NOVA SCHOOL OF SCIENCE & TECHNOLOGY

DEPARTAMENT OF CHEMISTRY

LARA PEDRO DUARTE CHAVES

Bachelor in Applied Chemistry

INVESTIGATION OF THE BIOACTIVE AND FUNCTIONAL PROPERTIES OF NOVEL EXOPOLYSACCHARIDES

MASTER IN BIOTECHNOLOGY

NOVA University Lisbon

September, 2024

NOVA SCHOOL OF SCIENCE & TECHNOLOGY

DEPARTAMENT OF CHEMISTRY

INVESTIGATION OF THE BIOACTIVE AND FUNCTIONAL PROPERTIES OF NOVEL EXOPOLYSACCHARIDES

LARA PEDRO DUARTE CHAVES

Bachelor in Applied Chemistry

Adviser: Patrícia Concórdio dos Reis,
Researcher, NOVA University Lisbon

Co-adviser: Tânia Sofia dos Santos Vieira,
Assistant Researcher, NOVA University Lisbon

Jury:

Chair: Ana Rita Cruz
Associate Professor with Aggregation, NOVA University Lisbon

Rapporteurs: Susana Isabel Conde Jesus Palma
Researcher, NOVA University Lisbon

Adviser: Patrícia Concórdio dos Reis,
Researcher, NOVA University Lisbon

MASTER IN BIOTECHNOLOGY

NOVA University Lisbon
September, 2024

Investigation Of The Bioactive And Functional Properties Of Novel Exopolysaccharides

To my grandma, you left too soon, but I hope I made you proud.

ACKNOWLEDGEMENTS

I would like to express my deepest gratitude to my advisor, Patrícia Reis, and co-advisor, Tânia Vieira, without whom I would not have been able to complete this thesis. I am immensely grateful for your unwavering guidance, patience, and empathy throughout this journey. Your shared scientific knowledge and constructive feedback have not only helped me improve but also shaped me as a student and scientist.

I would also like to extend my heartfelt thanks to the BioEng and Cell and Tissue Engineering research groups for welcoming me so warmly and making me feel like a part of your team. Thank you for your words of encouragement and for the understanding you have shown me throughout this process.

To my family, I want to express my immense gratitude for always standing by my side and encouraging me to overcome every challenge. A special thanks goes to my mother, for teaching me to be the person I am today and to never give up, and to my sister, the best friend anyone could ever ask for.

To my long-time friends, Beatriz and Eduarda, thank you for 10 years of unwavering friendship. Thank you for being there through the hardest moments and for encouraging me to reach for the best. Without you, I wouldn't be where I am today.

To my friends from Biotechnology, I am deeply grateful for sharing this journey with me. Your companionship and support have made this experience unforgettable. A special thanks goes to Filipa, because of you, I was able to break out of my shell and enjoy these last two years to the fullest. To Sofia, the wonderful friend I never imagined I would find, thank you for your kind and loving nature and for always being there, no matter what. And to Carolina, thank you for always showing me the bright side of life with your kind words.

Finally, to João, thank you for always being there for me, for caring for me, and for keeping me company through the toughest schedules. Your unwavering support has meant so much to me.

"Life is a play that does not allow testing. So, sing, cry, dance, laugh and live intensely, before the curtain closes and the piece ends with no applause."
(Charles Chaplin)

RESUMO

Os exopolissacarídeos (EPS) são macromoléculas promissoras com grande potencial para o desenvolvimento de produtos sustentáveis de base biológica em vários setores. Os ambientes marinhos, com as suas condições únicas e pouco exploradas, constituem fontes valiosas de microrganismos capazes de produzir EPS. Estes polímeros, especialmente aqueles que contêm açúcares raros, ácidos urónicos e grupos sulfatados, destacam-se pela sua elevada solubilidade, bem como pelas suas propriedades antioxidantes, fotoprotetoras e gelificantes, tornando-os ideais para aplicações nas indústrias cosmética, de saúde e alimentar.

O objetivo deste estudo parte por investigar as propriedades funcionais e biológicas de cinco EPS com composições distintas. O EPS RA19, rico em fucose, foi o único avaliado quanto às suas propriedades funcionais, demonstrando um comportamento não-Newtoniano e *shear-thinning*, uma forte capacidade de emulsificação com óleo de parafina e a aptidão para formar filmes estáveis, com ou sem plastificante, além de formar géis com Fe^{2+}. Estas características tornam-no adequado para aplicação em cosméticos e entrega de fármacos. No entanto, as suas propriedades biológicas foram limitadas à fotoproteção em queratinócitos, sem apresentar atividades antioxidantes ou cicatrizantes significativas.

O EPS SC4 demonstrou um excelente desempenho nas atividades fotoprotetora, antioxidante e cicatrizante, destacando o seu potencial para uso em cosméticos e engenharia de tecidos. O EPS AB5 evidenciou uma atividade fotoprotetora significativa, enquanto o EPS RD5, mostrou uma capacidade notável na cicatrização de feridas. Por fim, o EPS Mo169, apesar de não ter demonstrado propriedades fotoprotetoras ou cicatrizantes, revelou uma forte atividade antioxidante, sugerindo a sua aplicação na mitigação do stress oxidativo.

Palavras chave: Exopolissacarídeos (EPS), Propriedades Funcionais, Propriedades Biológicas, Fucose, Sulfatos, Aplicações

ABSTRACT

Exopolysaccharides (EPS) are promising macromolecules with significant potential for developing sustainable bio-based products across various sectors. Marine environments, with their unique conditions, serve as valuable but underexplored sources of novel EPS-producing microorganisms. EPS featuring rare sugar, uronic acid moieties, and sulfation are particularly attractive due to their enhanced solubility, antioxidant activity, photoprotection, and gelling capabilities, making them ideal for applications in cosmetics, healthcare, and food industries.

This study investigates the functional and biological properties of EPS RA19, a fucose-rich polymer. This polymer displayed non-Newtonian shear-thinning behavior, strong emulsification with paraffin oil, and the ability to form stable films with and without plasticizer, and Fe^{2+}-crosslinked gels, making it suitable for cosmetic and drug delivery applications. However, its biological activity was limited to photoprotection in keratinocytes, showing no antioxidant and wound healing activity.

Moreover, the bioactivity of four other EPS with previously demonstrated interesting functional properties was investigated. EPS SC4 exhibited superior photoprotective, antioxidant, and wound-healing properties, highlighting its potential in cosmetics and tissue engineering. EPS AB5 showed significant photoprotective activity, while EPS RD5, rich in uronic acids, demonstrated strong wound-healing capabilities. Finally, EPS Mo169, while lacking photoprotective or wound-healing properties, showed strong antioxidant activity, suggesting its use in oxidative stress reduction.

Keywords: Exopolysaccharides (EPS), Functional properties, Biological properties, Fucose, Sulfate, Applications

LIST OF CONTENTS

1 MOTIVATION AND BACKGROUND 1
1.1 Polysaccharides 1
1.2 Microbial Polysaccharides 2
1.3 Exopolysaccharides 2
1.4 Marine Biosphere: A rich source of microbial diversity 3
1.5 Polysaccharide rich in fucose 6
1.6 Sulfated polysaccharide 7
1.7 Applications 9
1.7.1 Biomedical Applications 9
1.7.2 Pharmaceutical Applications 10
1.7.3 Cosmetic Applications 11
1.7.4 Food Industries 12
1.8 Motivation 13
2 FUNCTIONAL PROPERTIES 15
2.1 Introduction 15
2.1.1 Thickening property 15
2.1.2 Film forming 16
2.1.3 Gelling capacity 16
2.1.4 Emulsifying ability 17
2.2 Materials and Methods 18
2.2.1 Materials 18
2.2.2 Characterization 18
2.2.3 Rheological Characterization 19
2.2.4 Films 20
2.2.5 Gels 21

2.2.6 Emulsions 22
2.3 Results and Discussion 23
2.3.1 Characterization 23
2.3.2 Rheological characterization 25
2.3.3 Films 31
2.3.4 Gels 34
2.3.5 Emulsions 38
2.4 Conclusion 42
3 BIOACTIVE PROPERTIES 45
3.1 Introduction 45
3.1.1 Antioxidant 45
3.1.2 Photoprotection 46
3.1.3 Wound healing 46
3.2 Materials and Methods 47
3.2.1 Materials 47
3.2.2 Cell culture 48
3.2.3 Cytotoxicity assay 48
3.2.4 Photoprotection 49
3.2.5 Antioxidant activity 50
3.2.6 Wound healing 51
3.2.7 Statistical Analysis 52
3.3 Results and Discussion 52
3.3.1 Cytotoxicity 52
3.3.2 Photoprotection 54
3.3.3 Antioxidant 56
3.3.4 Wound healing 58
3.4 Conclusion 60
4 CONCLUSIONS AND FUTURE WORK 61
4.1 General Conclusion 61
4.2 Future work 62

LIST OF FIGURES

Figure 1. FTIR spectra of EPS RA19 24
Figure 2. Thermogravimetric analysis curves of EPS RA19 25
Figure 3. Apparent viscosity (η) plotted as a function of shear rate (γ) for several EPS concentrations: 1 wt.%; 2 wt.%; 3 wt.%; 4 wt.%; 6 wt.%; 8 wt.%; 10 wt.%; 14 wt.%; 20 wt.%; and 24 wt.%. 26
Figure 4. Storage modulus G′ and loss modulus G′′ as functions of angular frequency for the aqueous solutions of EPS RA19 at various concentrations. 28
Figure 5. Apparent viscosity and oscillatory shear stress test for a gradient of temperatures. 29
Figure 6. Apparent viscosity and oscillatory shear stress test for different pH levels. 31
Figure 7. Photographs of the films 3wt.% EPS RA19 without glycerol and with glycerol are presented in the far left panel. SEM images: top view at ×250 magnification (left panel), top view at ×1000 magnification (center panel) and cross section view at ×250 magnification (right panel). 32
Figure 8. Optimization of iron (Fe^{2+}) concentration and EPS content. Test tubes showing varying concentrations of Fe^{2+} (40 mg and 60 mg) and EPS (2% and 4%) 37
Figure 9. Emulsions formulated with EPS RA19 at 0.5 and 1.0 wt.%, with O:W weight ratios of 2:3 and 3:2, using paraffin oil. 40
Figure 10. Apparent viscosity and oscillatory shear stress test for different emulsions. 41
Figure 11. Schematic representation of the cytotoxicity assay protocol, detailing the steps from cell seeding, treatment with test compounds, application of cytotoxicity assay reagent (resazurin) to measurement. Created in Inkscape. 49
Figure 12. Overview of the photoprotection assay protocol, illustrating the sequence from seeding cells, adding experimental and control treatments, subjecting one plate to UV irradiation and another left at room temperature, and measuring absorbance at 570 nm and 600 nm to assess photoprotective effects. Created in Inkscape. 50

Figure 13. Illustration of the oxidative stress assay protocol, showing the steps of seeding cells into a 96-well plate, adding H2-DCFDA, treating with EPS, inducing oxidative stress with H2O2 or UV light, and measuring fluorescence. Created in Inkscape. 51
Figure 14. Illustration of the wound healing assay protocol, showing the steps of seeding cells into a 12-well plate with silicone inserts, removing the silicone inserts to create uniform cell-free zones, and adding experimental and control treatments. Created in Inkscape. 52
Figure 15. Cytotoxicity effect of EPS RA19 on HaCaT, HFFF2 and Vero at different concentrations. Positive control was supplemented with medium and DMSO, and negative control was supplemented with only medium. 53
Figure 16. Metabolic viability of irradiated and non-irradiated HaCaT and HFFF2 cells 24h post exposure to UV radiation, for five EPS, RD5, SC4, AB5, RA19 and Mo169. Non irradiated cells supplemented with only medium, C-; Non irradiated cells supplemented with EPS, C+; Irradiated cells supplemented with only medium, I-; Irradiated cells supplemented with EPS, I+. 55
Figure 17. The impact of various EPS on the production of ROS (%) in HaCaT cells following exposure to UVB light, and hydrogen peroxide for 30 min. Ascorbic acid (AA) served as positive control.....58
Figure 18. Wound healing assay, with migration of HaCaT cells after treatment with EPS RD5, SC4, RA19 and Mo169 for 16h, 24h, 32h, and 48h post removal of insert.....59

LIST OF TABLES

Table 1. Examples of polysaccharides displaying source, properties and applications. 4
Table 2. Monosaccharide composition of EPS RA19 23
Table 3. Parameters of the Carreau model were estimated for various EPS concentrations, and 6 wt.% EPS under different pH and different temperatures 27
Table 4. Mechanical properties for films prepared with EPS RA19 with and without alongside reference values from literature 33
Table 5. The formation of gels under both standard and alkaline conditions was assessed by examining their strength and homogeneity 35
Table 6. Optimization of gel formation under standard conditions was evaluated based on their strength and homogeneity 36
Table 7. Emulsification activity was assessed at 24 h, and 30 days along with the stability of emulsions stabilized with EPS RA19 39
Table 8. Parameters of the Carreau model were estimated for various concentrations, and O:W ratios using paraffin as oil phase 42
Table 9. Monosaccharide composition of additional EPS used in biological assays 47

ACRONYMS

Ara	Arabinose
CPS	Capsular polysaccharide
DMEM	Dulbecco's Modified Eagle Medium
EPS	Exopolysaccharide
FBS	Fetal bovine serum
Fru	Fructose
Fuc	Fucose
GAG	Glycosaminoglycans
Gal	Galactose
GalA	Galacturonic Acid
Glc	Glucose
GlcA	Glucuronic Acid
GlcN	Glucosamine
GlcNAc	N-acetyl- glucosamine
HPLC	High Performance Liquid Chromatography
IdoA	Iduronic acid
LVE	Linear viscoelastic region
Man	Mannose
ManA	mannuronic acid
Mn	Number average molecular weight
Mw	Average molecular weight
PBS	Phosphate-buffered saline
PDI	Polydispersity index
PS	Penincilin-strepmycin

Rib	Ribose
RH	Relative humidity
Rha	Rhamnose
ROS	Reactive oxygen species
SE-HPLC	Size Exclusion-High Performance Liquid Chromatography
SEM	Scanning Electron Microscope
Suc	Sucrose
TFA	Trifluoroacetic acid
TG	Termogravimetric
TGA	Termogravimetric analysis
UV	Ultraviolet
WVP	Water vapor permeability
Xyl	Xylitol

SYMBOLS

κ	Kappa
ι	Iota
λ	Lambda
η	Apparent viscosity (Pa s)
λ	Time constant (s)
$\dot{\gamma}$	Shear rate (s^{-1})
η_0	Zero-shear rate viscosity (Pa s)
η_∞	Viscosity of the second Newtonian plateau (Pa s)
N_w	Molar flux of water vapor (mol m^{-2} s^{-1})
δ	Thickness of the film (m)
E_I	Emulsification index (%)
h_T	Overall height of the mixture after emulsification (mm)
h_e	Height of the emulsion layer (mm)
E_S	Emulsification stability (%)
T_{deg}	Degradation temperature (°C)
G'	Storage modulus
G''	Loss modulus

1

MOTIVATION AND BACKGROUND

1.1 Polysaccharides

Polysaccharides are the most prevalent high molecular weight polymers found in nature. They are formed by monosaccharides linked through glycosidic bonds. These fundamental building blocks define the structure of polysaccharides, which can be categorized into two main types: homopolysaccharides and heteropolysaccharides. Homopolysaccharides, like cellulose and pullulan, consist of repeating units of a single type of monosaccharide. In contrast, heteropolysaccharides, such as xanthan and hyaluronic acid, are made up of various monosaccharides, typically containing up to ten different types [1,2]. Common examples of monosaccharides often found in nature include simple sugars like D-galactose, L-fructose and D-glucose.

In addition, various derivatives of monosaccharides have been identified, such as amino sugars like D-galactosamine and D-glucosamine, and their derivatives. Simple sugar acids, including galacturonic and glucuronic acids, are also present, along with neutral sugars such as L-rhamnose, L-arabinose, and L-fucose. Polysaccharides can also contain organic acyl groups, such as acetyl, succinyl, and pyruvyl groups, and/or inorganic compounds (e.g., sulfate, fosfate) [2].

Polysaccharides can be further classified according to three key characteristics: the level of branching, the nature of glycosidic bond, and extension of their chains. Along with the wide array of monomeric combinations the glycosidic linkages themselves are highly versatile. They can exist in various configurations of the anomeric carbon, including α or β anomers, and the chosen carbon atom engaged on the bond. This originates polysaccharides that vary from having linear structures with a single type of monosaccharide to more complex structures with multiple branches and different types of monosaccharides [3]. Linkages such as β-1,4 or β-1,3

result in regions that are relatively stiffer. In contrast, α-1,2 and α-1,6 linkages facilitate a greater degree of flexibility in the backbone [4,5].

1.2 Microbial Polysaccharides

Microbial polysaccharides are classified into three distinct categories based on their cellular location and functional roles: intracellular polysaccharides, stored in the cytoplasm as vital reserves of carbon and energy (e.g., glycogen); cell wall polysaccharides, such as chitin, crucial for maintaining cellular structural integrity; and extracellular polysaccharides (EPS), which include free exopolysaccharides (EPS) and capsular polysaccharides (CPS). EPS are secreted by cells and play a multitude of essential roles in microbial physiology and interactions with the environment [5,6].

Free exopolysaccharides and capsular polysaccharides are found in the outer layer of the cell and bestow it with a protective barrier established between the environment and the cellular membrane. Whereas CPS are defined as polymers that interact with the surface of the cell via covalent bonds with phospholipids or lipid A molecules, EPS are expelled to the surface of the cell and are usually sloughed off as slime. Notwithstanding, these definitions are not so disconnected as they might seem, since some CPS are at times completely secreted from the cell and some EPS might be found loosely associated with the surface [3].

In comparison to plants and algae, microorganisms excel in polysaccharide production due to their rapid growth rates and adaptability. This allows for the manipulation of growth conditions in favor of enhancement of growth and production [7]. Given the wide variety of polysaccharides, encompassing both sugar monomers and non-carbohydrate groups, the chemical and physical characteristics of microbial polysaccharides show significant differences [5].

1.3 Exopolysaccharides

CPS primarily contribute to enhancing virulence and promoting pathogenesis, while free EPS serve diverse functions including protection against abiotic environmental stresses such as extreme temperatures, toxins, desiccation and salinity. Additionally, EPS also aids in promoting cell adhesion, acting as reserves for water and carbon storage. On solid surfaces EPS illicit bacterial community growth and proliferation, along with promoting cell adhesion, ultimately leading to the formation of biofilms [6].

Exopolysaccharides are sourced from a vast plethora of biological origins, encompassing microalgae, fungi, and bacteria, each contributing distinct polymers with varied biological functions and industrial applications. Bacterial production dominates the EPS landscape, exemplified by well-known polymers like gellan gum [8], levan [9] and xanthan gum [10]. Algae significantly enrich the EPS repertoire with notable examples such as alginate [11] and fungal EPS examples including pullulan [12], dextran [13], and lentinan [14]. Bacterial EPS can be acquired from strains inhabiting a variety of environments, ranging from freshwater and marine ecosystems to extreme conditions and soil habitats, further expanding their potential utility across different industries. Table 1 provides an extensive overview of various polysaccharides, detailing their sources and specific applications across multiple industries.

The advantages of bacterial EPS production lie in year-round availability, cost-effectiveness, and ease of access, making them highly valuable and versatile materials for diverse applications [15].

1.4 Marine Biosphere: A rich source of microbial diversity

Spanning more than 70% of the Earth's surface, the oceans cover approximately 360 million square kilometers, with an average depth of 3.7 kilometers [17]. These vast waters experience pressures up to 38 megapascals and maintain an average temperature of around 2 degrees Celsius. Within this expansive bodies of water thrives a rich diversity of life, highlighting its pivotal role in global biodiversity [18].

The unique environmental conditions of marine habitats create extreme ecological niches within marine ecosystems. These include deep-sea hydrothermal vents, volcanic zones underwater, saline lakes, polar sea ice, and microbial mats found in locations as diverse as Polynesian atolls [18].

Microbial mats, known locally in French Polynesia as “kopara” mats, are a consort of microbial layers superimposed to form a mat. These mats typically exhibit pH values ranging from 6 to 10.5, salt concentrations varying between 5 and 42 g L^{-1}, temperatures reaching 20°C at night and 42°C at midday, and light intensities that vary depending on their geographical location [19].

Table 1. Examples of polysaccharides displaying source, properties and applications. (Ara, L-arabinose; Fru, fructose; Fuc, L-fucose; Gal, galactose; Glc, glucose; GlcA, glucuronic acid; IdoA, iduronic acid; Man, mannose; ManA, mannuronic acid; GlcNAc, N-acetyl- glucosamine; Rha, rhamnose; Suc, sucrose; Xyl, xylose)

Microorganism	Polymer	Monomers	Source	Properties	Application	References
Klebsiella pneumoniae	Fucogel	GlcA, Fuc, Gal	Bacteria	Emulsifying, antimicrobial	Cosmetic Industry	[16]
Enterobacter cloacae	EPS 71a	Fuc, Gal, Glc, GlcA	Bacteria	High heavy metal, chelating capacity	Wastewater Treatment	[17]
Anoxybacillus gonensis YK25		Xyl, Suc, Glc, Gal, sulfate	Bacteria	Anticancer	Medical industry	[18]
Enterobacter A47	FucoPol	Fuc, Gal, Glc, pyruvate, succinate, acetate	Bacteria	Antioxidant, photoprotective, emulsifying, gelling, wound healing	Cosmetics Tissue engineering Drug delivery	[7,19-22]
Sphingomonas elodea	Gellan Gum	Rha, GlcA, Glc	Bacteria	Gelling, thickening	Food industry, Tissue engineering	[8,23]
Porphyridium cruentum		Gal, Xyl, Glc, GlcA, sulfate	Algae	Water retention, emulsifying, antioxidant, antibacterial	Food industry	[24]
Fucus serratus, Holothuria tubulosa	Fucoidan	Fuc, Sulfate, Acetate	Algae, invertebrates	Anti-tumor, anti-inflammatory, immunoregulator, anticoagulant	Medical, Pharmaceutic industry	[25,26]
Laminaria, Pseudomonas aeruginosa	Alginate	ManA, GlcA	Algae Bacteria	Gelling, films	Pharmaceutical, Tissue regeneration, Food industry	[11,27]
Xanthomonas	Xantham Gum	Glc, Man, GlcA	Bacteria	Gelling, films, thickening	Tissue engineering, Food industry, cosmetics	[10,28]
Clavibacter	Clavan	Glc, Gal, Fuc, pyruvic acid	Bacteria	Anti-tumor, moisturizing	Medical and cosmetic industry	[1,29]
Aureobasidium pullulans	Pullulans	Glc	Fungi	Films, antitumor, antiviral, antimicrobial	Food, cosmetics, biomedical	[12]
Rhodotorula mucilaginosa YMM19		Glc, Gal, glucopyranose	Fungi	Emulsifying, herbicidal	Pesticide	[30]

Table 1. (continuation) Examples of polysaccharides displaying source, properties and applications. (Ara, L-arabinose; Fru, fructose; Fuc, L-fucose; Gal, galactose; Glc, glucose; GlcA, glucuronic acid; IdoA, iduronic acid; Man, mannose; ManA, mannuronic acid; GlcNAc, N-acetyl- glucosamine; Rha, rhamnose; Suc, sucrose; Xyl, xylose)

Pediococcus pentisaceus E8	EPS E8	Ara, Man, Glc, Gal	Bacteria	Emulsifying, antioxidant	Food, pharmaceutical, cosmetic industry	[31]
Chondrus crispus Kappaphycus alvarezii	Carregeenans	Gal, 3,6-anhydrogalactose, sulfate	Algae	Gelling, thickening, stabilizing	Pharmaceutical, food, cosmetic industry	[32,33]
Bacillus sp., Halomonas sp.	Levan	Fru	Bacteria	Anti-oxidant, anti-inflammatory, anti-carcinogenic	Food, cosmetics, chemical, pharmaceutical industries	[6,15]
Lentinula edodes	Lentinan	Glc	Fungi	Anti-tumor, anti-inflammatory, anti-diabetes	Pharmaceutical industry	[14]
Weissella cibaria MED 17		Glc	Bacteria	Wound healing, antioxidant	Pharmaceutical industry	[34]
Weissella, Lactobacillus	Dextran	Glc	Bacteria	Water retention, wound healing, emulsifying	Tissue engineering, food industry	[6,13]
Ulva sp.	Ulvan	Rha, Xyl, IdoA, GlcA	Algae	Immunomodulating activity, antioxidant, anticancer, anticoagulant	Agriculture, medical, biomedical industry	[35]
Sclerotium rolfsii	Scleroglucan	Glc	Fungi	Water retention	Cosmetics, Agriculture industry	[36]
Papiliotrema terrestris PT22AV		Man, Glc	Fungi	Antibacterial, wound healing	Biomedical industry	[37]
Agrobacterium	Curdlan	Glc	Bacteria	Gelling, texturizer	Food, biomedical industry	[38]
Streptococcus sp., Bacillus sp.	Hyaluronic acid	GlcA, GlcNAc	Bacteria	Anti-carcinogenic, wound healing, water retention	Medical, cosmetic, pharmaceutical industry	[39]

The microbial community is mainly dominated by cyanobacteria, sulfurous and non-sulfurous photosynthetic bacteria and sulfate-reducing bacteria in the deeper layers, along with isolated microorganisms such as *Chromatium* sp. and *Rhodobacter* spp. [40]. Additionally, these mats harbor heterotrophic bacteria from genera such as *Pseudomonas*, *Alteromonas*, *Paracoccus*, and *Vibrio* recognized as primary producers of EPS [40].

As mentioned above, polysaccharides can be synthesized by various types of microorganisms. However, the ability to produce promising EPS is best demonstrated by extremophiles, microorganisms adapted to prosper in extreme environments such as thermophiles, psychrophiles, acidophiles, alkaliphiles and halophiles [41]. These organisms have evolved numerous adaptations to survive and thrive in harsh conditions imposed by extreme temperatures, pH levels, salt concentrations, and high radiation levels. The production of EPS serves as a crucial survival mechanism, providing extremophiles with essential water, nutrients, and metal ions [41]. Furthermore, EPS also acts as a protective barrier, shielding cells from toxic compounds, metals, and abiotic factors such as temperature fluctuations, pH variations, and pressure changes [6]. However, despite their potential, marine EPS remain under-explored and under-researched [42].

1.5 Polysaccharide rich in fucose

Rare sugars, such as L-rhamnose, uronic acids and L-fucose, are notably scarcer in nature compared to the more prevalent D-galactose and D-glucose [29]. Rare sugar exhibits distinctive properties that make them highly attractive for various fields of applications. Bacterial EPS containing rare sugars in their backbone are highly valuable, not merely due to their inherited properties, but also for their ability to yield pure rare sugar monosaccharides thorough hydrolysis and subsequent separation and purification steps [30].

Among these rare sugars, L-fucose, also known as 6-deoxy-L-galactose, is especially noteworthy. This monosaccharide is a common component in the structures of several glycans and glycolipids synthesized by mammalian cells. Fucose has two main structural features that set them apart from other six-carbon sugar monomers. Firstly, it lacks a hydroxyl group on the sixth carbon (C-6), and secondly, its configuration is L-configuration [43]. Microorganisms such as bacteria, microalgae, and fungi produce several fucose-containing EPS.

A notable example of a fucose-rich EPS produced by *Clavibacter* strains, in particular *C. michiganensis*, Clavan is a tetrasaccharide composed of repeating units of L-fucose, L-

galactose, L-glucose in 2:1:1 [29]. Clavan can help prevent colonization of tumor cells in the lungs and provide skin moisturization in cosmetic products (Table 1) [1].

Produced by bacteria belonging to *Enterobacteriaceae* family, such as *Citrobacter*, *Enterobacter*, and *Klebsiella*, colonic acid is a polyanionic heteropolysaccharide composed of D-galactose, L-fucose, D-glucose and glucuronic acid in molar ratios 2:2:1:1 [44]. Its polyanionic nature is conferred by the existence of uronic acid and pyruvate [45]. Colanic acid is widely employed in cosmetic applications for its excellent water retention properties, which are provided by its high molecular weight and abundant hydrophilic groups (Table 1) [44].

Fucogel, an anionic exopolysaccharide abundant in fucose and produced by *Klebsiella pneumoniae*, consists of a linear structure made up of repeating units of L-fucose, D-galactose, and glucuronic acid. [16]. This EPS is extensively used in the cosmetics industry due to its potent moisturizing and anti-aging properties [46]. Its self-emulsifying nature and ability to enhance skin hydration makes it a valuable ingredient in skincare formulations (Table 1) [46,47].

Numerous species within the *Enterobacter* genus have been documented to synthesize fucose-containing EPS. Fucopol, produced by *Enterobacter* A47, contains L-fucose, D-galactose, D-glucose, in molar ratio 1.6:1.3:1.1 [7]. Acyl substituents, namely acetate, pyruvate and succinate, were also detected in FucoPol's composition [7]. This EPS has been reported to have interesting physicochemical and biological properties, including emulsification [48], jellification [49], photoprotection [20] and cryopreservation (Table 1) [50]. *Enterobacter cloacae* produces an exopolysaccharide (EPS71a) with L-fucose, glucuronic acid, D-glucose, D-galactose in 2:1:1:1 molar ratio. The high content of glucuronic acid bestows EPS71a with negative charges and acidic properties, exhibiting a high heavy metal chelating capacity, making it very interesting for applications such as wastewater treatment (Table 1) [17].

1.6 Sulfated polysaccharide

Sulfated polysaccharides are a unique class of negatively charged polysaccharides characterized by the presence of sulfate groups attached to their sugar residues. These sulfate groups impart distinctive biochemical and biophysical properties that enhance the functionality and application range of these polysaccharides [51]. High sulfate content can enhance the hydrogen supply capacity and increase water solubility, improving antioxidant activity by stabilizing free radicals [52,53]. Contrastingly, an abnormally high content of sulfate can disrupt the EPS structures, reducing its potential [52].

Sulfated polysaccharides are synthesized by numerous marine organisms, including cyanobacteria, microalgae, and certain bacteria, and possess a broad spectrum of biological activities. Fucoidan, one of the most recognized sulfated polysaccharides, is predominantly derived from brown seaweed like *Fucus vesiculosus*, and a select group of marine invertebrates, including sea urchins, *Holothuria tubulosa*, and sea cucumbers [25,54]. Structurally fucoidans are very complex and devoid of regularity, however, all present high percentages of L-fucose residues in their backbone, along with varying degrees of sulfation and other monosaccharide components. Fucoidan has been extensively studied for its biological properties as anti-tumor, anti-inflammatory, immunoregulator, anticoagulant (Table 1) [26,55-57].

Carrageenan is a family of linear sulfated polysaccharides extracted from seaweeds such as *Chondrus crispus* [58] and *Kappaphycus alvarezii* [32]. It is composed of alternating galactose residues and 3,6-anhydrogalactose, with varying degrees of sulfation. The differences in the type and number of sulfate groups, lead to the classification of carrageenan into three main types: kappa (κ), iota (ι), and lambda (λ). Kappa Carrageenan (κ-Carrageenan) has one sulfate group per disaccharide unit and forms firm, rigid gels when potassium ions are present. I-Carrageenan, contains two sulfate groups per disaccharide repeating unit and forms elastic and soft gels in the presence of calcium ions. The most sulfated Carrageenan, lambda (λ), has three sulfate group per disaccharide unit. Unlike the previous, λ-Carrageenan does not form gels but acts as a thickening agent (Table 1) [59].

Beyond its use in the food industry, carrageenan has demonstrated antiviral properties by blocking viral entry into cells [60], and has shown immunomodulatory effects [61], making it useful in pharmaceutical formulations. Furthermore, In the cosmetics industry, carrageenan is utilized for its ability to enhance the texture and stability of products, as well as for its moisturizing properties [33].

Another noteworthy example is Ulvan, a versatile sulfated polysaccharide extracted from the cell walls of green macroalgae, particularly from species within the genera *Ulva* (commonly known as sea lettuce). Ulvan is composed of repeating disaccharide units, primarily consisting of rhamnose, xylose, glucuronic acid, and iduronic acid, and varied sulfation levels [35]. These structural features endow Ulvan with a wide range of biological activities, including antioxidant, antiviral, and anticoagulant properties. Its applications span multiple industries, from food and agriculture to pharmaceuticals and water treatment (Table 1) [62].

In recent years, EPS with a high sulfate content have attracted attention due to their potential properties. A sulfated EPS derived from *Chlorella* sp. demonstrates anti-hyperglycemic activity, making it a promising candidate for use as a nutraceutical or food additive [52].

Another sulfated EPS from *Porphyridium cruentum* has been shown to enhance microbiological quality and oxidative stability in minced beef meat, suggesting its potential for extending shelf life and producing healthier refrigerated meat products (Table 1) [24]. Additionally, the thermophilic bacteria *Anoxybacillus gonensis* YK25 produces an EPS with anticancer activity, indicating its potential application in the pharmaceutical industry (Table 1) [18].

1.7 Applications

Polysaccharides are increasingly recognized for their versatile applications in the biomedical , particularly in tissue engineering [63], wound healing [64] and drug delivery [63]. Their biocompatibility, biodegradability, and ability to form hydrogels make them excellent contenders for a range of biomedical applications [63].

1.7.1 Biomedical Applications

Tissue engineering and wound healing are key biomedical applications that utilize biomaterials to regenerate and repair damaged tissues, enhancing recovery and patient outcomes [65].

Tissue engineering is a multidisciplinary field that focuses on creating scaffolds that support cell attachment, proliferation, and differentiation to restore or regenerate damaged tissues and organs. EPS have emerged as promising scaffold materials due to their biocompatibility, biodegradability, and tunable mechanical properties [66].

EPS are particularly advantageous in tissue engineering because of their structural and functional resemblance to glycosaminoglycans (GAGs). GAGs are composed of repeating disaccharide units that include uronic acid residues and amino sugars, a composition mirrored by EPS [67]. This similarity enables EPS to emulate the natural cellular environment, enabling essential cellular processes [6]. Additionally, the sulfate groups in EPS enhance their interaction with growth factors and cytokines, stabilizing these molecules and boosting their biological activity [68].

Hyaluronic acid is another noteworthy EPS known for its hydrating and viscoelastic properties [69]. It can be naturally present in the extracellular matrix of connective tissues [69] or produced via biotechnology as EPS by bacteria, such as *Streptococcus* sp. and *Bacillus* sp. [39].

Hyaluronic acid-based scaffolds facilitate cell migration and proliferation, as well as nutrient diffusion, rendering them well-suited for applications in skin and wound healing [70]. Furthermore, they can be chemically modified to enhance their mechanical strength and

degradation rates, thereby enabling the adaptation of these scaffolds to specific tissue engineering requirements [70,71].

Xanthan gum is another EPS employed in biomedical applications. Its high viscosity, stability under diverse conditions, natural biocompatibility, and resistance to mechanical degradation render it useful for fabricating scaffolds that can support cellular growth *in vitro* [10]. Xanthan gum can be blended with other polymers to enhance its mechanical properties, making it suitable for soft tissue engineering [10].

FucoPol's biocompatibility and non-toxic nature make it an excellent candidate for wound healing applications in tissue engineering. It can be used to develop hydrogels and scaffolds that support cell proliferation and tissue regeneration, promoting faster and more efficient wound healing. FucoPol-based hydrogels can maintain a moist wound environment, which is crucial for optimal healing [19,22].

1.7.2 Pharmaceutical Applications

In pharmaceutical applications, drug delivery systems are crucial for enhancing the effectiveness and precision of treatments. These systems are carefully designed to release therapeutic agents in a controlled way, targeting specific areas in the body to boost therapeutic outcomes while reducing potential side effects [63]. Advanced drug delivery technologies, including nanoparticles, liposomes, and biodegradable polymers, facilitate precise modulation of drug release rates and distribution [72]. These sophisticated systems offer easy degradation, enhance bioavailability, and enable translocation across biological barriers, ensuring localized drug release [72]. Furthermore, the advancement of smart drug delivery systems, which respond to physiological triggers such as pH or temperature fluctuations, holds promise for highly targeted and responsive therapeutic interventions [73].

In drug delivery, EPS can be utilized to create various formulations such as hydrogels, nanoparticles, and microspheres that encapsulate drugs. These EPS-based delivery systems can administer drugs through oral, transdermal, intravenous, intramuscular, and targeted delivery routes, offering versatility in therapeutic applications. The ability of EPS to tailor release kinetics and enhance drug stability makes them valuable for optimizing drug delivery efficiency while minimizing side effects [72].

Alginate is one of the most widely used polymers in drug delivery due to its innate biocompatibility and low toxicity [74]. Its ability to gel in the presence of calcium ions makes it suitable for encapsulating a variety of drugs [11]. Alginate-based systems have been used to

deliver proteins, peptides, and small molecule drugs, particularly for the treatment of gastrointestinal disorders and applications in wound healing [11,75].

Notably, hyaluronic acid is utilized in drug delivery systems for its capacity to target specific cells, such as in cancer therapy, non-immunogenicity and biocompatibility. Hyaluronic acid-based hydrogels can encapsulate chemotherapeutic drugs and deliver them directly to tumor cells, reducing systemic toxicity, inhibiting metastasis and improving therapeutic outcomes [76].

Fucoidan has demonstrated potential in drug delivery due to its anticoagulant, anti-inflammatory and anti-metastatic properties. Fucoidan-based nanoparticles are being explored for their ability to deliver anti-cancer drugs and enhance the immune response. Their bioactivity and biocompatibility make them suitable for developing targeted and controlled release formulations [77].

1.7.3 Cosmetic Applications

EPS are highly effective at retaining moisture, creating hydrogels that keep the skin hydrated and elastic [78]. Their safety in formulations is guaranteed by their biocompatibility and biodegradability [79]. As a result, EPS are commonly used in anti-aging and skin-repair products, where they enhance effectiveness by decreasing visible wrinkles, softening and strengthening the skin and improving elasticity [78].

Hyaluronic acid is widely used for its exceptional ability to retain water. It can hold up to 1.000 times its weight in water, making it an excellent hydrating agent. Hyaluronic acid is incorporated into creams, serums, and lotions to improve skin hydration, elasticity, and overall appearance. Its use extends to anti-aging products where it helps to reduce the appearance of fine lines and wrinkles [69].

Commonly used in the cosmetic industry, alginate is an EPS that forms a gel-like texture when combined with calcium ions, making it ideal for inclusion in various cosmetic formulations such as lotions, masks and creams. It serves as an effective thickener, gelling agent, and stabilizer, enhancing the texture and stability of cosmetic products. Additionally, alginate's film-forming ability enhances adhesion to the skin, making it particularly useful in products designed for prolonged wear [80].

Valued for its moisturizing and bioactive properties, FucoPol offers hydration, smoothness, and spreadability when included in skincare formulations. These characteristics make it an ideal ingredient for lotions aimed at improving skin hydration and texture, as well as moisturizers designed to protect against UV rays [81].

Fucoidan is used to enhance skin repair and protection, due to particular bioactivities, such as photoprotection, antioxidation, anti-inflammation and anti-aging. It helps to reduce skin redness and irritation while providing a protective barrier against environmental stressors. Additionally, it promotes skin firmness and elasticity. Fucoidan is found in various topical skincare products, including creams, serums, and sunscreens, aimed at promoting skin health and resilience [80,82].

1.7.4 Food Industries

Public demand for food safety and quality has paved the path for the employment of EPS in food industries. EPS play a pivotal role in the food industry, due to their ability to change the food matrix improving texture, increasing viscosity and enhance mouthfeel, thereby ensuring product consistency and stability throughout shelf life [83]. They surge as a natural replacement for commercial additives due to their physicochemical characteristics and emulsifying, thickening, gelling and stabilizing properties [84].

The food industry is a vast and dynamic sector dedicated to the production, processing, packaging, and distribution of food products. EPS have gained prominence in the food industry due to their unique rheological properties, biocompatibility, and versatility. EPS are widely used as thickening and gelling agents in the food industry [84]. Alginate is a prominent example, being used to create gels and thicken various food products, such as sauces, dressings, and desserts. Additionally, alginate is widely used as an edible coating to extend the shelf life of perishable foods by acting as a barrier to moisture and gas exchange, thereby maintaining freshness. Its natural origin and biodegradability make alginate a preferred choice over synthetic additives, meeting the growing consumer demand for clean label ingredients in food products [27].

Another crucial application of EPS in the food industry is their role as emulsifiers and stabilizers. Xanthan gum is widely used to stabilize emulsions in products like beverages, salad dressings and sauces. Xanthan gum prevents the separation of oil and water phases, ensuring a consistent texture and appearance [85].

EPS such as gellan gum find application in food products for their ability to gel and form films. They serve as additives, stabilizers, and thickeners in confectionery, jams, and dairy products. Similar to alginates, these EPS can also act as a protective barrier against gastrointestinal conditions, owing to their resistance to heat and acidity [86].

1.8 Motivation

EPS are intriguing macromolecules that can play a key role in the development of sustainable bio-based products across various commercial sectors. Marine habitats, with their unique environmental conditions, are recognized as excellent sources of high-value biomolecules with enhanced properties. However, despite their significant potential for biodiscovery, marine environments remain underexplored and underutilized as sources of novel EPS-producing microorganisms.

EPS rich in rare sugars, such as fucose, are particularly noteworthy due to their distinctive properties, which make them highly attractive for numerous applications. These include antitumor activity, skin moisturization, anti-aging effects, enhanced skin hydration, photoprotection, and cryopreservation. Additionally, sulfated polysaccharides represent a unique class of negatively charged biomolecules. The presence of sulfate groups endows these polysaccharides with enhanced water solubility and improved biological and functional properties, such as antioxidant, antitumor and anti-inflammatory activities, as well as their use as thickening and gelling agents, and moisturizers.

Studying both the functional and biological properties of these EPS enables a comprehensive understanding of their potential in various applications. For instance, functional properties such as emulsifying, gelling, stabilizing, and film-forming capabilities can be crucial in fields like cosmetics and food technology. Meanwhile, their biological properties, including antioxidant activity, photoprotection, and wound healing, further underscore their potential for use in skincare and healthcare innovations.

With this in mind, in Chapter 2, the functional properties of a novel fucose-rich EPS were investigated. In Chapter 3, the bioactive properties of five EPS with different compositions, including the EPS from Chapter 2, were evaluated to determine their applicability in specific areas.

2

FUNCTIONAL PROPERTIES

2.1 Introduction

The demand for EPS has surged significantly over recent years owing to their unique physical-chemical properties, most notably their ability to form films, gels and emulsions, biocompatibility, biodegradability, and non-toxic nature [39]. These polysaccharides are rich in hydroxyl groups, making them valuable as hydrocolloids capable of altering the flow behavior and texture of various systems [87]. This versatility paves the way for numerous applications, including their use as thickening agents, gelling agents, emulsifiers, and stabilizers in industries such as food [86,87].

2.1.1 Thickening property

As thickening agents, EPS enhance the viscosity of aqueous solutions, improving the texture and mouthfeel of various products [85]. The thickening properties of EPS are attributed to their high molecular weight and capacity to create interconnected networks within solutions, which enhance viscosity by increasing resistance to flow, making EPS valuable additives in various applications requiring viscosity modulation, such as in food products, pharmaceuticals, and cosmetics [85].

Xanthan gum-based thickeners are preferred in the therapeutic management of dysphagia for their exceptional stability across diverse conditions typical of food and beverages, setting them apart from conventional thickeners [28]. Recently other EPS (e.g., scleroglucan, gellan gum and curdlan) have demonstrated properties akin to that of xanthan gum, and thus have been the subject of study for their prospective use as thickeners in dysphagia management (Table 1) [8,36,38].

2.1.2 Film forming

The biodegradable and biocompatible nature of EPS films offers an environmentally friendly alternative to traditional synthetic films. These films can protect food products from moisture loss, oxygen permeation, and microbial contamination, thereby extending shelf life and maintaining product quality [88]. In the pharmaceutical industry, EPS films can be used for controlled release drug delivery systems, where the film's properties regulate the rate and duration of drug release [89]. Additionally, EPS films have potential applications in wound dressings, where they can provide a protective barrier while promoting a moist healing environment [13].

EPS films have several drawbacks compared to traditional petroleum-based polymers, such as inferior chemical and thermal stability. Polysaccharides often result in brittle films with relatively poor mechanical properties, limiting their use in demanding packaging that requires high durability and tight sealing against moisture and gases. Moreover, EPS films tend to be highly sensitive to water and may degrade faster under humid conditions, affecting product shelf life and protection. Therefore, it is crucial to refine and enhance the properties of these films [88].

Several approaches can be employed to achieve this, including blending polysaccharides with other materials, modifying EPS structures to adjust biodegradability, permeability, and mechanical properties, and implementing cross-linking techniques to improve strength, stability, and barrier properties [88].

Known for its film-forming abilities, Xanthan Gum creates strong, flexible films that are biodegradable and can serve as protective coatings [90]. Pullulan forms transparent and edible films, which are used in food packaging to extend shelf life by protecting against moisture and oxygen (Table 1) [91].

2.1.3 Gelling capacity

Exopolysaccharide-based hydrogels are characterized by their three-dimensional, cross-linked polymer networks capable of holding substantial amounts of water, which imparts a gel-like consistency [78]. Notable for their high water retention, biocompatibility, and biodegradability, exopolysaccharide-based hydrogels are suitable for a wide range of applications, including biomedical, environmental and pharmaceutical sectors [78]. The unique water-retention capability is attributed to the hydrophilic groups attached to the polymer backbone, which engage in interactions with water molecules [78].

The interactions between cations and polymer chains are crucial in determining the characteristics of hydrogels. One of the primary methods for forming hydrogels is cation-mediated gelation. In this process, negatively charged moieties in the EPS interact with cations, leading to the formation of ionic crosslinks between different polymer chains [49,78]. Different cations, such as monovalent (e.g., K^+, Na^+), divalent (e.g., Mg^{2+}, Ca^{2+}), and trivalent (e.g., Al^{3+}, Fe^{3+}) ions, can have distinct effects on the hydrogel properties. For instance, divalent and trivalent cations create more robust crosslinking networks than monovalent cations, resulting in a hydrogel with greater tensile strength and remarkably tougher [78,92].

Natural polysaccharides have the ability to form gels with diverse textures and strengths, which can be finely adjusted by factors including pH levels, concentration, temperature variations, and the presence of ions or additives [93]. These gelling agents are extensively utilized in the food industry to enhance the texture and quality of products such as desserts, and dairy items [93]. For instance, gellan gum, composed of two units of glucose, one L-rhamnose and one L-glucuronic acid unit, can form both thermoreversible and thermostable gels, providing versatility in food formulations [23]. Alginate is capable of forming hydrogels with divalent cations, such as calcium (Ca^{2+}), which exhibit structural similarities to the matrices observed in living tissues. This property has led to its extensive utilization in a range of applications, including wound healing, drug delivery systems and tissue engineering [11]. Furthermore, FucoPol demonstrated considerable potential for the formation of hydrogel beads in the presence of divalent ion copper (II) (Cu^{2+}), and trivalent ion iron (III) (Fe^{3+}). This suggests a promising avenue for its potential applications in drug delivery [49].

2.1.4 Emulsifying ability

Microbial EPS possess excellent emulsifying properties enabling it to stabilize emulsions consisting of a mixture of oil and water. The effectiveness of EPS as emulsifiers can be attributed to their ability to reduce surface tension and form a protective layer around oil droplets, preventing coalescence [94]. This ability is crucial for the production of stable food products such as salad dressings, mayonnaise and sauces [94] Moreover, emulsions play a significant role in cosmetics and pharmaceutical lotions and creams [94].

The emulsions can be characterized as either oil-in-water (O:W) emulsions, where oil droplets are dispersed in a continuous water phase, or water-in-oil (W:O) emulsions, characterized by water droplets dispersed within a continuous oil phase [95].

FucoPol-based oil-in-water (O:W) emulsions containing olive oil and α-tocopherol demonstrated excellent viscosity and easy application. This, coupled with the additional

benefits of moisturization and antioxidant properties inherent to olive oil and α-tocopherol, renders them particularly well-suited for incorporation into cosmetic formulation [21]. Furthermore, microbial EPS synthesized by *Rhodotorula mucilaginosa* YMM19 have demonstrated significant emulsifying activity for farnesol, a natural herbicide. This highlights their promising potential for use in pesticide formulations (Table 1) [30]. Additionally, EPS-E8 derived from *P. pentosaceus* E8, exhibited exceptional stability and emulsifying efficacy for olive oil under extreme physicochemical conditions, underscoring its potential use in various sectors, including cosmetics, pharmaceuticals, and food manufacturing (Table 1) [31]

2.2 Materials and Methods

2.2.1 Materials

EPS RA19 was produced by culturing *Paracoccus zeaxanthinifaciens* subsp. *payriae* isolated from a "Kopara" mat in Rangiroa, French Polynesia [96]. The purified EPS was provided by Dr. Xavier Moppert from Pacific Biotech BP.

2.2.2 Characterization

2.2.2.1 Elemental analysis

The elemental analysis of the EPS was performed using a Thermo Finnigan-CE Instruments Flash EA 1112 CHNS series elemental analyzer (Italy). The samples underwent flash combustion in an oxygen-rich environment, causing the separation of gases (N_2, SO_2, H_2O, and CO_2) via gas chromatography. The nitrogen, carbon, hydrogen, and sulfur content was then determined using a thermal conductivity detector, as in Concórdio-Reis *et al.* [97].

2.2.2.2 EPS composition

The analysis described in Concórdio-Reis *et al.* [19] was performed to determine the composition of EPS. Dried samples of EPS (~5mg) were dissolved in 5mL of deionized water and subsequently hydrolyzed with trifluoroacetic acid (100 µL of 99% TFA) at 120 °C for 2 hours. After cooling the hydrolysates were filtered using an Eppendorf membrane filter, and afterward used to identify and quantify the constituent sugars by liquid chromatography (HPLC) using a Dionex Carbopac PA10 column (Thermo Scientific™ Dionex™, Sunnyvale, CA, USA) equipped with an amperometric detector. The analysis was carried out at 30°C with 4 mM NaOH as the eluent, at a flow rate of 0.9 mL min^{-1}. Standards ranging from 2.5 to 50 ppm of fucose (Carbosynth, Biosynth), rhamnose (Fluka Analytical, ≥99%), glucose (Acros Organics, >99%),

glucosamine (Sigma-Aldrich, Germany, ≥99%), arabinose (Tokyo Chemical Industry, >98%), mannose (Sigma-Aldrich, Germany, ≥99%), xylose (Sigma-Aldrich, Germany, ≥99%), galactose (Alfa Aesar, Johnson Matthey, Germany, 99%), ribose (Sigma-Aldrich, Germany, 98%), glucuronic acid (Alfa Aesar, ThermoFisher, Germany, >98%), and galacturonic acid (Fluka Analytical, ≥97%) were used for the determination and quantification of sugar monomers. The analysis was performed in duplicate.

2.2.2.3 Molecular mass distribution

Number and average molecular weights (Mn and Mw, respectively) of EPS, along with polydispersity index (PDI, Mn/Mw), were determined by Size Exclusion-High Performance Liquid Chromatography (SE-HPLC). The analysis was performed at 25°C on a KNAUER Smartline HPLC equipped with a Phenomenex Phenogel Linear LC Column 300 x 7.8 mm (USA), at a flow rate of 0.6 mL min^{-1}, using 0.1 M $LiNO_3$ as eluent. A 50 µL of EPS solution (0.5 w/v% in 0.1 M $LiNO_3$) was injected and a Water 2414 Refractive Index Detector was used for detection. A calibration curve generated with pullulan standards (P50 to P80) was used to calculate the values of Mn and Mw, as described in Concórdio-Reis *et al.* [97].

2.2.2.4 Fourier transform infrared spectroscopy

According to Concórdio-Reis [97], Fourier Transform Infra-Red (FTIR) Spectroscopy was recorded on a Perkin-Elmer Spectrum II spectrometer. The spectra were obtained between 500 and 4500 cm^{-1} after 10 scans, at room temperature.

2.2.2.5 Thermogravimetric analysis (TGA)

EPS samples (~10 mg) were characterized by Thermogravimetry (TG) using a Thermogravimetric Analyzer Labsys EVO (Setaram, France), with a heating rate of 10°C min^{-1}, from 25 to 800°C. The maximal thermal degradation temperature (T_{deg}, °C) corresponds to the temperature value obtained for the maximum decreasing peak of the sample mass, which corresponds to the highest degree slope, as described in Concórdio-Reis [2].

2.2.3 Rheological Characterization

The rheological experiments were carried out according to Concórdio-Reis [98]. An MCR92 modular compact rheometer (Anton Paar, Graz, Austria) equipped with a cone-plate geometry (angle 2°, diameter 35 mm, 0.145 mm gap) was used. Temperature was controlled at 25°C apart for the temperature dependent tests, with a Peltier system.

2.2.3.1 Apparent viscosity

To assess the rheological properties of the EPS, samples of dried polymer were dissolved in 5 mL of deionized water, and the solutions were stirred overnight at room temperature. Flow curves were obtained using a steady-state flow ramp across a shear rate range of 0.01 s^{-1} to 700 s^{-1}. Steady-state measurements were conducted for various polymer concentrations (1-24 wt.%). Additionally, the apparent viscosity of a 6 wt.% EPS solution was evaluated under various conditions, including different pH levels (3-9) and the presence of 0.01M NaCl and 0.01M HCl.

To characterize the flow behavior of EPS solutions, the Carreau model (Equation 1) was employed, where η_0 is the zero-shear rate viscosity (Pa s), λ is a time constant (s), $\dot{\gamma}$ is the shear rate (s^{-1}), η is the apparent viscosity (Pa s), n is the viscosity exponent and), η_∞ is the viscosity of the second Newtonian plateau (Pa s). Since the second Newtonian plateau was not reached during the experiments, the equation was modified by assuming η_∞ values significantly lower than η and η_0. The experimental results were then fitted to this adjusted model.

$$\eta = \eta_\infty + \frac{\eta_0 - \eta_\infty}{[1+(\lambda\dot{\gamma})^2]^{\frac{1-n}{2}}} \quad (1)$$

2.2.3.2 Oscillatory shear tests

To establish the linear viscoelastic region (LVE) of the EPS solutions, amplitude sweep tests were conducted at varying strain levels (0.01–100%, 1 Hz). Following this, the storage modulus (G') and loss modulus (G") were assessed for EPS solutions at multiple concentrations (1–24 wt.%). Frequency sweep experiments were then performed at a consistent strain within the LVE, covering a frequency range of 0.01 to 10 Hz. Furthermore, the effects of pH levels (3–9) and the addition of salts such as NaCl and HCl on both moduli were examined using a 6 wt.% EPS solution.

2.2.3.3 Effect of temperature

A 6 wt.% EPS solution was subjected to oscillatory and steady-state tests at various temperatures (0-45 °C). The temperature ramp flow analysis involved maintaining a constant shear rate of 10 s^{-1} while varying the temperature from 0 to 95 °C, with heating and cooling rates set at 6 °C min^{-1}.

2.2.4 Films

The filmogenic properties of EPS RA19, encompassing both preparation and characterization of the films, were evaluated following the methods described by Concórdio-Reis [99].

2.2.4.1 Films' preparation

Two aqueous solutions were prepared by dissolving 1.5 or 3 wt.% EPS in deionized water, under constant stirring. Sodium azide (10 mg L^{-1}) was added to the solutions to avert microbial growth. Posterior tests were performed using 3 wt.% EPS solution and adding 15 $wt._{glycerol}.wt._{polymer}^{-1}$ % glycerol as a plasticizer. The mixture was stirred until homogeneity was achieved.

Afterwards, 30mL of the solutions were cast in petri dishes with a diameter of 88 mm and left to dry in an incubator (Raypa, Spain) at 30°C for around a week. The films were then peeled from the petri dish and placed in a desiccator (Normax, Portugal), for at least 1 week, conditioned with a 53% relative humidity (RH), attained by adding a saturated solution of $Mg(NO_3)_2$. A thermohygrometer (Vaisala, Finland) was used to monitor the RH. The films' thickness was measured using a micrometer (Mitutoyo, UK), in 3 points.

2.2.4.2 Morphological Characterization

The morphology of the EPS films was examined using a Hitachi TM 3030Plus Tabletop Scanning Electron Microscope (SEM). The mounted samples were then coated with a thin layer of gold/palladium in preparation for analysis. The samples used for the cross-section were previously frozen in liquid nitrogen and broken.

2.2.4.3 Mechanical properties

Tensile tests carried out with a texture analyzer (TMS-Pro, Food Technology Corporation, England) fitted with a 250 N loading cell. Film samples were cut into rectangular strips, 15mmx50mm and 20mmx50mm. The samples were held by tensile grips and stretched with a crosshead speed of 0.5mm s^{-1} until rupture.

Young's modulus (εm, MPa), which represents the material's stiffness and resistance to deformation under tensile or compressive stress, was determined from the initial slope of the stress-strain curve within the elastic region. Elongation at break (ε, %) comparing the final length the original length. The tensile strength at break (Ƈ, MPa) was calculated by dividing the maximum force applied at failure by the initial cross-sectional area. At least three replicates of each sample were analyzed.

2.2.5 Gels

The gel forming capacity of EPS RA19 was tested as described in Concórdio-Reis *et al.* [100]. The cation-mediated gels were prepared using divalent cations ($CuSO_4{\cdot}5H_2O$, Riedel-de Haën, Sigma-Aldrich, Germany; $MgSO_4{\cdot}7H_2O$, LabChem, Portugal; $FeSO_4{\cdot}7H_2O$, AppliChem Panreac, Barcelona, Spain; $CaCl_2{\cdot}2H_2O$, AppliChem Panreac, Barcelona, Spain; $ZnCl_2$, Sigma-

Aldrich, Germany; $AgNO_3$, Fluka, Honeywell, North Carolina, United States) and a trivalent cation ($FeCl_3 \cdot 6H_2O$, Sigma-Aldrich, Germany). Primarily a 5mL solution of EPS was prepared, after which, the metal salt was added, and the solution was agitated until homogenization was achieved.

To assess the influence of polymer concentration and cation amount, subsequent tests were carried out with Fe(II) and Cu(II). Different conditions were performed using 2-8 wt.% EPS and the salts containing 10-60 mg of cation.

Gels were evaluated by visual inspection and categorized based on their strength and consistency: (+++) homogenous gels that maintained their gel structure in a tube-inversion test; (++) homogenous gels that homogeneous gels that failed to retain their structure in the tube-inversion test; (+) weak, non-homogenous gels that do not maintain their gel structure in a tube-inversion test; (-) no gel formation; and (pp) for formation of precipitate.

2.2.6 Emulsions

2.2.6.1 Preparation and characterization

The emulsification potential of the EPS was tested with, almond, paraffin and olive oil. Emulsions (5 mL in 10 mL tubes) were prepared by mixing the oils with EPS aqueous solutions (0.5–4 wt.%) in the vortex for 2 minutes. The oil and aqueous phases were weighted to obtain different O:W ratios (2:3, 3:2, 4:1, 3:1, and 2:1).

After 24h and 30 days the emulsification index (E_I, %) was calculated using Equation 2, where h_T (mm) denotes the total height of the mixture following the emulsification process, and h_e (mm) corresponds to the height of the emulsion layer.

$$E_I = \frac{h_e}{h_T} \times 100 \quad (2)$$

The emulsification stability (E_S, %) was determined by dividing the E_I measured after 30 days by the E_I measured after 24h (Equation 3).

$$E_S = \frac{Final\ E_I}{Inicial\ E_I} \times 100 \quad (3)$$

2.2.6.2 Rheological properties

The different EPS emulsions were subjected to steady-state and oscillatory tests, performed as described above (sections 2.2.3.1 and 2.2.3.2, respectively). The temperature was controlled at 25°C.

2.3 Results and Discussion

2.3.1 Characterization

2.3.1.1 Elemental Analysis

The exopolysaccharide was primarily composed of carbon (27.11 wt.%) and hydrogen (5.11%). Furthermore, the presence of nitrogen was detected in trace amounts (0.98 wt.%), likely due to the presence of amino sugar monomers. Notably a high content of sulfates, 14.58 wt.% was detected. Nevertheless, this sulfate content is still lower than the 29 wt.% originally reported in G. Raguénès et. al [96]. Sulfated polysaccharides such as Ulvan, with a sulfate content of 2.3-40 wt.%, are comparable to the degree of sulfation of EPS RA19. Conversely, carrageenan and fucoidan present higher degrees of sulfation, at 25-39% and 20-30%, respectively. Several bacterial species are also known to produce EPS with lower degrees of sulfation, Including *Alteromonas*, with a sulfation degree of 2.0-3.4 wt.% [100], *Enterobacter cloacae*, which produces EPS71a with a sulfation degree of 7 wt.% [17], and *Labrenzia* sp. PRIM-30, which has a sulfate content of 4.76 wt.% [101].

2.3.1.2 EPS composition

EPS RA19 is a heteropolysaccharide composed of neutral monomers, glucose, galactose, fucose, and rhamnose, the amino sugar glucosamine and simple sugar acids, glucuronic acid and galacturonic acid (Table 2). Galactose and rhamnose are the main neutral sugars with 34.42 mol% and 23.64 mol%, respectively, followed by fucose with 22.10 mol%. The content of uronic acids is relatively low, 5.31 mol% compared to the published for the same polysaccharide [96]. However, in contrast to the results found by G. Raguénès et. al. [96], this batch presents two different uronic acids, instead of only glucuronic acid. Another discovery is the presence of glucosamine, which was not previously reported by G. Raguénès et. al [96]. This discovery is further supported by the nitrogen content determined through elemental analysis.

Table 2. Monosaccharide composition of EPS RA19 (Fuc, L-fucose; Gal, galactose; GalA, galacturonic acid; GlcN, glucosamine; Glc, glucose; Rha, rhamnose; N/A, not applicable)

EPS RA19	Monosaccharide composition (mol%)						
Reference	Fuc	Gal	GalA	GlcN	Glc	GlcA	Rha
This study	22.10± 2.51	34.42 ± 5.56	4.64 ± 0.31	1.28 ± 0.16	13.25 ± 2.95	0.67 ± 0.04	23.64 ± 2.41
[96]	14.7	11.7	2.9	N/A	4.4	N/A	12.4

2.3.1.3 Molecular mass distribution

The molecular mass distribution analysis demonstrated that the polysaccharide possesses a relatively high average molecular weight (Mw) of 1.06 ± 0.07 x10^6 Da with a polydispersity index of 1.11 ± 0.02, indicative of homogeneity. This molecular weight is slightly lower than the previously reported value for the same EPS, which was 3.2 x10^6 Da [96]. Nonetheless, the value obtained is within range for exopolysaccharides, which typically exhibit high molecular weights. For example, the fucose-rich EPS FucoPol has a molecular weight of 5.8 x 10^6 Da, while xanthan gum and gellan gum range from 0.4 to 15 x 10^6 Da and 0.24 to 2.2 x 10^6 Da, respectively [7,79].

2.3.1.4 Fourier transform infrared spectroscopy

The FTIR spectrum of the EPS RA19 (Figure 1) presented a broad band past 3000cm^{-1}, resulting from an O-H stretching vibration, along with a characteristic vibration of a C-H stretching between 2850-2960cm^{-1}. Moreover, the spectrum expresses an intense peak at 1634.7cm^{-1}, singular to uronic acids C=O. Comparatively to the spectrum published by G. Raguénès *et al.* [96] the peak is less intense, probably related to fewer uronic acid monomers in the polysaccharide chain than previously reported, which is further established by the findings of the EPS composition. Additionally, the presence of an intense peak at 1212.0cm^{-1} indicates the presence of ester sulfates linked to the polysaccharide. This peak is also less intense than previously reported, consistent with the findings in section 2.3.1.2.

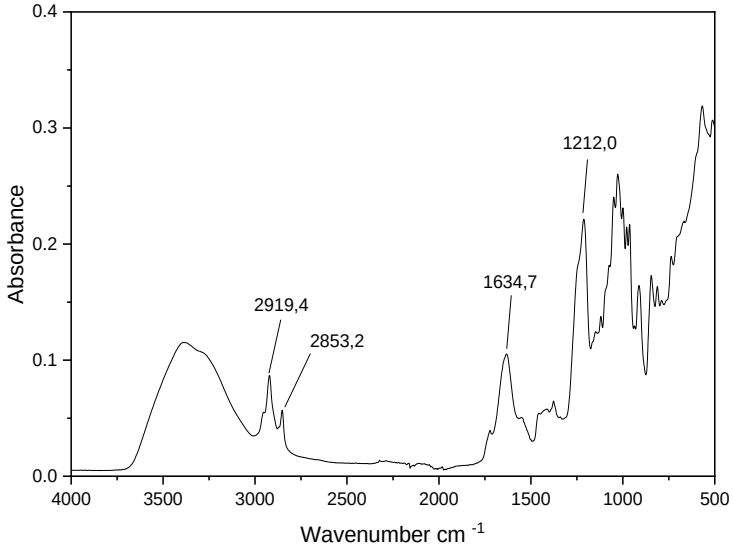

Figure 1. FTIR spectra of EPS RA19

2.3.1.5 Thermogravimetric analysis

Thermal degradation of polysaccharides usually occurs in three phases. In the first phase, with the increase of temperature from 35 to 140ºC a decrease of 15.0% of weight was registered, this happens due to moisture loss [100]. The second phase showed a weight loss of 15.5%, which occurred between 140 and 203 ºC, and was related to the decomposition of the side chains [100]. The highest weight loss was registered on the third phase (201-491ºC), with a decrease of 30.3% in weight concomitant with the scission of the main chain of the polysaccharide [100]. The high percentage of char (45.8%) might be related to the high amount of inorganic content [100]. The degradation temperature (T_{deg}) was found to be 184.6ºC, marked by a significant weight loss at this temperature. Although this value is relatively low, it falls within the reported range for other microbial EPS (130–300 ºC) [100,102,103]. This low degradation temperature is attributed to the high sulfur content, promoting desulfation, which requires less energy than water elimination, and in return the sulfuric acid, which can only be decomposed or volatilized at temperatures above 380ºC, aids in acid-catalyzed dehydration, thereby lowering the thermal stability [104].

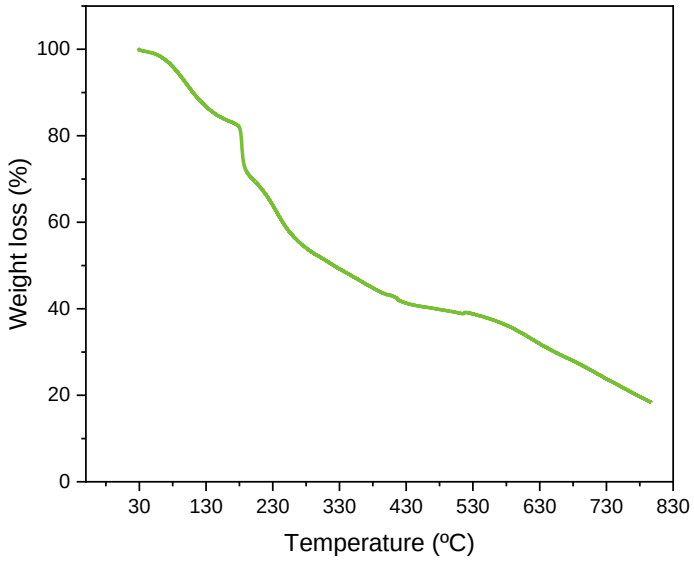

Figure 2. Thermogravimetric analysis curves of EPS RA19

2.3.2 Rheological characterization

Understanding the rheological properties of EPS is crucial for predicting their behavior under varying environmental conditions like pH, temperature, and ionic strength, which directly affect their flow and structural characteristics. These properties are essential for determining

the suitability of EPS in industries such as cosmetics, pharmaceuticals, and food, where stability and viscosity are often required, even at low concentrations [105]. Therefore, optimizing EPS rheological behavior is critical to ensuring their functionality across diverse industrial applications.

2.3.2.1 Rheological properties in aqueous medium

The viscosity of fucose containing sulfated EPS RA19 was assessed over a range of concentrations. The flow curves obtained for the different concentrations ranging from 1–24 wt.% are presented in Figure 3. At all tested concentrations, the EPS solutions behaved as a non-Newtonian liquid with shear thinning or pseudoplastic behavior, characterized by a progressive decrease of viscosity with the increase of shear rate, which has been frequently reported for other EPS [21,36,38,100].

As the shear rate increases, this behavior is defined by microstructural rearrangements that lead to the disruption of molecular interactions, which include entanglements, as well as electrostatic, hydrophobic, and hydrogen bonding interactions. [98]. At low shear rates, polysaccharide chains form entangled aggregates, leading to high viscosity due to increased resistance [98]. As shear rate increases, these interactions are disrupted, causing alignment of polymer molecules in the direction of flow, which results in a reduction in viscosity, as illustrated in Figure 3 [98,106].

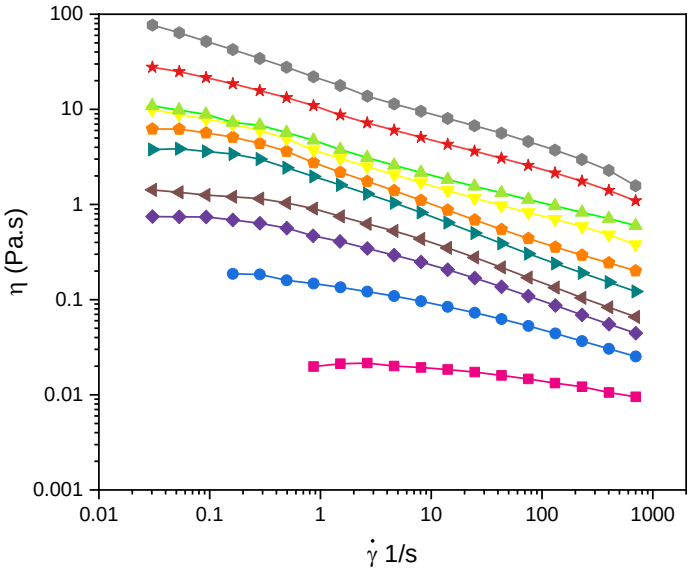

Figure 3. Apparent viscosity (η) plotted as a function of shear rate ($\dot{\gamma}$) for several EPS concentrations: 1 wt.% (■); 2 wt.% (●); 3 wt.% (◆); 4 wt.% (◀); 6 wt.% (▶); 8 wt.% (⬟); 10 wt.% (▼); 14 wt.% (▲); 20 wt.% (★); and 24 wt.% (⬢).

The flow curves (Figure 3) for concentrations exceeding 1 wt.% were evaluated using the Carreau model, with the estimated parameters detailed in Table 3. The findings indicated that as the EPS concentration rose from 1 to 24 wt.%, the zero shear viscosity (η_0) rose significantly from 0.021 to 21.7 Pa s. This is due to the exponential rise in viscosity with increasing polymer concentration, caused by the greater entanglement of macromolecules. At higher concentrations, polysaccharide molecules are closer together, leading to more interactions and the formation of entangled aggregates, which increases flow resistance and, in turn, viscosity [98,107]. Moreover, the time constant also increased from 0.142 to 1.506 s with EPS concentration, indicating longer relaxation times as more entanglements between the biopolymer molecules form and new interactions develop more slowly. Consequently, the transition from Newtonian to shear-thinning behavior shifted to lower shear rates [98,105].

Table 3. Parameters of the Carreau model were estimated for various EPS concentrations, and 6 wt.% EPS under different pH and different temperatures.

EPS (wt.%)	pH	Temperature (°C)	η_0 (Pa s)	λ (s)	n	R^2	MRE [a] (%)
1	7	25	0.021	0.142	0.839	0.992	1.499
2			0.141	0.418	0.711	0.998	2.021
3			0.455	0.575	0.617	0.998	2.112
4			0.853	0.598	0.576	0.999	1.260
6			1.754	0.634	0.555	0.997	1.595
8			2.745	1.130	0.592	0.998	2.418
10			3.506	1.139	0.676	0.996	1.953
14			4.354	1.360	0.710	0.995	1.850
20			11.215	1.467	0.683	0.999	1.567
24			21.700	1.506	0.654	0.995	2.947
6	3	25	1.714	2.741	0.497	0.996	2.316
	5		0.201	0.944	0.743	0.999	0.406
	9		0.081	0.599	0.796	0.988	0.711
6	7	0	6.440	1.909	0.489	1.000	0.030
		15	3.803	1.754	0.535	1.000	0.202
		35	2.590	1.696	0.572	1.000	0.246
		45	1.820	1.694	0.600	1.000	0.509

[a] $\mathrm{MRE} = \frac{\sum_{i=1}^{j} \left| \frac{(x_{\mathrm{exp\ i}} - x_{\mathrm{model\ i}})}{x_{\mathrm{exp\ i}}} \right|}{j} \times 100$

Figure 4 illustrates the effect of polymer concentration (1–24%) on both the storage modulus (G') and the loss modulus (G''). The storage modulus (G') represents the material's

elastic behavior, indicating its ability to store energy, while the loss modulus (G'') reflects the viscous contribution, indicating energy loss [98].

The EPS solution displayed liquid-like behavior, characterized by G'' higher than G', showing no ability to form a gel network in the dilute regime. At certain concentrations, above 1 wt.% EPS, G' increased at faster rates than G'' as the frequency rose, suggesting that EPS RA19 behaves as a viscoelastic fluid [108]. This trend suggests that this EPS may be suitable for use as a thickener [109]. Similar behavior has been reported for EPS produced by *Clavibacter michiganensis* [108], composed of L-fucose, D-galactose, and D-glucose 2:1:1 molar ratio and a molecular weight of 1.09×10^6 Da. The frequency sweeps at various concentrations showed G'' exceeding G', reflecting liquid-like behavior, while the frequency dependence of G′ became more pronounced than that of G'' as EPS concentration increased. To better understand the changes in the distance between G' and G'' across different concentrations, further tests need to be conducted.

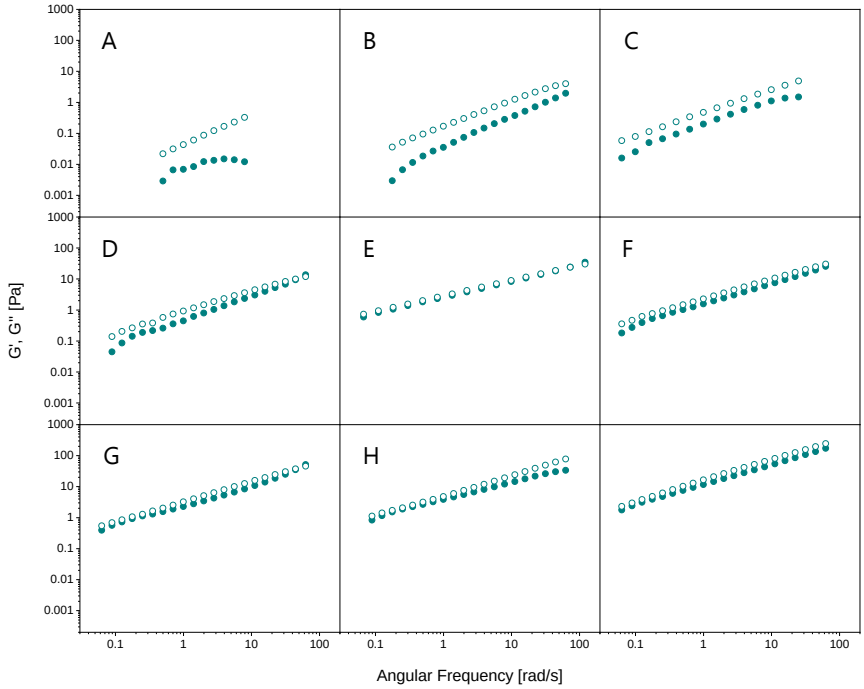

Figure 4. Storage modulus G′ (●) and loss modulus G′′ (○) as functions of angular frequency for the aqueous solutions of EPS RA19 at various concentrations: (A) 1 wt.%; (B) 2 wt.%; (C) 3 wt.%; (D) 4 wt.%; (E) 6 wt.%; (F) 8 wt.%; (G) 10 wt.%; (H) 14 wt.%; (I) 20 wt.%.

2.3.2.2 Effect of temperature

Temperature has a significant impact on the rheology of EPS by affecting both intra- and intermolecular hydrogen bonds as well as the movement of molecular chains. Changes in temperature can lead to new interactions within the polymers, resulting in the formation of

aggregates or gel-like structures [98,110]. The effect of temperature (from 0 to 45°C) on the viscosity of a 6 wt.% EPS RA19 solution was assessed, with the resulting flow curves illustrated in Figure 5A and the corresponding parameters from the fitted Carreau model provided in Table 3.

As the temperature increased from 0 to 45°C, the apparent viscosity of the solution decreased, while the shear-thinning behavior remained consistent. Higher temperatures also caused the transition from the Newtonian to the shear-thinning regime to occur at higher shear rates, indicating faster formation of new interactions at elevated temperatures [98]. This is because polymer entanglement and network formation rely on hydrogen bonding interactions and Van der Waals forces, which are weakened as thermal motion increases at higher temperatures. As a result, molecular movement becomes easier, reducing intermolecular entanglements and lowering the solution's viscosity [98,110]. This trend is reflected in the Carreau model parameters (Table 3), where the zero-shear viscosity (η_0) dropped from 6.440 to 1.820 Pa s, and a reduction in relaxation time (λ) from 1.909 to 1.694 seconds as the temperature rose from 0 to 45°C. Similar results have been reported, EPS Mo169 maintained its shear thinning behavior at temperatures up to 95°C [98], EPS obtained from *Leuconostoc citreum*-BMS strain was able to retain its entangled structure at temperatures between 25 and 45°C [109]. Similarly, Levan produced from *Bacillus mojavensis* was able to maintain its entangled structure at 40 and 50°C [111].

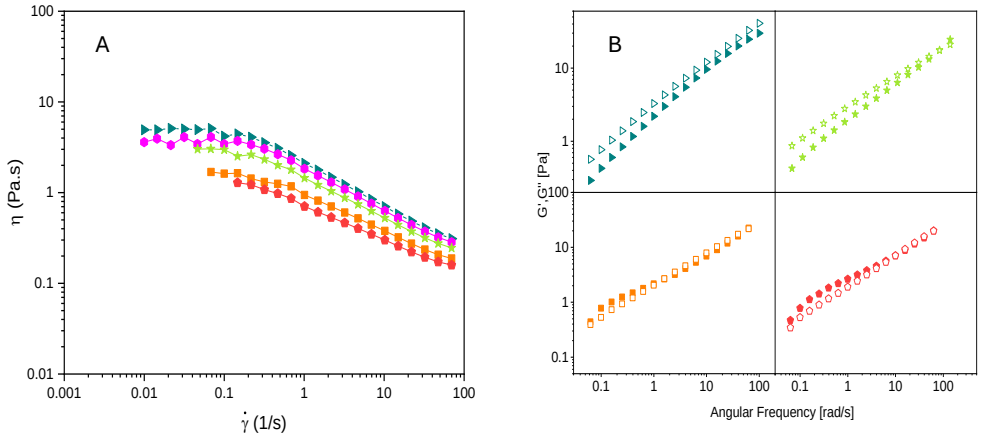

Figure 5. Apparent viscosity and oscillatory shear stress test for a gradient of temperatures. (A) Apparent viscosity (η) as a function of shear rate ($\dot{\gamma}$) for diverse EPS concentrations under various temperatures: 0°C (▶); 5 °C (●); 15 °C (★); 35 °C (■); 45 °C (⬟). (B) Storage modulus G′ (solid symbols) and loss modulus G′′ (open symbols) as functions of angular frequency.

The effect of temperature (0-45ºC) on both the storage modulus and the loss modulus, is illustrated in Figure 5B. Between 0 and 5ºC, G'' consistently exceeded G' across all frequencies, indicating that the polymer solution retained its liquid-like properties. At higher temperatures, above 35ºC, G' surpassed G'' at low frequencies, suggesting a solid-like behavior. However, with increasing frequency, G'' quickly became dominant again, pointing to the loss of this structure and a return to liquid-like behavior. The decrease in viscous modulus with rising temperature aligns with the previously observed reduction in viscosity under similar conditions. Similarly, Han, Du *et al.* [112] studied the effect of temperature on the viscosity of EPS produced by *Sporidiobolus pararoseus* JD-2 and observed that increasing the temperature from 10 to 80ºC resulted in a decrease in G''.

2.3.2.3 Effect of pH

The influence of pH on the viscosity of EPS RA19 at 6 wt.% was analyzed, with viscosity measurements recorded at four different pH values, 3, 5, 7, and 9. The EPS exhibited its highest viscosity at neutral pH (7), with an estimated zero-shear viscosity (η_0) of 1.754 Pa s, suggesting that under neutral conditions, the polymer achieves optimal intermolecular interactions and chain entanglement, resulting in enhanced resistance to flow. In contrast, the lowest viscosity was observed at pH 9, where the estimated η_0 was 0.081 Pa s. The reduced viscosity under alkaline conditions may be attributed to a decrease in intermolecular associations, reducing repulsion, which likely affects the hydrodynamic volume of the EPS molecules, reducing their effective size and viscosity. It has been reported that hydrogen bonds may be weakened by hydroxyl groups [112,98].

At pH 3 and pH 5, the sulfate and uronic acid groups play a crucial role in determining the viscosity of the EPS. Sulfate groups, which have a pKa of -3 and 2, remain deprotonated at both pH levels, contributing to the overall negative charge of the polymer. However, the uronic acids behave differently, glucuronic acid has a pKa of 3.28 [114], and, similarly, galacturonic acid has a pKa of 3.51 [114]. These are protonated at pH 3, while at pH 5, they are deprotonated. The deprotonation of the carboxyl groups in the uronic acids at pH 5 introduces additional negative charges, which, in conjunction with the already deprotonated sulfate groups, results in increased electrostatic repulsion.

As repulsion increases, the EPS chains adopt a more expanded conformation, reducing entanglements and facilitating molecular movement, which results in decreased viscosity. This behavior aligns with the findings observed at pH 5 [98].

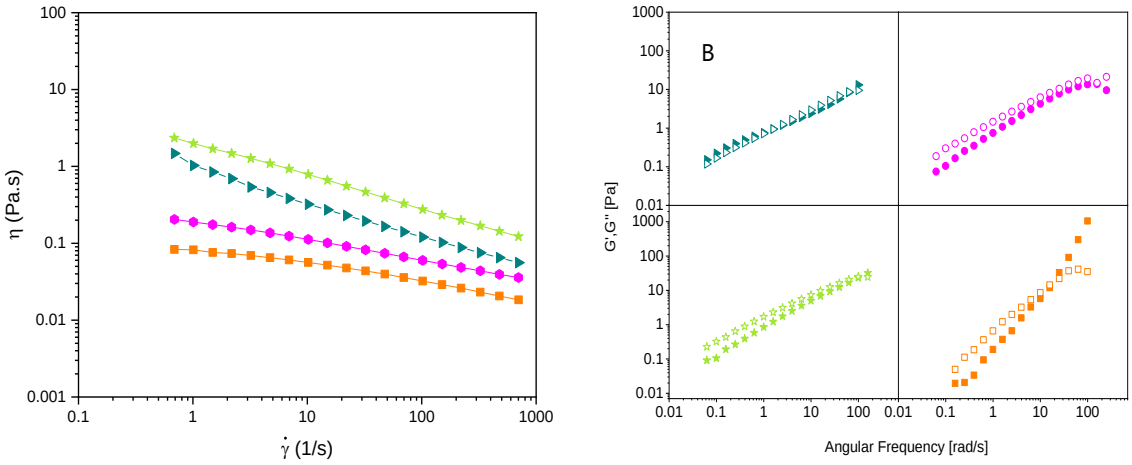

Figure 6. Apparent viscosity and oscillatory shear stress test for different pH levels. (A) Apparent viscosity (η) as a function of shear rate ($\dot{\gamma}$) for diverse EPS concentrations under various pH value: pH 3 (▶); pH 5 (●); pH 7 (★); pH 9 (■). (B) Storage modulus G′ (solid symbols) and loss modulus G′′ (open symbols) as functions of angular frequency.

Figure 6B illustrates the effect of pH on both the storage and loss moduli. Across all pH conditions tested, G'' remained higher than G', indicating that the EPS retained its liquid-like characteristics, showing minimal impact from pH variations. This suggests that the EPS was not significantly altered by changes in pH.

Polysaccharides generally exhibit notable pH-dependent behavior in their viscoelastic properties, particularly at extreme values (below pH 4 and above pH 10) [98]. For example, the EPS produced by *Alteromonas macleodii* Mo 169 maintained a weak gel-like structure at pH 5 but lost this structure at pH 3 and pH 9 [98]. Conversely, as reported by Y. Abid *et al.* [109], the EPS produced by *Leuconostoc citreum* was largely unaffected by pH changes, maintaining a liquid-like behavior, similar to the results observed in this study.

2.3.3 Films

To ensure EPS films are suitable for practical applications, it is important to assess their mechanical properties, as these influence the material's overall performance. Whether used in bio-adhesives, wound dressings, or packaging, the strength, flexibility, and barrier properties of the films must be balanced to meet the demands of each application [13,115,116].

2.3.3.1 Morphological characterization

Glycerol is a commonly used plasticizer that improves the flexibility and elasticity of films by reducing intermolecular forces between polymer chains [99]. It acts as a softening agent, allowing the material to retain moisture and preventing cracks. This results in smoother, more

uniform films with enhanced mechanical properties, such as better tensile strength and flexibility, making them more suitable for applications requiring durability and homogeneity [117].

The filmogenic properties of EPS R19 were initially tested using 1.5 wt.% and 3 wt.% concentrations. Images of the films formed are shown in Figure A1. The film formed with 1.5 wt.% EPS was more fragile, and brittle compared to the one formed with 3 wt.% EPS. Similar findings were observed with kefiran-based films, where an increase in polymer concentration led to greater film thickness [118]. Therefore, further testing was conducted using 3 wt.% EPS. in Figure 7, films formed by 3% EPS RA19 with and without glycerol are shown in panels A and B, respectively. The further left panel shows that both films are opaque; however, there are noticeable differences in their texture. The film without glycerol (Figure 7A) has a more uneven and rough surface, whereas the film formed with glycerol (Figure 7B) is smoother. These observations are further supported by the SEM images. The top-view (center panels) and cross-section (right panel) SEM of the film without glycerol highlights surface irregularities, while the film with glycerol appears more compact and homogeneous. Nevertheless, even without glycerol, the film shows good structural integrity and homogeneity, although its mechanical properties are likely inferior to the film that contains glycerol. J. Piermaria *et al.* reported that incorporating glycerol as a plasticizer resulted in films with more compact structures and a smoother appearance [118].

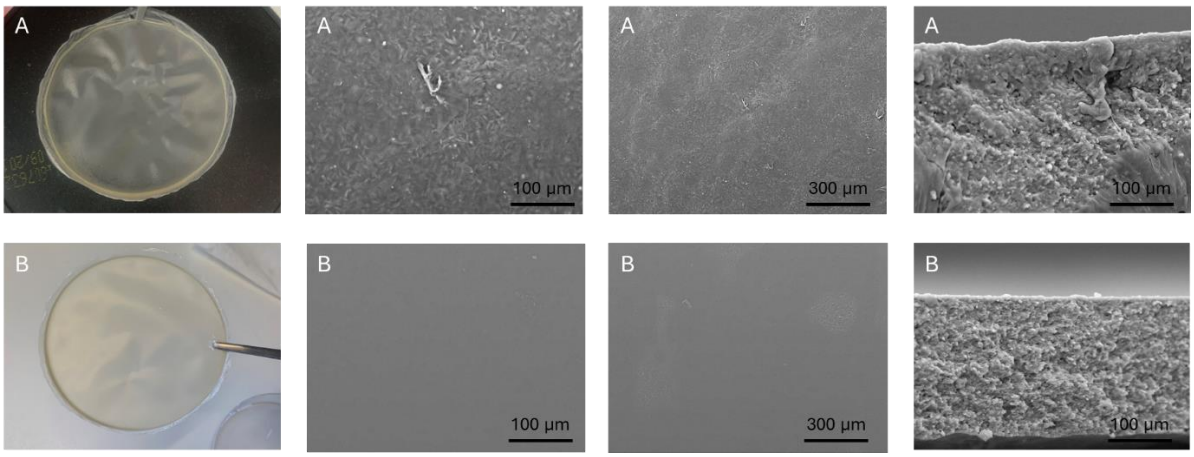

Figure 7. Photographs of the films 3wt.% EPS RA19 without glycerol (A) and with glycerol (B) are presented in the far left panel. SEM images: top view at ×250 magnification (left panel), top view at ×1000 magnification (center panel) and cross section view at ×250 magnification (right panel).

2.3.3.2 Mechanical properties

Tensile tests were conducted on films formulated with 3 wt.% EPS, both with and without the addition of glycerol, and the mechanical properties obtained are summarized in Table 4. Young's modulus indicates the material's stiffness, offering insights into how the film's

flexibility and mechanical properties relate to its chemical composition [116]. Elongation at break is the increase in film length (%) before breakage and tensile strength is the maximum stress a film can withstand before breaking [115].

The film without glycerol was brittle and rigid since it showed high Young's modulus and tensile strength values and low deformation at break ones, 1.65±0.21 MPa, 13.57±0.97 MPa and 5.56±1.82 %, respectively. Comparatively, glycerol improved the flexibility of the film, characterized by a decrease of Young's modulus and tensile strength, and an increase in elongation at break, 1.50±0.28 MPa, 12.65±1.24 MPa and 14.41±1.87 %, respectively. This behavior results from glycerol reducing intermolecular forces between polymer chains as well as supporting the formation of H-bonds between glycerol and EPS molecules which increases the free volume and the molecular mobility of the polymer [119].

Table 4. Mechanical properties for films prepared with EPS RA19 with and without alongside reference values from literature (Ƈ, Tensile Strength at break; ε, Elongation at break; εm, Young's Modulus)

EPS	Plasticizer ($wt._{glycerol}.wt._{polymer}^{-1}$ %)	Mechanical Properties			Reference
		Ƈ (MPa)	ε (%)	εm (MPa)	
RA19	-	13.57±0.97	5.56±1.82	165±21.2	This study
	15	12.65±1.24	14.41± 1.87	150±28.3	This study
Kefiran	-	40.92	2.70	N/A	[118]
	15	15.15	116.69	N/A	
Chitosan	-	31.13	10.60	N/A	[117]
Chitosan	15	41.6	24.7	1193	[120]
Chitosan with *Alteromonas* sp. EPS		39.5-42.7	16.6-23.7	1008-1186	
Alteromonas EPS A	60	4.55	47.0	10	[99]
Alteromonas EPS B-F	30	10.8-23.6	2.8-37.7	65-1100	
FucoPol	30	3.1	54.9	2.8	[121]
Alginate and Pectin	50	22.5-42.3	5.9-14.9	N/A	[122]
Pectin	5	4.99-6.91	45.8-523	N/A	[123]

Comparing films is challenging due to the numerous variables affecting their mechanical behavior, such as differences in polymer chemical composition, molecular weight, and preparation methods, including polymer concentration and the type and amount of plasticizer used, as well as relative humidity at which films are conditioned [99]. Increasing the plasticizer content helps reduce interactions between polymer chains and enhances molecular mobility, resulting in more flexible films [124]. The choice of plasticizer is also crucial, as different plasticizers affect EPS behavior in various ways, particularly based on their molecular weight. Low

molecular weight plasticizers tend to promote stronger interactions among EPS chains, leading to improved mechanical properties [124]. Additionally, higher relative humidity directly impacts film elasticity, with water acting as a plasticizer in hydrophilic films, especially in plasticized films, as non-plasticized films show little tendency to absorb water [125].

Nevertheless, the values of Ƈ, ε, and εm for the films prepared in this study fall within the ranges reported for various polysaccharide-based films: 3.10–42.7 MPa, 2.70–116.69 %, and 2.8–1193 MPa, respectively (Table 4).

2.3.4 Gels

EPS are particularly effective at crosslinking with heavy metals due to their high content of uronic acids, sulfates, and other ionizable groups, which facilitate strong interactions with cations such as Mg^{2+}, Cu^{2+}, Zn^{2+}, Fe^{2+}, Ca^{2+}, and Fe^{3+}. These interactions enhance the stability and performance of hydrogels. The use of these cations as crosslinkers also imparts valuable biological properties to the gels. For instance, Fe^{2+} offers antibacterial [126] and anti-inflammatory effects [127] while promoting cell proliferation [128]; Fe^{3+} provides stimuli-responsive capabilities, redox properties, and photosensitivity [129]; and Cu^{2+} contributes antimicrobial activity and prothrombotic effects by promoting coagulation and platelet activation [130]. As a result, these cation-mediated gels show great potential for applications in wound healing and tissue engineering.

2.3.4.1 Screening for cations

The gelation ability of the polymer was evaluated in the presence of various cations, including divalent ions (Fe^{2+}, Cu^{2+}, Ca^{2+}, Ag^{2+}, Zn^{2+}, Mg^{2+}) and the trivalent ion Fe^{3+}, under both alkaline and neutral conditions (Table 5). Images of gels formed with 1 wt.% EPS under alkaline and standard conditions, as well as gels formed with 0.5 wt.% EPS under alkaline conditions, are presented in Appendix (Figure A2). Gel formation was assessed based on strength and homogeneity, using the following criteria: (+++) homogeneous gels that retained their structure in a tube-inversion test; (++) homogeneous gels that did not retain their structure in the tube-inversion test; (+) weak, non-homogeneous gels that did not retain their structure; (-) no gel formation; and (pp) indicating the formation of a precipitate.

As presented in Table 5, under standard conditions, only Fe^{3+} led to precipitate formation for both polymer concentrations, with no gel formation observed. Under alkaline conditions, EPS RA19 was able to form gels with Cu^{2+} at 0.5 wt.% and with Fe^{2+}, Fe^{3+}, and Cu^{2+} at 1 wt.%. Alkaline conditions appeared to enhance gelation, which was expected since higher pH values

increase the number of ionized carboxyl groups. This raises the total number of COO^- groups in the molecular chain, providing more crosslinking points. As a result, both the strength and the rate of gel formation are improved [131].

Table 5. The formation of gels under both standard and alkaline conditions was assessed by examining their strength and homogeneity: (++) homogenous gels that do not maintain their gel structure in a tube-inversion test; (+) weak, non-homogenous gels that do not maintain their gel structure in a tube-inversion test; (-) no gel formation; and (pp) for formation of precipitate.

EPS (wt.%)	Salt	Salt concentration (mg ml^{-1})	Deionized water	NaOH (2 M)
0.5	$FeSO_4$	10	(-)	(-)
	$CaCl_2$		(-)	(-)
	$AgNO_3$		(-)	(-)
	$FeCl_3$		pp	(-)
	$ZnCl_2$		(-)	(-)
	$MgSO_4$		(-)	(-)
	$CuSO_4$		(-)	(+)
1	$FeSO_4$		(-)	(+)
	$CaCl_2$		(-)	(-)
	$AgNO_3$		(-)	(-)
	$FeCl_3$		pp	(+)
	$ZnCl_2$		(-)	(-)
	$MgSO_4$		(-)	(-)
	$CuSO_4$		(-)	(+)

Previous studies on EPS RA19 concluded that it has a strong affinity for both copper and iron, consistent with the findings of this study [132]. This affinity can be attributed to the ionizable groups present in the polymer chain, such as carboxyl groups from uronic acids and sulfate groups [132]. It has been hypothesized that hydroxyl groups present in the backbone of EPS RA19 might be involved in chelation of divalent ions, while, the sulfate groups are known to uptake trivalent ions [132].

EPS synthesized by *Alteromonas* strains isolated from French Polynesia demonstrated a strong affinity for divalent ions, including Ca^{2+}, Mg^{2+}, Fe^{2+}, and Cu^{2+}. EPS A and C, which are richest in galactose, were able to form gels with Fe^{2+} under standard conditions. EPS B formed gels with Cu^{2+} under alkaline conditions, likely due to its high uronic acid content [100].

Similarly, fucose-rich FucoPol exhibited excellent metal-binding capacity, forming gels with Fe^{3+} under standard conditions and with Cu^{2+} under alkaline conditions [22,49].

2.3.4.2 Effect of cation concentration

Given the ability of EPS RA19 to form gels with Fe^{3+}, Fe^{2+}, and Cu^{2+} under alkaline conditions, the effect of these cations at varying concentrations was examined under standard conditions. As shown in Table 6, the concentration of Fe^{3+} did not impact the gelling ability of EPS, as no gels were formed with this cation. In contrast, both divalent cations formed homogeneous gels with EPS RA19. For Fe^{2+}, increasing the salt concentration resulted in stronger gels, as higher concentrations provided more ions to bond with ionizable groups in the polymer chain (Figure 8). Conversely, no correlation was observed between salt concentration and gel strength for Cu^{2+}. Additionally, all gels formed with copper gradually lost their integrity over time, likely due to weaker crosslinking bonds, suggesting that the gel structure was not stable.

Table 6. Optimization of gel formation under standard conditions was evaluated based on their strength and homogeneity: (+++) homogenous gels that maintained their gel structure in a tube-inversion test; (++) homogenous gels that do not maintain their gel structure in a tube-inversion test; (+) weak, non-homogenous gels that do not maintain their gel structure in a tube-inversion test; (-) no gel formation.

EPS (wt.%)	Salt	Salt concentration (mg ml^{-1})	Standard condition
2	$FeSO_4$	10	(+)
		40	(+++)
		60	(+++)
4		20	(++)
		40	(+++)
		60	(+++)
2	$CuSO_4$	10	(+)
		40	(+)
		60	(+)
4		20	(++)
		40	(++)
		60	(++)
2	$FeCl_3$	20	(-)
		40	(-)
		60	(-)

The gelling ability of κ-carrageenan improved with increasing salt concentration (Ca^{2+}), as this enhanced the formation of gel networks [133]. Similarly, a study on EPS Mo169 demonstrated that increasing both polymer and cation concentrations, which raises crosslinking density, resulted in stronger and more compact gels [134].

2.3.4.3 Effect of EPS concentration

The effect of EPS concentration was assessed within the range of 2-4 wt.% (Table 6). Increasing the EPS concentration from 1 wt.% (Table 5) to 2 wt.% did not influence gel formation with Fe^{3+}, as no gels were observed at either concentration. In contrast, for Fe^{2+}, gel formation was initiated at 2 wt.%, with further increases up to 4 wt.% resulting in enhanced gel strength and homogeneity, particularly at lower ion concentrations (Figure 8). Similarly, for Cu^{2+}, gels formed at 2 wt.%, and increasing the EPS concentration to 4 wt.% further improved both the strength and uniformity of the gels across all cation concentrations. The enhancement in gel strength with increasing polymer concentration is likely due to the greater availability of anionic groups, which enables cations to form additional bonds, thereby increasing crosslinking density [134]. Similarly, increasing the concentration of EPS Mo169 resulted in the formation of stronger and more compact gels with Fe(III) [134]. Additionally, studies on FucoPol support these findings, as higher polymer concentrations also led to increased gel strength with Fe(III) [22].

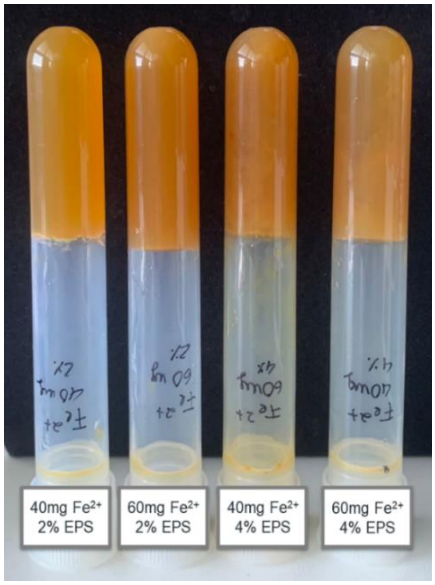

Figure 8. Optimization of iron (Fe^{2+}) concentration and EPS content. Test tubes showing varying concentrations of Fe^{2+} (40 mg and 60 mg) and EPS (2% and 4%).

The findings indicate that Fe^{2+} is the most promising crosslinker for forming stable gels with EPS RA19, demonstrating superior gelling capacity and stability compared to Cu^{2+} and Fe^{3+}. This makes Fe^{2+}-crosslinked gels particularly well-suited for applications such as drug delivery and tissue engineering, where gel strength and stability are crucial for optimal performance.

2.3.5 Emulsions

2.3.5.1 Preparation and characterization

Three different oil phases were used to prepare emulsions with EPS RA19, paraffin oil, olive oil, and almond oil, which are commonly used in cosmetic applications. Paraffin oil, a derivative of petroleum is commonly used for its occlusive properties, which help to lock in moisture and its ability to regulate viscosity in cosmetic formulations [135]. Olive oil, known for its rich composition of fatty acids, antioxidants, and vitamins, is highly valued for its nourishing, anti-inflammatory effects on the skin [136]. Almond oil, abundant in vitamins and essential fatty acids, is frequently incorporated into cosmetics for its moisturizing, emollient, and skin-restructuring effects [137]. By combining these oils with EPS as emulsifiers, formulations can be enhanced in both stability and skin benefits, supporting a growing trend toward natural and multifunctional cosmetic products.

The emulsification assays were conducted by mixing the EPS at a concentration of 0.5 wt.% with oil phases in two different ratios, 2:3 and 3:2, using paraffin, olive oil, and almond oil (Table 7). The results for the 2:3 ratio showed no significant differences in the emulsification index (E_I), with all emulsions displaying an E_I above 50%, which is considered the threshold for an effective emulsifier after 24 hours of formation [109]. However, for the 3:2 ratio, there was a clear distinction between the oils. The emulsion with paraffin exhibited the highest E_I at 78.9±1.6% (Figure 9), while those with almond and olive oil showed much lower values of 17.1±1.6% and 18.6±0.0%, respectively (Figure A3). All emulsions demonstrated excellent stability over a 30-day period. Nonetheless, the emulsion with almond oil at the 3:2 ratio not only had a low emulsification index but also displayed reduced stability compared to the others, leading to its exclusion from subsequent experiments.

Table 7. Emulsification activity was assessed at 24 h ($E_{I\ (24h)}$), and 30 days ($E_{I\ (30days)}$) along with the stability of emulsions (E_S) stabilized with EPS RA19. Data are shown as the average±standard deviation (SD) (n = 2). N/A, not applicable.

wt.%	(O:W)	Oil Phase	$E_{I\ (24h)}$	$E_{I\ (30days)}$	E_S
0.5	2:3	Paraffin	53.41±1.61	50.00±1.64	93.62±0.04
		Almond oil	53.66±1.85	52.33±1.34	97.52±0.05
		Olive oil	51.19±1.68	51.16±0.00	99.95±0.03
	3:2	Paraffin	78.89±1.57	76.92±1.20	97.51±0.02
		Almond oil	17.05±1.61	14.61±1.61	85.69±0.12
		Olive oil	18.60±3.29	18.39±3.26	98.85±0.25
1	2:3	Paraffin	55.68±1.61	46.59±1.61	83.67±0.04
		Olive oil	56.47±0.94	51.72±1.83	91.59±0.04
	3:2	Paraffin	80.00±6.29	79.35±5.22	99.18±0.10
		Olive oil	56.82±16.07	50.56±7.99	88.99±0.29
	4:1	Paraffin	12.12±4.75	N/A	N/A
	3:1		9.63±1.48	N/A	N/A
	2:1		18.82±6.45	N/A	N/A
2	3:2	Paraffin	63.33±4.71	62.22	98.25
4			37.78±3.14	35.56	94.12
6			58.89±4.71	55.56	94.34
8			41.11±1.57	40.00	97.30

The same ratios were evaluated using 1 wt.% of EPS with paraffin and olive oil as the oil phases. While the emulsification index for paraffin-based emulsions increased, the change was not as pronounced compared to olive oil-based emulsions, which saw a significant rise from 18.6±0.0% to 56.8±0.0%. Emulsification stability remained high across all formulations. However, due to the superior performance of paraffin, particularly in terms of emulsification index and overall stability, subsequent tests focused exclusively on this oil phase. The high emulsification index is likely due to the presence of uronic acids and deoxysugars like fucose and rhamnose in the EPS, which render it lipophilicity, facilitating adsorption at the oil-water interface, lowering interfacial tension, and promoting the formation of stable droplets [138,139].

Given that the emulsification index increased with a higher oil phase content, additional ratios with increased paraffin levels (4:1, 3:1, and 2:1) were tested. Surprisingly, these ratios

resulted in a significantly lower emulsification index, ranging from 9.6% to 18.8%, compared to the 3:2 ratio. This decrease may be due to reaching a critical volume fraction, where the system undergoes either phase inversion (shifting from O:W to W:O) or complete breakdown, leading to phase separation [140].

To assess the influence of EPS concentration on emulsification behavior, a range of concentrations from 2 to 8 wt.% was tested at a constant O:W ratio of 3:2. The results indicated no clear correlation between EPS concentration and the emulsification index at either 24 hours or 30 days. However, the emulsion with 1 wt.% EPS consistently demonstrated the highest emulsification index overall, being, therefore, the optimal concentration of polymer. This is in line with findings by Jiang *et al.* [31], who reported that beyond 1 mg mL^{-1} of EPS E8, further increases in polymer concentration did not affect the emulsification activity. Similarly, Kavitake *et al.* [141] found no consistent trend between EPS concentration and emulsion activity beyond 0.75 wt.% EPS. This stabilization of the emulsification index at higher polymer concentrations is likely due to saturation adsorption, where the emulsifier exceeds the amount needed to fully cover the droplet surfaces, leaving excess EPS in the continuous phase (water) without stabilizing additional droplets [140,142].

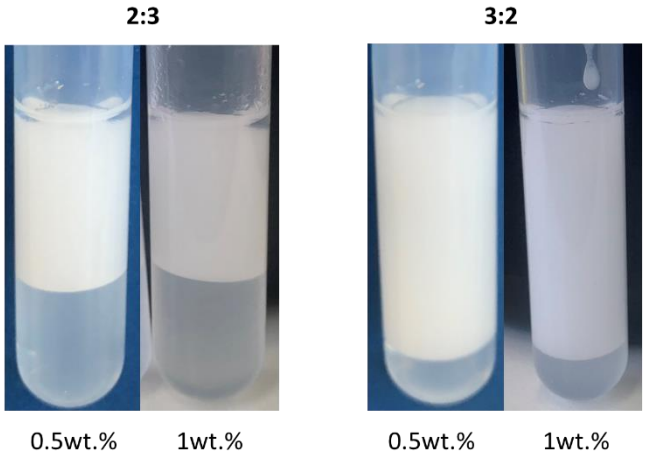

Figure 9. Emulsions formulated with EPS RA19 at 0.5 and 1.0 wt.%, with O:W weight ratios of 2:3 and 3:2, using paraffin oil.

2.3.5.2 Rheological properties

The effect of EPS concentration on the viscosity of emulsions with a 3:2 O:W ratio was evaluated at different EPS concentrations: 0.5 wt.%, 1 wt.%, 2 wt.%, 4 wt.%, 6 wt.%, and 8 wt.%. Additionally, the influence of the oil phase content was examined for emulsions with varying O:W ratios (4:1, 3:1, and 2:1) using paraffin as the oil phase and 1 wt.% EPS. The flow curves

and the parameters from the fitted Carreau model are presented in Figure 10 and Table 8, respectively.

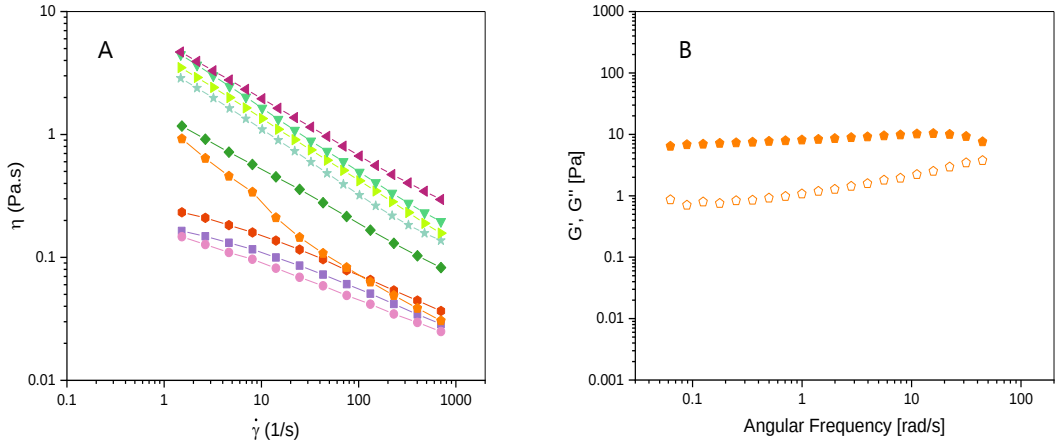

Figure 10. Apparent viscosity and oscillatory shear stress test for different emulsions. (A) Apparent viscosity (η) as a function of shear rate ($\dot{\gamma}$) for emulsions with a 3:2 O:W ratio at different EPS concentrations: 0.5 wt.% (⬟), 1 wt.% (◆), 2 wt.% (★), 4 wt.% (▶), 6 wt.% (▼) and 8 wt.% (◀); and for emulsions with varying O:W ratios using paraffin as the oil phase with 1 wt.% EPS: 4:1 (■), 3:1(●) and 2:1 (⬢). (B) Angular frequency dependencies of storage G′ (full symbols) and loss G'' (open symbols) moduli.

The results showed that as the EPS concentration increased from 1 to 8 wt.%, the zero-shear viscosity (η_0) rose significantly from 2.578 to 8.618 Pa s (Table 8). This indicates that the higher EPS concentration led to an increase in viscosity, likely due to unabsorbed EPS remaining in the continuous phase and acting as a thickening agent [143].

Regarding the increase in oil phase content, the viscosities of emulsions with oil-to-water ratios of 4:1, 3:1, and 2:1 were not significantly different, with estimated zero-shear viscosities (η_o) of 0.165, 0.149, and 0.230 Pa s, respectively. However, compared to the viscosity at a 3:2 ratio, with a zero-shear viscosity of 2.578 Pa s for the same EPS concentration, there was a noticeable decrease. This can be attributed to phase inversion, where the continuous phase shifts to oil [142]. These findings are consistent with the results presented in the previous section 2.3.5.1.

Table 8. Parameters of the Carreau model were estimated for various concentrations, and O:W ratios using paraffin as oil phase

EPS (wt.%)	O:W	η_0 (Pa s)	λ (s)	n	R^2	MRE[b] (%)
0.5	3:2	1.852	1.197	0.404	0.995	3.016
1		2.578	3.882	0.562	1.000	0.972
2		4.403	1.391	0.688	1.000	1.192
4		6.128	1.933	0.696	1.000	0.344
6		8.313	2.186	0.663	1.000	1.090
8		8.618	2.484	0.476	1.000	0.630
1	4:1	0.165	0.344	0.492	0.997	1.656
	3:1	0.149	0.516	0.478	0.996	1.021
	2:1	0.230	0.320	0.540	0.996	1.338

[b] $\mathrm{MRE} = \frac{\sum_{i=1}^{j}\left|\frac{(x_{\exp i} - x_{\mathrm{model}\, i})}{x_{\exp i}}\right|}{j} \times 100$

The behavior of both the storage and loss moduli for the emulsion containing 0.5 wt.% EPS and a 3:2 oil-to-water ratio with paraffin oil is illustrated in Figure 10B. Even at this low concentration, G' remains consistently higher than G'' across all frequencies, indicating a weak gel-like behavior [98]. This contrasts with the behavior observed for EPS in water, as discussed in section 2.2.3, where a liquid-like behavior was seen at various concentrations of EPS, temperatures, and pH levels.

2.4 Conclusion

This chapter explores the functional properties of EPS RA19, produced by *Paracoccus zeaxanthinifaciens* subsp. *payriae*, isolated from a "Kopara" mat in French Polynesia. The EPS is rich in galactose, rhamnose and fucose, along with sulfates, and uronic acids, which endow the EPS with negative charges. The potential of this EPS as a thickening, gelling, film-forming, and emulsifying agent was evaluated.

Rheological characterization demonstrated that EPS RA19 exhibited notable non-Newtonian shear-thinning behavior and liquid-like properties under steady-state and dynamic oscillatory measurements, respectively. These behaviors persisted across different temperature and pH conditions, indicating the robustness of the EPS under varying environmental factors.

The film-forming ability of EPS RA19 was tested both with and without a plasticizer. Results showed that the polymer produced promising films with good structural integrity and homogeneity, even in the absence of a plasticizer. Regarding mechanical properties, films

without glycerol had higher Young's modulus and tensile strength, along with lower elongation at break. The addition of glycerol improved the flexibility of the films, reducing Young's modulus and tensile strength while increasing elongation at break.

In terms of gel formation, EPS RA19 was able to form gels in the presence of Fe^{2+} and Cu^{2+}, though the latter showed instability over time, suggesting limited structural integrity. Increasing the concentrations of both the polymer and Fe^{2+} resulted in stronger, more homogeneous gels, making Fe^{2+}-crosslinked gels particularly suitable for applications such as drug delivery and tissue engineering.

The emulsifying properties of EPS RA19 were tested with olive oil, paraffin oil, and almond oil, as well as different EPS concentrations and oil-to-water ratios. EPS RA19 showed excellent emulsification and stabilization potential with paraffin oil, achieving the highest emulsification index at an optimal oil-to-water ratio of 3:2 and 1 wt.% EPS. This combination demonstrated high stability over 30 days, and rheological analysis revealed that viscosity increased with higher EPS concentrations. Therefore, this EPS has potential in high value applications, such as cosmetic, formulation, tissue engineering and drug delivery.

3

BIOACTIVE PROPERTIES

3.1 Introduction

Microbial EPS have garnered significant interest due to their diverse bioactivities, including antioxidant [144], wound healing [145], photoprotective [20], and antimicrobial effects [144], non-toxic nature and close compatibility with biological systems [39], making them highly sought-after in applications where these properties are paramount considerations.

3.1.1 Antioxidant

Reactive oxygen species (ROS) are a collection of highly reactive molecules, comprising superoxide radicals ($O2^{\bullet -}$), hydroxyl radicals ($OH^{\bullet}$), hydrogen peroxide (H_2O_2), as well as various peroxides (ROOR') and hydroperoxides (ROOH), generated as by-products of cellular metabolism primarily within the mitochondria, in oxidative phosphorylation [146]. Exogenous stimuli, such as salinity, prolongated exposure to UV rays and metal toxicity, can also induce the overproduction of ROS [146].

In excess, these species pose a significant threat to cellular integrity due to their highly reactive nature. ROS can inflict oxidative damage on vital cellular components such as proteins, lipids, and DNA, potentially culminating in cell death if left unchecked [147]. Cells counteract this oxidative stress through a range of defense mechanisms, including the production of antioxidant enzymes and compounds [148]. EPS have emerged as compounds capable of scavenging ROS, thereby mitigating oxidative stress and shielding cells from harm [149-151].

Natural polysaccharides can act as antioxidants in their own right, through mechanisms such as chelating metals and scavenging ROS, or enhance the activity of endogenous antioxidant enzymes, offering potential therapeutic benefits in combating oxidative stress-related diseases and promoting overall cellular health [149]. For example, the high concentration of negatively charged groups in FucoPol endowed the EPS with significant antioxidant potential, aiding cells in protecting against the deleterious H_2O_2 exposure [150]. Fucoidan extracted from

Fucus vesiculosus exhibits superior antioxidant effect in comparison to fucoidan from Ascophyllum nodosum, which is ascribed to its elevated fucose and sulfate content [151].

3.1.2 Photoprotection

An organism's ability to protect itself from harmful UV radiation is crucial, especially from UVA and UVB rays, as UVC is largely absorbed by the ozone layer [152]. UV radiation can cause cellular dysfunction and increase oxidative stress, leading to detrimental effects on the organism's health [152,153]. An effective strategy involves the use of polysaccharides as photoprotectors due to their capability to absorb UV radiation, thus preventing it from reaching vital cellular components [20]. In addition, these polymers can enhance repair mechanisms in UV-induced damaged cells and act as scavengers of ROS generated by UV exposure [154].

Studies have demonstrated the protective effects of EPS in various contexts. For instance, EPS derived from *Lactobacillus reuteri* have been shown to protect human skin fibroblasts from UVA-induced damage by enhancing antioxidant enzyme activities and reducing cell apoptosis (Table 1) [154]. FucoPol, produced by *Enterobacter* A47 effectively protects epithelial cells and keratinocytes from UVA and UVB, through the absorption of UV radiation [20].

3.1.3 Wound healing

Wound healing is a complex process characterized by the occurrence of several somewhat overlapping phases, which can be delineated as follows: hemostasis, inflammation, new tissue formation, and tissue remodeling [155]. Hemostasis occurs immediately after an injury to prevent excessive bleeding by forming blood clots through platelet aggregation and fibrin clot creation [155]. Uncontrolled bleeding can lead to excessive blood loss and potentially death. To address this, materials that aid in rapid hemostasis are being developed [156].

Subsequently, an inflammatory response is initiated, characterized by the influx of immune cells, including macrophages and neutrophils, which are responsible for clearing debris and combating infection against pathogens, such as viruses, bacteria and other microorganisms [155]. Proliferation is marked by the formation of new connective tissue, where fibroblasts synthesize collagen, and endothelial cells form new blood vessels (angiogenesis), leading to the development granulation tissue. Epithelial cells then migrate over the wound bed to re-establish the skin barrier. Remodeling entails the maturation and reorganization of collagen fibers, thereby strengthening tissue over the course of several months or years. Disruptions at any stage have the potential to result in chronic wounds or abnormal scarring [155]. Prolonged

inflammation can lead to chronic wounds, whereas excessive collagen deposition during remodeling can cause hypertrophic scarring or keloids, both of which have a bearing on the functional and cosmetic outcomes of wound healing [155,157].

Bioactive materials, such as EPS, have significantly improved tissue repair through multiple mechanisms, including promoting cell proliferation and migration [145], enhancing collagen synthesis and modulating the inflammatory response [158]. By maintaining a moist wound environment and providing a biocompatible matrix, EPS helps support faster wound closure and tissue regeneration [64]. The inclusion of EPS in advanced wound care products underscores their importance in improving healing outcomes, reducing recovery times and minimizing scarring, making them valuable in medical and therapeutic applications [159].

For example, Fucoidan enhanced wound healing by promoting blood vessel formation and deposition of collagen [160]. EPS extracted from the bacterium *Weissella cibaria* MED17 exhibited wound healing capacity and the ability to repair DNA damage (Table 1) [34]. In a study conducted in animals, it was shown that EPS synthesized by *Papiliotrema terrestris* PT22AV had the ability to facilitate the recruitment of keratinocytes, fibroblasts and macrophages aiding in reducing the inflammation phase (Table 1) [37].

3.2 Materials and Methods

3.2.1 Materials

For the biological tests, four additional exopolysaccharides were investigated. The processes of bacterial isolation, EPS production, and composition analysis were completed prior to this thesis under the PROMICON project (Table 9).

Table 9. Monosaccharide composition of additional EPS used in biological assays (Ara, L-arabinose; Fuc, L-fucose; Gal, galactose; GalA, galacturonic acid; Glc, glucose; GlcN, glucosamine; Man, mannose; Rha, rhamnose; Rib, ribose)

	Monosaccharide composition (mol%)								
EPS	Ara	Fuc	Gal	GalA	Glc	GlcN	Man	Rha	Rib
SC4	26	-	-	1	22	52	-	-	-
RD5	-	27	14	10	14	18	-	13	-
AB5	4	3	9	6	67	12	-	-	-
Mo169	-	-	6	-	21	52	18	-	3

Alteromonas macleodii Mo169 was isolated from a giant clam in the marine environment of Moorea Island lagoon, French Polynesia. Bacterial isolation, EPS production, and

composition analysis were performed before this thesis in collaboration with Pacific Biotech BP (Table 9).

All the polymers were sterilized in a DIGITHEAT-TFT Drying Oven (J.P. Selecta, Spain), at 120°C for 2h in a sealed Schott flask.

3.2.2 Cell culture

Biological assays were conducted using HaCaT (human immortalized keratinocyte, obtained from ATCC, USA), HFFF2 (Human fetal foreskin fibroblasts, obtained from ECACC, UK) and Vero cell line (monkey kidney epithelial cells, VERO CCL-81, obtained from ATCC, USA). HaCaT cells were cultured in Dulbecco's Modified Eagle medium (DMEM) High Glucose (4.5 g L^{-1}) from Biowest (L0103), supplemented with 10% (v/v) of fetal bovine serum (FBS) from Biowest, and 1% (v/v) penincilin-strepmycin (PS) from Gibco. Both HFFF2 and Vero cells were cultured in DMEM Low Glucose (1g L^{-1}) from Biowest (L0060) supplemented with 10% (v/v) FBS and 1% (v/v) PS. All cells were maintained at 37ºC with 5% CO_2, as described by Concórdio-Reis *et al.*[19], and Guerreiro *et al.* [50].

3.2.3 Cytotoxicity assay

The cytotoxicity assays were performed according to the methodology described by Guerreiro *et al.* [20] according to the International Standard ISO 10993-5. Cell viability was assessed using the resazurin colorimetric assay (from Alfa Aesar). Resazurin is a small dye that is reduced to resorufin by cellular reductases in viable cells. This reaction shifts the absorbance of the dye from 600 nm (resazurin) to 570 nm (resorufin) [161].

The HaCaT, HFFF2 and Vero cells were seeded individually into 96 well-plates at 25.000 cell cm^{-2}, 30.000 cell cm^{-2} and 20.000 cell cm^{-2}, respectively, in standard DMEM culture medium, and allowed to grow for 24 hours in the incubator at 37ºC in a 5% CO_2 humidified atmosphere. Afterwards, cells were supplemented with the EPS diluted in the appropriate medium for each cell type (25-0.75 mg mL^{-1}). Simultaneously, the cells were incubated with only cultivation medium as the negative control (viable cells), and with cultivation medium supplemented with 10% DMSO as the positive control (non-viable cells). After incubating for 24h, 100µL of DMEM:resazurin (50% of 0.04 g L^{-1} of resazurin diluted in PBS + 50% medium) solution was added to assess cell viability, followed by 3h incubation at 37ºC in a 5% CO_2 before reading the absorbance at 570 and 600 nm. The optical density was measured using an Agilent BioTek Synergy LX Multi-Mode Microplate Reader (Agilent, USA) and cell viability was expressed in

terms of percentage of living cells relative to the negative control (Figure 11). A minimum of two independent experiments were performed in quadruplicate.

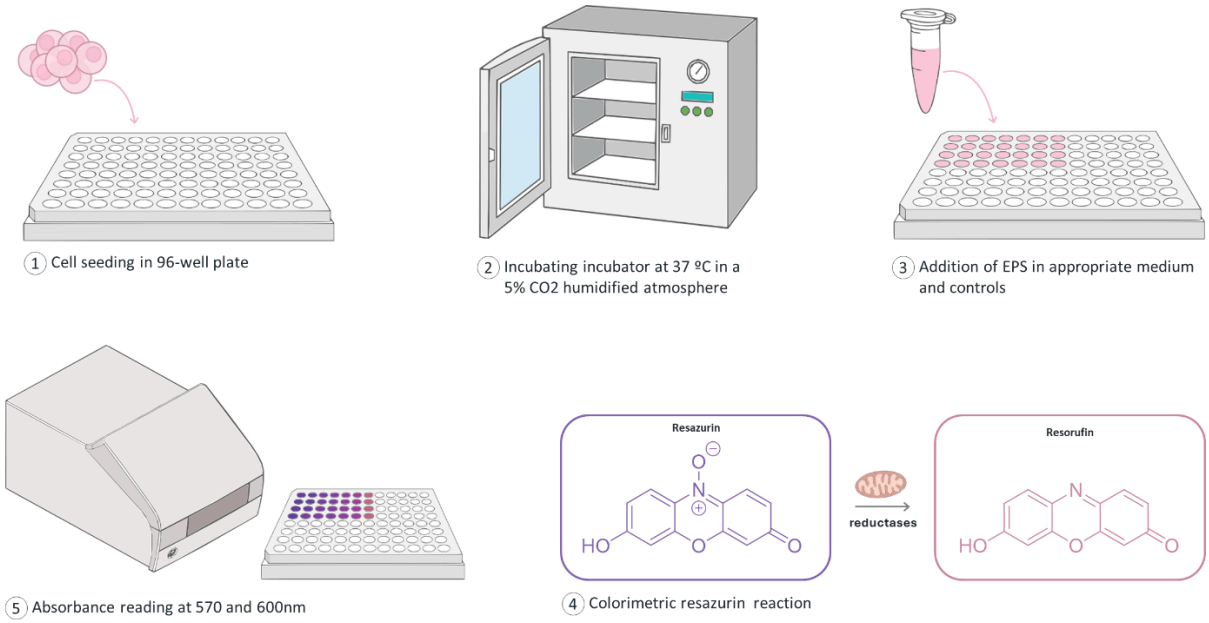

Figure 11. Schematic representation of the cytotoxicity assay protocol, detailing the steps from cell seeding, treatment with test compounds, application of cytotoxicity assay reagent (resazurin) to measurement. Created in Inkscape.

3.2.4 Photoprotection

To evaluate the photoprotective activity of EPS RA19, EPS SC4, EPS RD5, EPS AB5 and EPS obtained from *Alteromonas macleodii* Mo169. The protocol described by Guerreiro *et al.* [20] was followed with minor modifications. HaCaT and HFFF2 cells were seeded in a 12-well plate at densities of 25.000 cell cm^{-2} and 30.000 cell cm^{-2}, respectively, using standard DMEM culture medium. After a 24-hour growth period in an incubator at 37ºC in a 5% CO_2 humidified atmosphere, the cells were supplemented with either DMEM (control) or DMEM containing 1.5 g L^{-1} EPS. Two conditions were tested: (i) cells were irradiated with a 254 nm ultraviolet lamp in a flow chamber for 30 minutes, and (ii) cells were left at room temperature for the same duration. Viability was assessed 2 hours and 24 hours post-irradiation using the resazurin colorimetric assay, as described above in section 3.2.3. The experimental design of the assay is represented in (Figure 12). A minimum of two independent experiments were performed in quadruplicate.

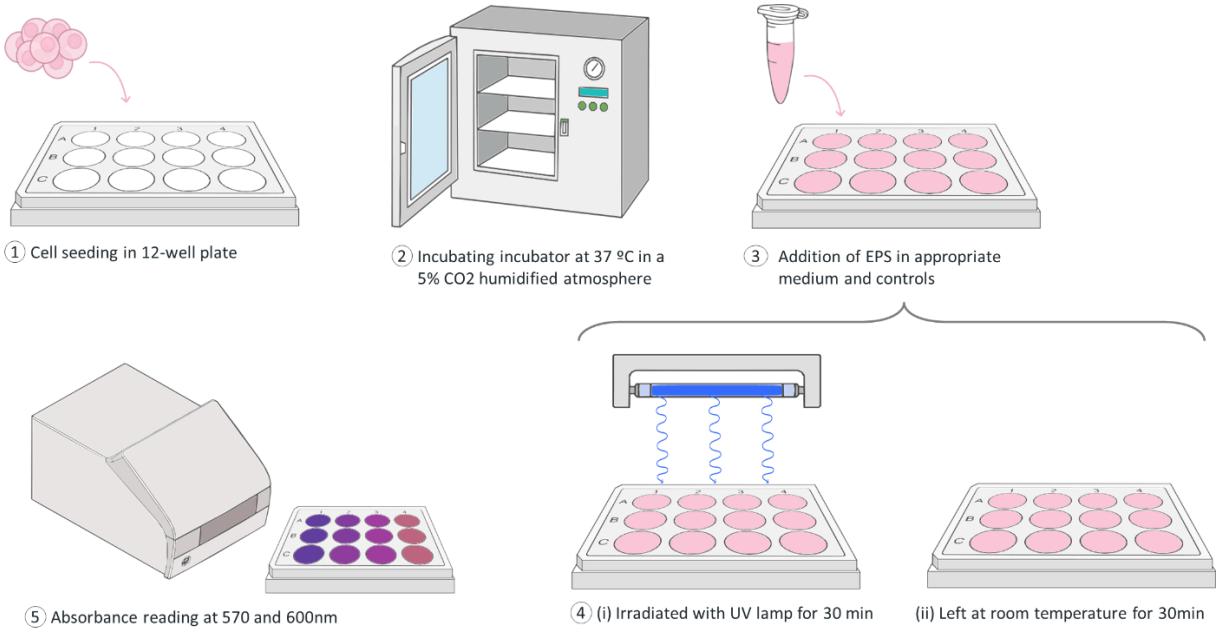

Figure 12. Overview of the photoprotection assay protocol, illustrating the sequence from seeding cells, adding experimental and control treatments, subjecting one plate to UV irradiation and another left at room temperature, and measuring absorbance at 570 nm and 600 nm to assess photoprotective effects. Created in Inkscape.

3.2.5 Antioxidant activity

To evaluate the antioxidant activity of the EPS, the protocol described by Nunes *et al.* [162] was followed.

Intracellular ROS generation was assessed using a fluorometric assay with 2,7'-dichloro-dihydrofluorescein diacetate (H_2-DCFDA, obtained from Merck). This non-fluorescent probe is converted by cellular esterases into 2,7'-dichlorodihydrofluorescein (H_2DCF), which also lacks fluorescence. Upon reaction with ROS such as hydrogen peroxide (H_2O_2), hydroxyl radicals, and other peroxides, H_2DCF is rapidly oxidized to the highly fluorescent dichlorofluorescein (DCF) [162].

HaCaT cells were seeded at a density of 25.000 cell cm^{-2} in 96-well plates and left for 24h in an incubator at 37ºC in a 5% CO_2 humidified atmosphere. The culture medium was removed and 20µM of H_2-DCFDA was added to each well and the plates were incubated at 37ºC for 30 min. Afterwards, the volumes were discarded, and the 1.5 wt.% EPS solutions and 1 mg mL^{-1} ascorbic acid (positive control) were incubated for a further 1 hour. Subsequently, oxidative stress was induced by adding a solution of 500 µM hydrogen peroxide (H_2O_2) or exposing cells to a 254 nm ultraviolet lamp in a flow chamber for 30 minutes. Before ROS levels were determined by fluorescence (excitation wavelength 485 nm, emission wavelength 520 nm) using an

Agilent BioTek Synergy LX Multi-Mode Microplate Reader (Agilent, USA), the volume of the wells exposed to UV were discarded and PBS was added (Figure 13).

A minimum of two independent experiments were performed in quadruplicate (n=4) and reported as a percentage of ROS reduction determined according to Equation 4.

$$ROS\ (\%) = \frac{fluorescence\ of\ exposed\ cells}{fluorescence\ of\ unexposed\ control} \times 100 \quad (4)$$

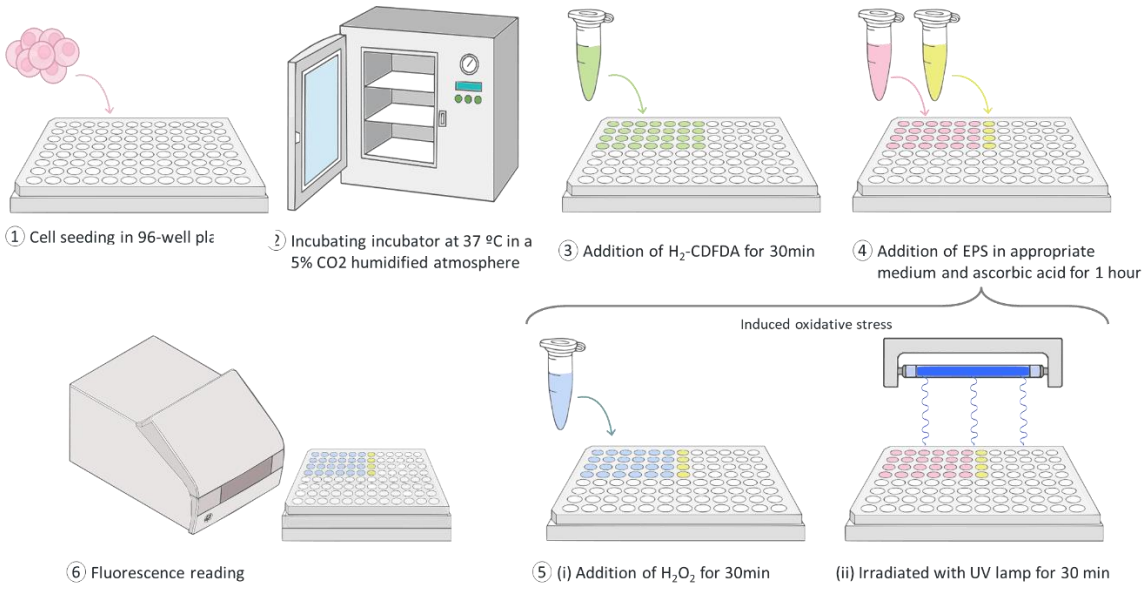

Figure 13. Illustration of the oxidative stress assay protocol, showing the steps of seeding cells into a 96-well plate, adding H2-DCFDA, treating with EPS, inducing oxidative stress with H2O2 or UV light, and measuring fluorescence. Created in Inkscape.

3.2.6 Wound healing

The wound healing property of EPS RA19 was assessed according to protocol described by Concórdio-Reis *et al.* [19], with a few modifications. HaCaT cells were seeded at a density of 60.000 cells cm^{-2} on four defined cell-free gaps silicon inserts (Ibidi, Germany) placed in 12-well plates. The cells were left to grow to confluence (24h). Afterwards, the silicon inserts were removed, and each well was washed twice with PBS to remove non-adherent cells. Then, the cells were supplemented with the 1.25 wt.% EPS solutions (Figure 14).

A NIKON Eclipse Ti-S optical microscope connected to a NIKON D610 digital camera was used for image collection at different time points: 0, 16, 24, 32, 42h. To measure the wound area, image analysis was performed using ImageJ 1.56g software (USA). The wound area was defined between the border lines, and the percentage of the recovered wound area was calculated using the following Equation 5.

$$Wound\ area\ recovered\ (\%) = \frac{(Initial\ area) - (Final\ area)}{Initial\ area} \times 100 \quad (5)$$

The results were expressed in terms of mean ± SD of four replicates (n=4) of one independent experiment.

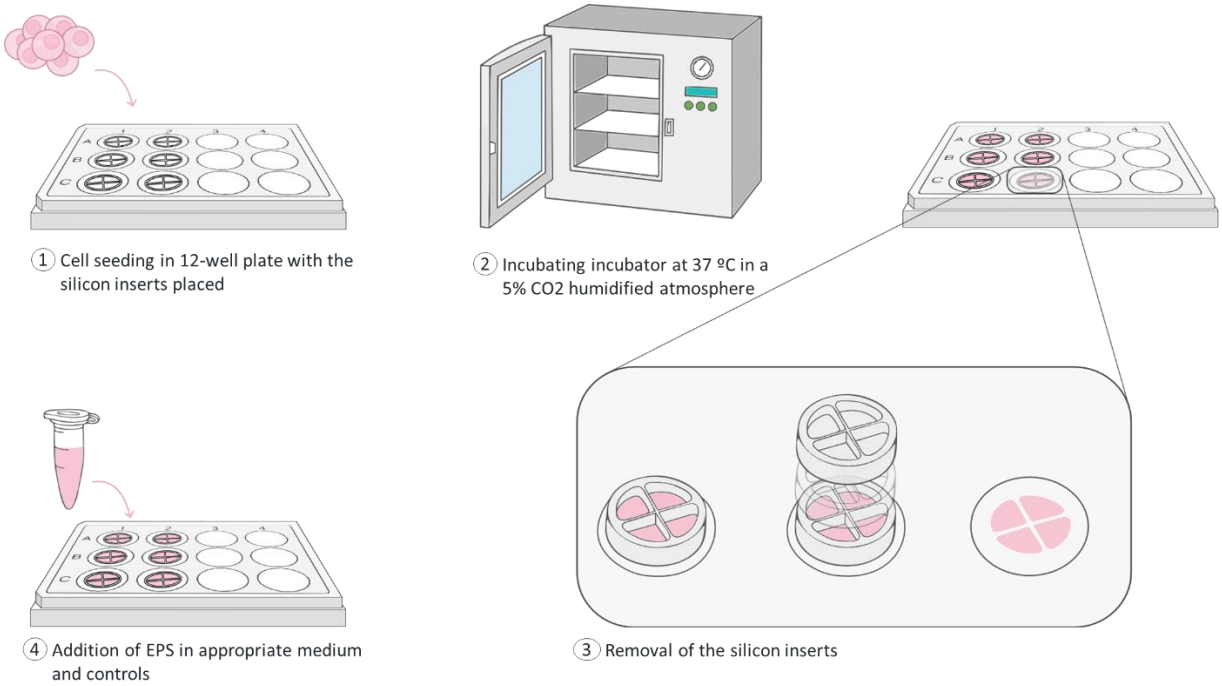

Figure 14. Illustration of the wound healing assay protocol, showing the steps of seeding cells into a 12-well plate with silicone inserts, removing the silicone inserts to create uniform cell-free zones, and adding experimental and control treatments. Created in Inkscape.

3.2.7 Statistical Analysis

All experiments were conducted in at least duplicate, and the results are expressed as mean ± SD. Statistical significance across datasets was evaluated using two-way ANOVA. GraphPad Prism 8 software (GraphPad Software, Inc., San Diego, CA, USA) was employed for statistical analysis, with $P < 0.05$ considered statistically significant.

3.3 Results and Discussion

3.3.1 Cytotoxicity

Evaluating the cytotoxicity of EPS is crucial for applications in cosmetics, biomedical, and medical fields due to the need for safety, biocompatibility, and effectiveness [79,163]. EPS used in these industries often come in direct contact with skin or internal tissues, so ensuring they

do not cause harm or trigger immune responses is essential [163]. With this in mind, the potential cytotoxicity of EPS RA19 was tested for three different cell lines. Both fibroblasts and keratinocytes are the leading cells found in the skin layers, dermis and epidermis, respectively, and play an important role in cutaneous regeneration in the inflammatory phase, contributing to wound healing of the damaged tissue [164]. Vero cell line is, amongst other cells, recommended by ISO 10993-5 international standard for the performance of cytotoxicity assays [165].

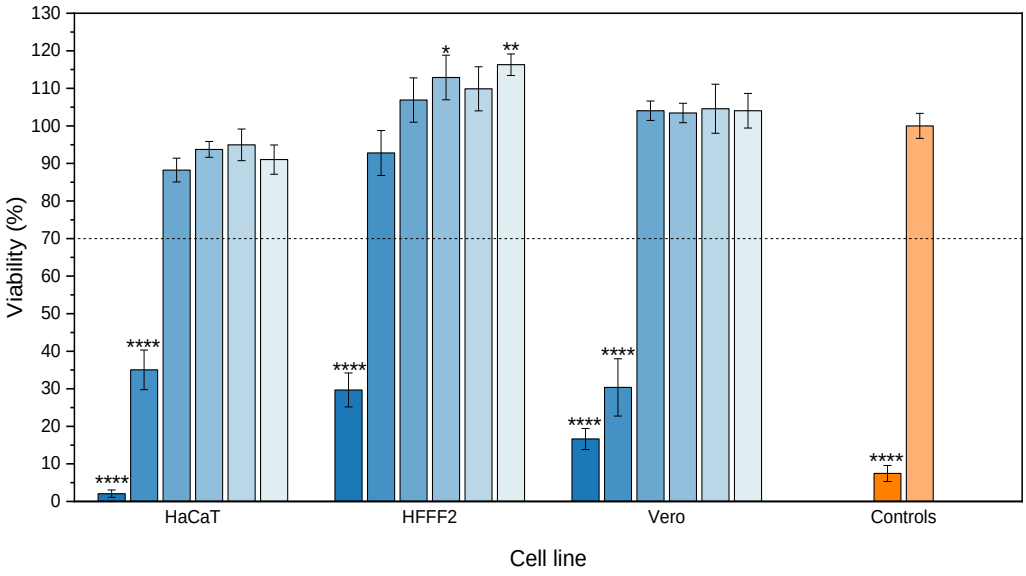

Figure 15. Cytotoxicity effect of EPS RA19 on HaCaT, HFFF2 and Vero at different concentrations: 25 g L^{-1}, (■), 12.5 g L^{-1}, (■), 6.3 g L^{-1}, (■), 3.2 g L^{-1}, (■), 1.6 g L^{-1}, (□) 0.8 g L^{-1}, (□). Positive control was supplemented with medium and DMSO (■), and negative control was supplemented with only medium (□). Statistically significant differences comparing samples with the negative control were assessed according to Two way ANOVA (*, p≤0.05, **, p≤0.01, **** p≤0.0001).

The toxicity of the EPS was evaluated for concentrations ranging from 25 g L^{-1} to 0.8 g L^{-1}. The negative control (C-), which was only supplemented with complete culture medium, represents a viability of 100%, meaning that all cells are alive. Contradictorily, in the positive control (C+), the cytotoxic condition in which 10% DMSO was added to supplement the medium, a viability of 7.44±2.13% was obtained, confirming the test's sensitivity to cell viability.

According to ISO 10993-5 standards [165], EPS RA19 is considered non-cytotoxic at concentrations up to 6 g L^{-1}, with cell viability remaining above 70% for all tested cell lines. At higher concentrations, cell viability was significantly inferior compared to the negative control, while at lower concentrations no significant difference in cell viability was observed. Considering these results this polysaccharide can be considered non-cytotoxic at concentrations below 6 g L^{-1} and used for further biological studies.

These findings are consistent with the literature where other EPS have been shown to be non-cytotoxic within certain concentration ranges. For example, at concentrations between 0.01 and 1 mg mL^{-1}, EPS produced by *Lactobacillus reuteri* SJ47 has no toxic effects on cells [154]. Similarly, EPS AC210 has been reported to be non-cytotoxic at concentrations between 0 and 1 mg mL^{-1} [97]. In contrast, Fucopol has shown no cytotoxicity at concentrations up to 10 mg mL^{-1} [50].

3.3.2 Photoprotection

Photoprotection involves both primary and secondary defense mechanisms. Primary protection relies on compounds that shield the skin by absorbing, reflecting, or blocking UV radiation. Secondary defenses, such as antioxidants, help neutralize ROS and reduce the cascade of harmful reactions triggered by UV exposure. Together, these systems work to minimize UV-induced damage and provide long-term skin protection [166].

To determine the suitability of a biomaterial as a photoprotector, it is crucial to evaluate its effectiveness in providing UV protection, given the significant risks associated with prolonged UV exposure, such as photoaging and skin cancer [152]. With this in mind, the potential of EPS as natural photoprotective agents was tested, focusing on their ability to shield the skin from harmful UV radiation and mitigate the associated long-term damage.

As EPS RA19 showed a similar cytotoxicity range to Fucopol, the concentration for this assay was based on the 2.5 mg mL^{-1} used in the Fucopol photoprotection studies. However, as some EPS, such as RD5 and SC4, did not fully dissolve at this concentration, a lower concentration of 1.5 mg mL^{-1} was used instead. While the cytotoxicity of the other EPS was not individually tested, their similarity to EPS RA19 led to the decision to test all EPS at the same concentration. Additionally, the literature confirms that EPS do not exhibit cytotoxicity at this concentration [50].

Two sets of 12-well plates were cultured with HaCaT and HFFF2 cell lines, in which for each respective cell line, one plate was maintained at room temperature (C+, C-), while the other plate was exposed to UV radiation for a 30 minute period (I+, I-). Figure A4 and Figure 16, showcase the metabolic activity of irradiated and non-irradiated HaCaT and HFFF2 cells, after 2h and 24h post radiation, respectively, the latter, was used to assess any delayed radiation-induced damage.

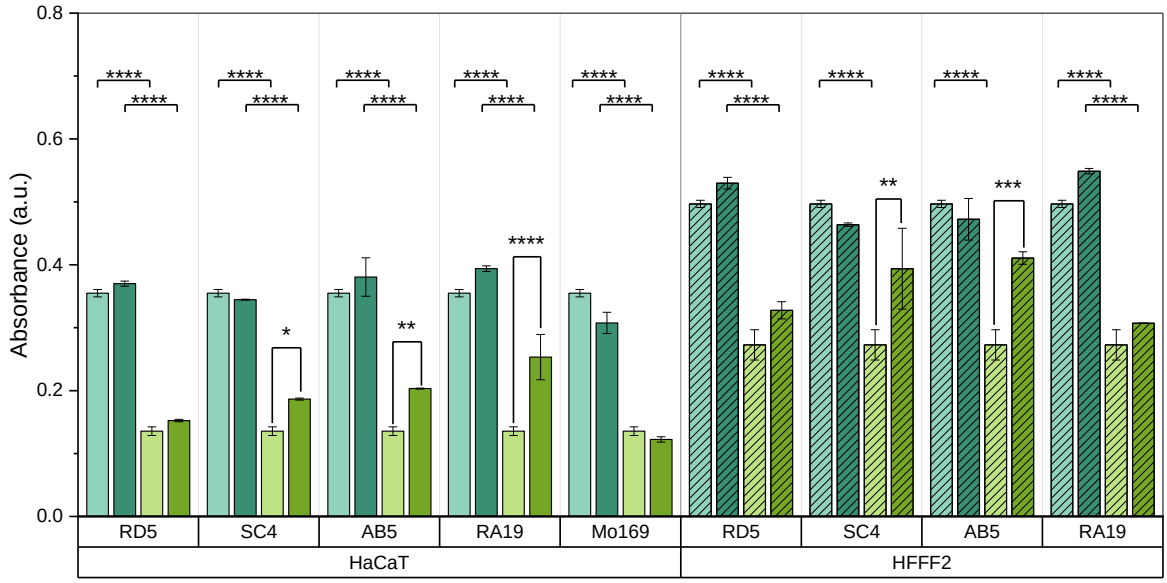

Figure 16. Metabolic viability of irradiated and non-irradiated HaCaT (clear bars) and HFFF2 cells (striped bars) 24h post exposure to UV radiation, for five EPS, RD5, SC4, AB5, RA19 and Mo169. Non irradiated cells supplemented with only medium, C-, (□); Non irradiated cells supplemented with EPS, C+, (■); Irradiated cells supplemented with only medium, I-, (□); Irradiated cells supplemented with EPS, I+, (■). Statistically significant differences comparing samples were determined according to Two way ANOVA (*, p≤0.05, **, p≤0.01, ***, p≤0.001, **** p≤0.0001).

At the 2-hour post-irradiation time point, no significant reduction in cell viability was observed between the irradiated cells (I+, I-) and the control cells (C+, C-) as depicted in Figure A4. For HaCaT, after 24 hours, cells treated with EPS SC4, AB5, and RA19 showed a significant increase in viability compared with the cells without EPS (I-), indicating the potential photo-protective effects of these polymers. Conversely, both EPS RD5 and Mo169 exhibited significant photodegradability after 24h post-irradiation, reducing their effectiveness as a protective agent.

For the HFFF2 cell line, the EPS demonstrated similar behaviors to those observed in the HaCaT cells, except for RA19. Compared to HaCaT, HFFF2 cells supplemented with EPS RA19 did not show statistical difference between I+ and I- group, indicating that for this cell line EPS RA19 does not have protective effect. This indicates that certain EPS might specifically target and protect particular skin cell types from UV damage. A similar result was observed for EPS produced from a *Paenibacillus* isolate, where the EPS reduced UVB-induced cell death in keratinocyte cells but not in fibroblasts [167]. In contrast, the other EPS tested displayed similar difference between I- and I+ across both cell lines, implying that they have comparable photoprotective effects on both HaCaT and HFFF2 cells.

Previous studies have demonstrated that sulfated polysaccharides possess strong photoprotective properties. For example fucoidan isolated from *Hizikia fusiforme*, rich in both sulfate and fucose, similarly to EPS RA19, proved to protect HaCaT cells against UVB-induced photodamage [168]. The fucoidan purified from brown seaweed *Saccharina japonica* also enhanced the viability of HaCaT cells exposed to UVB radiation [169].

EPS SC4 and AB5 exhibited similar behaviors, both demonstrating strong photoprotection in both cell lines, with a statistically significant difference between I+ and I- at the 24-hour mark. AB5 consistently showed higher significance values than EPS SC4, suggesting it has greater photoprotective activity. Furthermore, in HaCaT cells, neither polymer showed a statistically significant difference between C+ and I+, which was not observed with other EPS in either cell line. This may indicate that UV exposure did not significantly affect the cells, allowing them to remain viable and continue proliferating. In contrast, EPS RD5 and Mo169 showed no photoprotective activity in either cell line, as no significant difference was observed between the irradiated groups.

Since EPS SC4 is primarily composed of arabinose, this could be linked to its demonstrated photoprotective activity. Although no studies have specifically attributed photoprotection to arabinose alone, research suggests that polysaccharides rich in arabinose may endow the polysaccharide with antioxidant properties [170,171]. These antioxidant effects are likely related to photoprotection, as antioxidants play a critical role in mitigating UV-induced oxidative stress, which is a key factor in preventing skin damage caused by solar radiation [172]. Interestingly, EPS AB5, the only other EPS in this study containing arabinose, albeit in smaller amounts, also demonstrates photoprotective potential. However, AB5 has a relatively high content of uronic acids, which have been shown to possess photoprotective activity [173]. FucoPol, known for its photoprotective activity [20], has a composition similar to EPS RD5, yet RD5 does not exhibit any photoprotection despite this similarity.

3.3.3 Antioxidant

Sunscreens in their composition are endowed with a combination of UV filters, which ensure protection over a broad spectrum of UV radiation, and antioxidants, which help stabilizing the formulation and add additional protection against UV mediated oxidative stress [174]. With the constant innovation of the cosmetic industry, multifunctional compounds are a prerequisite in the development of new cosmetic products, therefore it is important to find biomaterials which show good photoprotective and antioxidant activities [53].

An *in vitro* assay was conducted to evaluate the antioxidant capacity of EPS RD5, SC4, Mo169, and RA19, specifically their effectiveness in mitigating ROS generation. UV radiation induces the formation of ROS, including hydroxyl radicals, superoxide anions, and hydrogen peroxide [54]. Hydrogen peroxide, in turn, interacts with redox-active transition metals (e.g., Fe^{2+}), producing hydroxyl radicals via the Fenton reaction [55]. In this assay, HaCaT cells were seeded in 96-well plates, and ROS generation was triggered by exposing the cells to either hydrogen peroxide or UV radiation for 30 minutes. This setup enabled a comprehensive evaluation of each EPS's ability to counteract oxidative stress and protect cellular health.

Ascorbic acid, most commonly known as vitamin C, is the second most used active ingredient in topical cosmetic formulations, for its antioxidant and photoprotective activities [53]. Therefore, it was used as positive control to compare the efficacy of the EPS as antioxidants.

The results obtained (Figure 17) revealed that all tested EPS generated ROS in response to exogenous stimuli, though their antioxidant activity varied. This was evident from reduced ROS production, similar to the positive control, indicating their capacity to mitigate ROS formation. Notably, in HaCaT cells exposed to UV light (Figure 17A), EPS SC4 and Mo169 exhibited the strongest antioxidant potential, though their ROS reduction was still significantly weaker than the positive control, highlighting their comparatively lower antioxidant effectiveness. Under hydrogen peroxide treatment (Figure 17B), RD5 exhibited the poorest antioxidant activity, with a larger deviation from the positive control. Overall, while all EPS demonstrated some level of antioxidant capacity, their effectiveness was generally less pronounced than the positive control. This suggests that while EPS have antioxidant activity, their effectiveness is less pronounced compared to the positive control. To comprehensively evaluate the antioxidant activity of the EPS, further testing is required, particularly focusing on optimizing concentration, as previous studies have demonstrated that the antioxidant properties of EPS improve with increasing concentration [53,144].

EPS RA19 demonstrated strong photoprotective activity (Figure 16) but showed limited antioxidant effects, illustrated by an almost 100% production of ROS. In contrast, EPS Mo169 and SC4, which both contain high levels of glucosamine in their backbone, did not produce as many ROS as the other polysaccharides, exhibiting a significant ability to reduce UV-induced ROS formation. This aligns with existing literature, which highlights glucosamine's excellent antioxidant properties, including its strong chelating effect on ferrous ions and its role in protecting macromolecules from oxidative damage caused by hydroxyl radicals [56]. Among the two, SC4 stands out as the most promising candidate for cosmetic sunscreen applications, as it combines both effective photoprotective and antioxidant properties, making it well-suited

for comprehensive skin protection. Additionally, despite RD5's compositional similarity to FucoPol, which has reported antioxidant properties [150], RD5 does not display any measurable antioxidant activity, as it produces almost three times more ROS than the positive control.

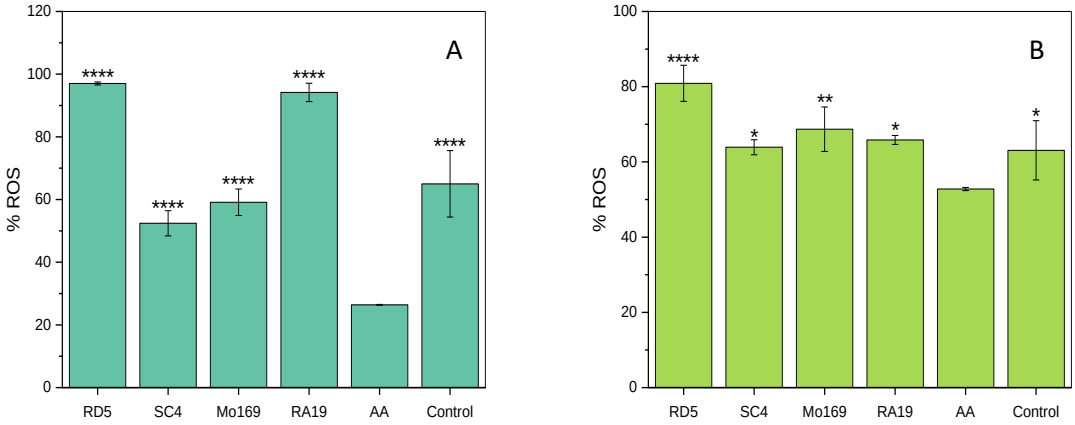

Figure 17. The impact of various EPS on the production of ROS (%) in HaCaT cells following exposure to (A) UVB light, and (B) hydrogen peroxide for 30 min. Ascorbic acid (AA) served as positive control. Statistically significant differences comparing samples with the positive control were assessed according to Two way ANOVA (*, $p \leq 0.05$, **, $p \leq 0.01$, **** $p \leq 0.0001$).

Interestingly, the reduced effectiveness of ascorbic acid in mitigating ROS induced by hydrogen peroxide, compared to UV-induced ROS, may be attributed to the potential for ascorbic acid to occasionally reduce Fe^{3+} to Fe^{2+}, which can further enhance the Fenton reaction and lead to more ROS formation, potentially reducing its overall protective effect in cells exposed to hydrogen peroxide [175].

The significant production of ROS observed in the control group is a reflection of the natural ROS production, as cells typically generate lower levels of ROS under normal conditions [146].

3.3.4 Wound healing

The wound healing capacity of EPS RD5, SC4, RA19 and Mo169 was assessed after 16, 24, 32 and 48h post removal of inserts, which left the wells with a defined cell-free gap, and the monitoring of cell migration was evaluated through the measurement of the area between wound edges. The wound recovery was calculated as a ratio relative to control (Figure 18), and images of the evolution of wound healing for the control and respective EPS are displayed in Figure A5.

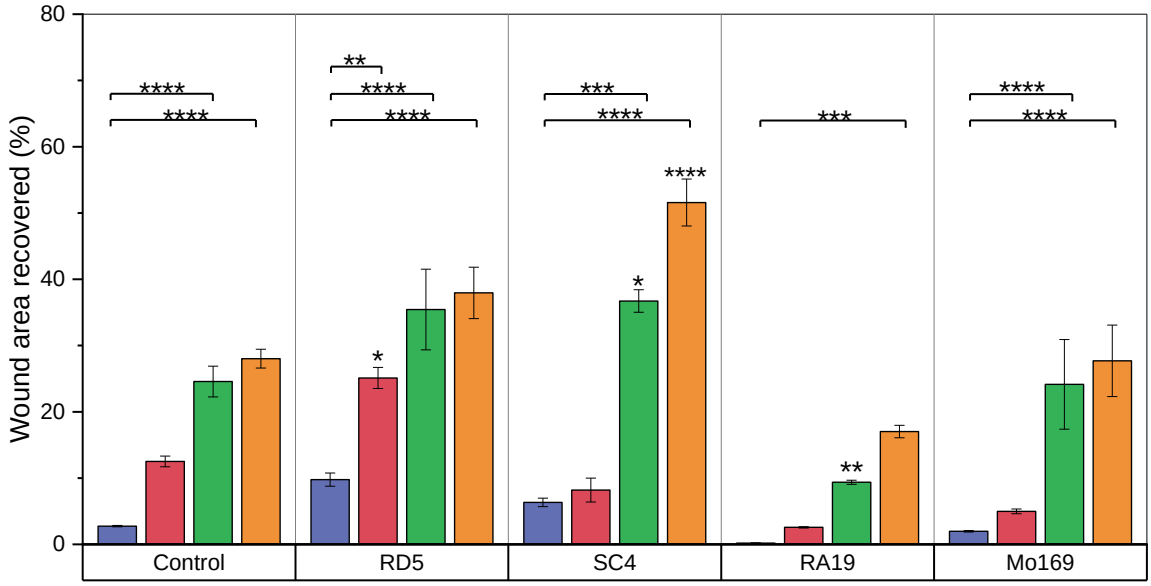

Figure 18. Wound healing assay, with migration of HaCaT cells after treatment with EPS RD5, SC4, RA19 and Mo169 for 16h (■), 24h (■), 32h (■), and 48h (■) post removal of insert. Statistically significant differences comparing samples with the control for the respective time points and between time points for each EPS were assessed according to Two way ANOVA (*, p≤0.05, **, p≤0.01, **** p≤0.0001).

Among the tested EPS, only SC4 and RD5 demonstrated superior cell migration compared to the control, which was treated with medium alone, indicating strong wound healing activity. SC4 was particularly effective, with wound recovery at 48 hours, nearly double that of the control group. This accelerated healing, highlighted by a highly significant difference compared to the control, suggests that SC4 may stimulate faster cell migration and tissue repair, positioning it as a potential candidate for therapeutic applications in wound treatment. Similarly, RD5 exhibited significant wound recovery, consistently outperforming the control group at every time point. This aligns with the statistically significant difference in cell migration observed between the EPS RD5 and the control at each time point, further confirming its potential in promoting wound recovery.

In contrast, while RA19 and Mo169 demonstrated some degree of cell migration/proliferation over the 48-hour period, their wound recovery did not surpass that of the control group. This implies that these EPS may not be as effective and not the best candidates for therapeutic agents aimed at enhancing wound healing and tissue regeneration.

Interestingly, EPS SC4 and RD5 exhibited significantly enhanced wound healing properties compared to EPS RA19 and Mo169. RD5, characterized by its high uronic acid content (10 mol%), may facilitate wound repair through interactions with cellular receptors, potentially modulating immune responses, as supported by previous research [174].

In contrast, SC4, with its elevated arabinose content (26 mol%), may promote tissue closure and recovery, likely attributed to the anti-inflammatory properties of arabinose [177,178].

3.4 Conclusion

This chapter examines the bioactive properties of five different EPS, RA19, previously tested for its functional properties; EPS SC4, AB5, RD5, and EPS Mo169, produced by *Alteromonas macleodii* Mo169, which was isolated from a giant clam in the Moorea Island lagoon, French Polynesia.

The cytotoxicity of EPS RA19 was assessed, showing that concentrations up to 6 mg/ml did not induce toxic effects in HaCaT, HFFF2, or Vero cells. Photoprotection assays revealed that RA19 predominantly protected HaCaT cells but was less effective for HFFF2 cells. EPS SC4 and AB5 exhibited the highest photoprotective activity, while EPS RD5 showed moderate activity, and EPS Mo169 did not display any photoprotective properties. Antioxidant activity tests indicated that RA19 and RD5 had limited antioxidant capacity, while EPS Mo169 and SC4 demonstrated strong antioxidant activity. Overall, EPS SC4 emerged as the best candidate for cosmetic sunscreen applications due to its excellent photoprotective and antioxidant properties.

Regarding wound healing, EPS RA19 and Mo169 did not show significant improvements compared to the control, suggesting a lack of wound healing activity. In contrast, EPS RD5 and SC4 displayed highly promising results, positioning them as potential therapeutic agents for promoting wound healing and tissue regeneration.

4
CONCLUSIONS AND FUTURE WORK

4.1 General Conclusion

This dissertation investigates the functional and biological properties of EPS, each with unique characteristics and potential applications. Specifically, EPS RA19, a fucose-rich polymer, was studied for both its functional and biological properties. In contrast, EPS SC4, AB5, RD5, and Mo169 were primarily evaluated for their biological properties.

EPS RA19 demonstrated potential applications across several fields. Rheological studies revealed that this polymer exhibits non-Newtonian shear-thinning behavior and liquid-like properties in steady-state and dynamic oscillatory measurements, respectively. Additionally, films formed from EPS RA19 alone exhibited good structural integrity and homogeneity, even without a plasticizer. The incorporation of glycerol enhanced the flexibility of the films, improved the mechanical properties, and resulted in a smoother, more compact structure. EPS RA19 also formed gels in the presence of Fe^{2+} and Cu^{2+}; however, only Fe^{2+} produced stable gels that maintained their structure over time. Increasing the concentrations of both the polymer and Fe^{2+} further strengthened and homogenized the gels, making Fe^{2+}-crosslinked gels suitable for applications such as drug delivery and tissue engineering. EPS RA19 also formed highly stable emulsions with paraffin oil at an optimal O:W of 3:2 and 1 wt.% EPS, suggesting its suitability for cosmetic formulations.

In terms of biological properties, EPS RA19 was non-cytotoxic at concentrations up to 6 mg ml^{-1} and showed good photoprotection in keratinocytes. However, it exhibited limited antioxidant activity and was ineffective as a wound-healing agent.

In contrast, EPS SC4 showed remarkable biological activity, with excellent photoprotective and antioxidant properties, positioning it as a strong candidate for cosmetic applications. Its outstanding wound-healing capabilities further highlight its potential use in tissue engineering. EPS AB5 was primarily investigated for its photoprotective potential, showing good activity in both cell lines evaluated.

EPS RD5, while exhibiting moderate photoprotective activity and limited antioxidant capacity, stood out for its strong wound-healing potential. This positions it as a promising candidate for tissue engineering applications, where wound repair is critical.

Finally, EPS Mo169, produced by *Alteromonas macleodii*, did not show significant photoprotective or wound-healing properties. However, its strong antioxidant activity suggests potential for applications focused on oxidative stress reduction.

4.2 Future work

This study highlights several areas that warrant further investigation. First, a more detailed structural characterization of EPS RA19 is required, with a focus on its glycosidic linkage composition and acyl content. This will provide a deeper understanding of the polymer's complex mechanisms.

The optimization of EPS-based films should be explored further by adjusting the type and concentration of plasticizers. Assessing their gas and water vapor permeability will be essential for comprehensive characterization. To further enhance their mechanical and barrier properties for a wider range of applications, the incorporation of functional additives or blending with other polymers should also be considered.

Further characterization of EPS RA19-Fe^{2+} gels is necessary, including compression tests, water content determination, swelling studies, and cytotoxicity assessments. These evaluations are crucial to determine the potential application of these gels in drug delivery and tissue engineering.

In vivo studies of EPS-based emulsions should be conducted to assess their applicability in cosmetic formulations. These studies should include skin compatibility testing, irritation and allergic reaction assessments, and sensory evaluations. Additionally, the rheological behavior of these emulsions under varying temperatures and pH should be investigated to confirm their stability and emulsifying activity across a wide range of conditions.

Further testing is also needed to optimize the antioxidant activity of the EPS, with a focus on concentration and exposure conditions. Similarly, photoprotection studies should be expanded to include a broader range of concentrations and exposure times to better understand their protective potential.

Finally, the sulfate content of EPS RA19 presents an opportunity for further research into their anti-inflammatory and antimicrobial properties. Investigating these biological activities could expand the scope of its applications in biomedical and therapeutic fields.

BIBLIOGRAPHY

[1] Y. A. G. Mahmoud, M. E. El-Naggar, A. Abdel-Megeed, and M. H. El-Newehy, "Recent advancements in microbial polysaccharides: Synthesis and applications," *Polymers (Basel).*, vol. 13, no. 23, p. 4136, 2021, doi: 10.3390/polym13234136.

[2] A. S. A. Mohammed, M. Naveed, and N. Jost, "Polysaccharides; Classification, Chemical Properties, and Future Perspective Applications in Fields of Pharmacology and Biological Medicine (A Review of Current Applications and Upcoming Potentialities)," *J. Polym. Environ.*, vol. 29, no. 8, pp. 2359–2371, 2021, doi: 10.1007/s10924-021-02052-2.

[3] P. Cescutti, "Bacterial capsular polysaccharides and exopolysaccharides," in *Microbial Glycobiology*, First Edit., Elsevier Inc., 2010, ch. 6, pp. 93–108. doi: 10.1016/B978-0-1237-4546-0.00006-7.

[4] C. Delbarre-Ladrat, C. Sinquin, L. Lebellenger, A. Zykwinska, and S. Colliec-Jouault, "Exopolysaccharides produced by marine bacteria and their applications as glycosaminoglycan-like molecules," *Front. Chem.*, vol. 2, 2014, doi: 10.3389/fchem.2014.00085.

[5] F. Freitas, C. A. V. Torres, D. Araújo, and I. Farinha, "Advanced Microbial Polysaccharides," in *Biopolymers for Biomedical and Biotechnological Applications*, Wiley, 2021, ch. 2, pp. 19–62. doi: 10.1002/9783527818310.

[6] S. S. Nadda, Ashok Kumar, Sajna K. V, *Microbial Exopolysaccharides as Novel and Significant Biomaterials*. 2021. doi: 10.1007/978-3-030-75289-7.

[7] F. Freitas *et al.*, "Fucose-containing exopolysaccharide produced by the newly isolated Enterobacter strain A47 DSM 23139," *Carbohydr. Polym.*, vol. 83, no. 1, pp. 159–165, 2011, doi: 10.1016/j.carbpol.2010.07.034.

[8] O. Torres, A. Yamada, N. M. Rigby, T. Hanawa, Y. Kawano, and A. Sarkar, "Gellan gum: A new member in the dysphagia thickener family," *Biotribology*, vol. 17, pp. 8–18, 2019, doi: 10.1016/j.biotri.2019.02.002.

[9] R. Srikanth, C. H. S. S. S. Reddy, G. Siddartha, M. J. Ramaiah, and K. B. Uppuluri, "Review on production, characterization and applications of microbial levan," *Carbohydr. Polym.*, vol. 120, pp. 102–114, 2015, doi: 10.1016/j.carbpol.2014.12.003.

[10] A. Kumar, K. M. Rao, and S. S. Han, "Application of xanthan gum as polysaccharide in tissue engineering: A review," *Carbohydr. Polym.*, vol. 180, pp. 128–144, 2018, doi: 10.1016/j.carbpol.2017.10.009.

[11] K. Y. Lee and D. J. Mooney, "Alginate: Properties and biomedical applications," *Prog.*

Polym. Sci., vol. 37, no. 1, pp. 106–126, 2012, doi: 10.1016/j.progpolymsci.2011.06.003.
[12] P. G. Mahendra Rai, Magdalena Wypij, Avinash P. Ingle, Joanna Trzcinska-Wencel, "Emerging Trends in Pullulan-Based Antimicrobial Systems for Various Applications," *Int. J. Mol. Sci.*, vol. 22, no. 24, p. 13596, 2021, doi: 10.3390/ijms222413596.
[13] S. Priya *et al.*, "Exploring polysaccharide-based bio-adhesive topical film as a potential platform for wound dressing application: A review," *Carbohydr. Polym.*, vol. 327, p. 121655, 2024, doi: 10.1016/j.carbpol.2023.121655.
[14] M. Zhang, Y. Zhang, L. Zhang, and Q. Tian, "Mushroom polysaccharide lentinan for treating different types of cancers: A review of 12 years clinical studies in China," in *Progress in Molecular Biology and Translational Science*, 1st ed., vol. 163, Elsevier Inc., 2019, ch. 13, pp. 297–328. doi: 10.1016/bs.pmbts.2019.02.013.
[15] A. I. Netrusov, E. V. Liyaskina, I. V. Kurgaeva, A. U. Liyaskina, G. Yang, and V. V. Revin, "Exopolysaccharides Producing Bacteria : A Review," *Microorganisms*, vol. 11, no. 6, p. 1541, 2023, doi: 10.3390/microorganisms11061541.
[16] O. Guetta, K. Mazeau, R. Auzely, M. Milas, and M. Rinaudo, "Structure and properties of a bacterial polysaccharide named fucogel," *Biomacromolecules*, vol. 4, no. 5, pp. 1362–1371, 2003, doi: 10.1021/bm030033h.
[17] A. Iyer, K. Mody, and B. Jha, "Characterization of an exopolysaccharide produced by a marine Enterobacter cloacae," Indian Journal of Experimental Biology.
[18] Y. I. Karadayi, G. Aykutoglu, N. P. Arslan, M. O. Baltaci, A. Adiguzel, and M. Taskin, "Production of water-soluble sulfated exopolysaccharide with anticancer activity from Anoxybacillus gonensis YK25," *J. Chem. Technol. Biotechnol.*, vol. 96, no. 5, pp. 1258–1266, 2020, doi: 10.1002/jctb.6638.
[19] P. Concórdio-Reis *et al.*, "Silver nanocomposites based on the bacterial fucose-rich polysaccharide secreted by Enterobacter A47 for wound dressing applications: Synthesis, characterization and in vitro bioactivity," *Int. J. Biol. Macromol.*, vol. 163, pp. 959–969, 2020, doi: 10.1016/j.ijbiomac.2020.07.072.
[20] B. M. Guerreiro, F. Freitas, J. C. Lima, J. C. Silva, and M. A. M. Reis, "Photoprotective effect of the fucose-containing polysaccharide FucoPol," *Carbohydr. Polym.*, vol. 259, p. 117761, 2021, doi: 10.1016/j.carbpol.2021.117761.
[21] S. Baptista, J. R. Pereira, C. V. Gil, C. A. V. Torres, M. A. M. Reis, and F. Freitas, "Development of Olive Oil and α-Tocopherol Containing Emulsions Stabilized by FucoPol: Rheological and Textural Analyses," *Polymers (Basel).*, vol. 14, no. 12, p. 2349, 2022, doi: 10.3390/polym14122349.
[22] D. Araújo *et al.*, "Novel Hydrogel Membranes Based on the Bacterial Polysaccharide FucoPol: Design, Characterization and Biological Properties," *Pharmaceuticals*, vol. 16, no. 7, p. 991, 2023, doi: 10.3390/ph16070991.
[23] F. Raquel Maia, V. M. Correlo, J. M. Oliveira, and R. L. Reis, "Natural Origin Materials for Bone Tissue Engineering: Properties, Processing, and Performance," in *Principles of Regenerative Medicine*, Third Edit., Elsevier Inc., 2019, ch. 32, pp. 535–558. doi: 10.1016/B978-0-12-809880-6.00032-1.
[24] H. Ben Hlima *et al.*, "Sulfated exopolysaccharides from Porphyridium cruentum: A useful strategy to extend the shelf life of minced beef meat," *Int. J. Biol. Macromol.*, vol. 193, pp. 1215–1225, 2021, doi: 10.1016/j.ijbiomac.2021.10.161.
[25] M. I. Bilan, A. A. Grachev, A. S. Shashkov, N. E. Nifantiev, and A. I. Usov, "Structure of a

fucoidan from the brown seaweed Fucus serratus L.," *Carbohydr. Res.*, vol. 341, no. 2, pp. 238–245, 2005, doi: 10.1016/j.carres.2005.11.009.
[26] B. Li, F. Lu, X. Wei, and R. Zhao, "Fucoidan: Structure and bioactivity," *Molecules*, vol. 13, no. 8, pp. 1671–1695, 2008, doi: 10.3390/molecules13081671.
[27] R. G. Puscaselu, A. Lobiuc, M. Dimian, and M. Covasa, "Alginate: From food industry to biomedical applications and management of metabolic disorders," *Polymers (Basel).*, vol. 12, no. 10, p. 2417, 2020, doi: 10.3390/polym12102417.
[28] E. K. Hadde, B. Mossel, J. Chen, and S. Prakash, "The safety and efficacy of xanthan gum-based thickeners and their effect in modifying bolus rheology in the therapeutic medical management of dysphagia," *Food Hydrocoll. Heal.*, vol. 1, p. 100038, 2021, doi: 10.1016/j.fhfh.2021.100038.
[29] C. Roca, V. D. Alves, F. Freitas, and M. A. M. Reis, "Exopolysaccharides enriched in rare sugars: Bacterial sources, production, and applications," *Front. Microbiol.*, vol. 6, 2015, doi: 10.3389/fmicb.2015.00288.
[30] Y. M. M. Mohammed, M. M. G. Saad, and S. A. M. Abdelgaleil, "Production, characterization and bio-emulsifying application of exopolysaccharides from Rhodotorula mucilaginosa YMM19," *3 Biotech*, vol. 11, no. 7, 2021, doi: 10.1007/s13205-021-02898-2.
[31] G. Jiang *et al.*, "Exopolysaccharide Produced by Pediococcus pentosaceus E8: Structure, Bio-Activities, and Its Potential Application," *Front. Microbiol.*, vol. 13, 2022, doi: 10.3389/fmicb.2022.923522.
[32] R. Rupert, K. F. Rodrigues, V. Y. Thien, and W. T. L. Yong, "Carrageenan From Kappaphycus alvarezii (Rhodophyta, Solieriaceae): Metabolism, Structure, Production, and Application," *Front. Plant Sci.*, vol. 13, 2022, doi: 10.3389/fpls.2022.859635.
[33] M. H. Shafie *et al.*, "Application of Carrageenan extract from red seaweed (Rhodophyta) in cosmetic products: A review," *J. Indian Chem. Soc.*, vol. 99, no. 9, p. 100613, 2022, doi: 10.1016/j.jics.2022.100613.
[34] Ö. Kahraman-Ilıkkan *et al.*, "The wound healing effect and DNA damage repair of exopolysaccharide extracted from Weissella cibaria MED17," *Bioact. Carbohydrates Diet. Fibre*, vol. 31, p. 100400, 2024, doi: 10.1016/j.bcdf.2023.100400.
[35] J. T. Kidgell, M. Magnusson, R. de Nys, and C. R. K. Glasson, "Ulvan: A systematic review of extraction, composition and function," *Algal Res.*, vol. 39, p. 101422, 2019, doi: 10.1016/j.algal.2019.101422.
[36] X. Li *et al.*, "Characterisation of the molecular properties of scleroglucan as an alternative rigid rod molecule to xanthan gum for oropharyngeal dysphagia," *Food Hydrocoll.*, vol. 101, p. 105446, 2020, doi: 10.1016/j.foodhyd.2019.105446.
[37] M. Hamidi *et al.*, "Exopolysaccharide from the yeast Papiliotrema terrestris PT22AV for skin wound healing," *J. Adv. Res.*, vol. 46, pp. 61–74, 2023, doi: 10.1016/j.jare.2022.06.012.
[38] Y. Wei, Y. Guo, R. Li, A. Ma, and H. Zhang, "Rheological characterization of polysaccharide thickeners oriented for dysphagia management: Carboxymethylated curdlan, konjac glucomannan and their mixtures compared to xanthan gum," *Food Hydrocoll.*, vol. 110, p. 106198, 2021, doi: 10.1016/j.foodhyd.2020.106198.
[39] A. A. Waoo *et al.*, "Microbial exopolysaccharides in the biomedical and pharmaceutical industries," *Heliyon*, vol. 9, no. 8, p. e18613, 2023, doi: 10.1016/j.heliyon.2023.e18613.

[40] J. Guézennec, X. Moppert, G. Raguéns, L. Richert, B. Costa, and C. Simon-Colin, "Microbial mats in French Polynesia and their biotechnological applications," *Process Biochem.*, vol. 46, no. 1, pp. 16–22, 2011, doi: 10.1016/j.procbio.2010.09.001.
[41] J. Wang, D. R. Salem, and R. K. Sani, "Extremophilic exopolysaccharides: A review and new perspectives on engineering strategies and applications," *Carbohydr. Polym.*, vol. 205, pp. 8–26, 2018, doi: 10.1016/j.carbpol.2018.10.011.
[42] R. Jeewon, A. A. Aullybux, D. Puchooa, N. Nazurally, A. F. Alrefaei, and Y. Zhang, "Marine Microbial Polysaccharides : An Untapped Resource for Biotechnological Applications," *Mar. Drugs*, vol. 21, no. 7, p. 420, 2023, doi: 10.3390/md21070420.
[43] D. J. Becker and J. B. Lowe, "Fucose: Biosynthesis and biological function in mammals," *Glycobiology*, vol. 13, no. 7, pp. 41R-53R, 2003, doi: 10.1093/glycob/cwg054.
[44] S. Li *et al.*, "Combinatorial Metabolic Engineering and Enzymatic Catalysis Enable Efficient Production of Colanic Acid," *Microorganisms*, vol. 10, no. 5, p. 1877, 2022, doi: 10.3390/microorganisms10050877.
[45] M. Rättö *et al.*, "Colanic acid is an exopolysaccharide common to many enterobacteria isolated from paper-machine slimes," *J. Ind. Microbiol. Biotechnol.*, vol. 33, no. 5, pp. 359–367, 2006, doi: 10.1007/s10295-005-0064-1.
[46] C. Robert, A. M. Robert, and L. Robert, "Effect of a fucose-rich polysaccharide preparation on the age-dependent evolution of the skin surface micro-relief," *Pathol. Biol.*, vol. 51, no. 10, pp. 586–590, 2003, doi: 10.1016/j.patbio.2003.09.009.
[47] L. Robert, I. Fodil-Bourahla, L. Bizbiz, and A. M. Robert, "Effects of L-fucose and fucose-rich oligo- and polysaccharides (FROP-s) on collagen biosynthesis by human skin fibroblasts. Modulation of the effect of retinol, ascorbate and α-tocopherol," *Biomed. Pharmacother.*, vol. 58, no. 1, pp. 65–70, 2004, doi: 10.1016/j.biopha.2003.06.003.
[48] S. Baptista and F. Freitas, "Formulation of the Polysaccharide FucoPol into Novel Emulsified Creams with Improved Physicochemical Properties," *Molecules*, vol. 27, no. 22, p. 7759, 2022, doi: 10.3390/molecules27227759.
[49] L. Fialho *et al.*, "Cation-mediated gelation of the fucose-rich polysaccharide FucoPol: preparation and characterization of hydrogel beads and their cytotoxicity assessment," *Int. J. Polym. Mater. Polym. Biomater.*, vol. 70, no. 2, pp. 90–99, 2019, doi: 10.1080/00914037.2019.1695205.
[50] B. M. Guerreiro, F. Freitas, J. C. Lima, J. C. Silva, M. Dionísio, and M. A. M. Reis, "Demonstration of the cryoprotective properties of the fucose-containing polysaccharide FucoPol," *Carbohydr. Polym.*, vol. 245, p. 116500, 2020, doi: 10.1016/j.carbpol.2020.116500.
[51] S. Raveendran, Y. Yoshida, T. Maekawa, and D. S. Kumar, "Pharmaceutically versatile sulfated polysaccharide based bionano platforms," *Nanomedicine Nanotechnology, Biol. Med.*, vol. 9, no. 5, pp. 605–626, 2013, doi: 10.1016/j.nano.2012.12.006.
[52] K. Guehaz *et al.*, "A sulfated exopolysaccharide derived from Chlorella sp. exhibiting in vitro anti-α-d-Glucosidase activity," *Arch. Microbiol.*, vol. 206, no. 5, 2024, doi: 10.1007/s00203-024-03940-6.
[53] J. H. Xie *et al.*, "Sulfated modification, characterization and antioxidant activities of polysaccharide from Cyclocarya paliurus," *Food Hydrocoll.*, vol. 53, pp. 7–15, 2016, doi: 10.1016/j.foodhyd.2015.02.018.
[54] Y. Chang *et al.*, "Primary structure and chain conformation of fucoidan extracted from

sea cucumber Holothuria tubulosa," *Carbohydr. Polym.*, vol. 136, pp. 1091–1097, 2016, doi: 10.1016/j.carbpol.2015.10.016.
[55] L. M. Cao, Z. X. Sun, E. C. Makale, G. K. Du, W. F. Long, and H. R. Huang, "Antitumor activity of fucoidan: a systematic review and meta-analysis," *Transl. Cancer Res.*, vol. 10, no. 12, pp. 5390–5405, 2021, doi: 10.21037/tcr-21-1733.
[56] E. Apostolova *et al.*, "Immunomodulatory and anti-inflammatory effects of fucoidan: A review," *Polymers (Basel).*, vol. 12, no. 10, p. 2338, 2020, doi: 10.3390/polym12102338.
[57] W. A. J. P. Wijesinghe, Y. Athukorala, and Y. J. Jeon, "Effect of anticoagulative sulfated polysaccharide purified from enzyme-assistant extract of a brown seaweed Ecklonia cava on Wistar rats," *Carbohydr. Polym.*, vol. 86, no. 2, pp. 917–921, 2011, doi: 10.1016/j.carbpol.2011.05.047.
[58] M. Álvarez-Viñas *et al.*, "Efficient extraction of carrageenans from Chondrus crispus for the green synthesis of gold nanoparticles and formulation of printable hydrogels," *Int. J. Biol. Macromol.*, vol. 206, pp. 553–566, 2022, doi: 10.1016/j.ijbiomac.2022.02.145.
[59] A. Ali and S. Ahmed, "Carrageenans: Structure, Properties and Applications," in *Marine Polysaccharides*, First Edit., 2019, ch. 3, pp. 29–52. doi: 10.1201/9780429058929-3.
[60] M. Álvarez-Viñas, S. Souto, N. Flórez-Fernández, M. D. Torres, I. Bandín, and H. Domínguez, "Antiviral activity of carrageenans and processing implications," *Mar. Drugs*, vol. 19, no. 8, p. 437, 2021, doi: 10.3390/md19080437.
[61] E. Cicinskas, A. A. Kalitnik, Y. A. Karetin, M. S. G. Mohan Ram, A. Achary, and A. O. Kravchenko, "Immunomodulating Properties of Carrageenan from Tichocarpus crinitus," *Inflammation*, vol. 43, no. 4, pp. 1387–1396, 2020, doi: 10.1007/s10753-020-01216-x.
[62] A. K. P. Grace Sathyanesan Anisha, Tessy Augustianath, Savitha Padmakumari, Reeta Rani Singhania, Ashok Pandey, "Bioresource Technology Reports Ulvan from green macroalgae : Bioactive properties advancing tissue engineering , drug delivery systems , food industry , agriculture and water treatment," *Bioresour. Technol. Reports*, vol. 22, p. 101457, 2023, doi: 10.1016/j.biteb.2023.101457.
[63] L. Lei, Y. Bai, X. Qin, J. Liu, W. Huang, and Q. Lv, "Current Understanding of Hydrogel for Drug Release and Tissue Engineering," *Gels*, vol. 8, no. 5, p. 301, 2022, doi: 10.3390/gels8050301.
[64] S. Shen, X. Chen, Z. Shen, and H. Chen, "Marine polysaccharides for wound dressings application: An overview," *Pharmaceutics*, vol. 13, no. 10, p. 1666, 2021, doi: 10.3390/pharmaceutics13101666.
[65] M. Downer, C. E. Berry, J. B. Parker, L. Kameni, and M. Griffin, "Current Biomaterials for Wound Healing," *Bioengineering*, vol. 10, no. 12, p. 1378, 2023, doi: 10.3390/bioengineering10121378.
[66] A. Zanotti, L. Baldino, and E. Reverchon, "Production of Exopolysaccharide-Based Porous Structures for Biomedical Applications: A Review," *Nanomaterials*, vol. 13, no. 22, p. 2920, 2023, doi: 10.3390/nano13222920.
[67] B. F. Cress, J. A. Englaender, W. He, D. Kasper, R. J. Linhardt, and M. A. G. Koffas, "Masquerading microbial pathogens: Capsular polysaccharides mimic host-tissue molecules," *FEMS Microbiol. Rev.*, vol. 38, no. 4, pp. 660–697, 2014, doi: 10.1111/1574-6976.12056.
[68] K. Zeng, T. Groth, and K. Zhang, "Recent Advances in Artificially Sulfated

Polysaccharides for Applications in Cell Growth and Differentiation, Drug Delivery, and Tissue Engineering," *ChemBioChem*, vol. 20, no. 6, pp. 737–746, 2019, doi: 10.1002/cbic.201800569.

[69] B. Bravo, P. Correia, J. E. Gonçalves Junior, B. Sant'Anna, and D. Kerob, "Benefits of topical hyaluronic acid for skin quality and signs of skin aging: From literature review to clinical evidence," *Dermatol. Ther.*, vol. 35, no. 12, 2022, doi: 10.1111/dth.15903.

[70] A. Di Mola, M. R. Landi, A. Massa, U. D'Amora, and V. Guarino, "Hyaluronic Acid in Biomedical Fields: New Trends from Chemistry to Biomaterial Applications," *Int. J. Mol. Sci.*, vol. 23, no. 22, p. 14372, 2022, doi: 10.3390/ijms232214372.

[71] A. Marinho, C. Nunes, and S. Reis, "Hyaluronic acid: A key ingredient in the therapy of inflammation," *Biomolecules*, vol. 11, no. 10, p. 1518, 2021, doi: 10.3390/biom11101518.

[72] I. Saha and S. Datta, "Bacterial exopolysaccharides in drug delivery applications," *J. Drug Deliv. Sci. Technol.*, vol. 74, p. 103557, 2022, doi: 10.1016/j.jddst.2022.103557.

[73] T. C. Ezike *et al.*, "Advances in drug delivery systems, challenges and future directions," *Heliyon*, vol. 9, no. 6, p. e17488, 2023, doi: 10.1016/j.heliyon.2023.e17488.

[74] M. A. S. Abourehab *et al.*, "Alginate as a Promising Biopolymer in Drug Delivery and Wound Healing: A Review of the State-of-the-Art," *Int. J. Mol. Sci.*, vol. 23, no. 16, p. 9035, 2022, doi: 10.3390/ijms23169035.

[75] P. Paul, G. Nandi, M. A. Abosheasha, and H. Bera, "Alginate-based systems for protein and peptide delivery," in *Tailor-Made and Functionalized Biopolymer Systems: For Drug Delivery and Biomedical Applications*, Elsevier, 2021, pp. 85–113. doi: 10.1016/B978-0-12-821437-4.00011-6.

[76] C. P. Fu *et al.*, "Hyaluronic Acid-Based Nanocarriers for Anticancer Drug Delivery," *Polymers (Basel).*, vol. 15, no. 10, p. 2317, 2023, doi: 10.3390/polym15102317.

[77] C. S. Chiang *et al.*, "Fucoidan-based nanoparticles with inherently therapeutic efficacy for cancer treatment," *Pharmaceutics*, vol. 13, no. 12, p. 1986, 2021, doi: 10.3390/pharmaceutics13121986.

[78] A. Berradi, F. Aziz, M. E. Achaby, N. Ouazzani, and L. Mandi, "A Comprehensive Review of Polysaccharide-Based Hydrogels as Promising Biomaterials," *Polymers (Basel).*, vol. 15, no. 13, p. 2908, 2023, doi: 10.3390/polym15132908.

[79] F. Benhadda *et al.*, "Marine versus Non-Marine Bacterial Exopolysaccharides and Their Skincare Applications," *Mar. Drugs*, vol. 21, no. 11, p. 582, 2023, doi: 10.3390/md21110582.

[80] H. S. Kalasariya, C. E. Maya-Ramírez, J. Cotas, and L. Pereira, "Cosmeceutical Significance of Seaweed: A Focus on Carbohydrates and Peptides in Skin Applications," *Phycology*, vol. 4, no. 2, pp. 276–313, 2024, doi: 10.3390/phycology4020015.

[81] S. Baptista, J. R. Pereira, B. M. Guerreiro, F. Baptista, J. C. Silva, and F. Freitas, "Cosmetic emulsion based on the fucose-rich polysaccharide FucoPol: Bioactive properties and sensorial evaluation," *Colloids Surfaces B Biointerfaces*, vol. 225, p. 113252, 2023, doi: 10.1016/j.colsurfb.2023.113252.

[82] T. Morais, J. Cotas, D. Pacheco, and L. Pereira, "Seaweeds compounds: An ecosustainable source of cosmetic ingredients?," *Cosmetics*, vol. 8, no. 1, 2021, doi: 10.3390/COSMETICS8010008.

[83] A. P. JB Prajapat, "Food and Health Applications of Exopolysaccharides produced by

Lactic acid Bacteria," *Adv. Dairy Res.*, vol. 1, no. 2, 2013, doi: 10.4172/2329-888x.1000107.
[84] E. Korcz and L. Varga, "Exopolysaccharides from lactic acid bacteria: Techno-functional application in the food industry," *Trends Food Sci. Technol.*, vol. 110, pp. 375–384, 2021, doi: 10.1016/j.tifs.2021.02.014.
[85] D. Saha and S. Bhattacharya, "Hydrocolloids as thickening and gelling agents in food: A critical review," *J. Food Sci. Technol.*, vol. 47, no. 6, pp. 587–597, 2010, doi: 10.1007/s13197-010-0162-6.
[86] S. Pirsa and K. Hafezi, "Hydrocolloids: Structure, preparation method, and application in food industry," *Food Chem.*, vol. 399, p. 133967, 2023, doi: 10.1016/j.foodchem.2022.133967.
[87] A. Sullo and I. T. Norton, *Food Colloids and Emulsions*, First Edit. Elsevier, 2015. doi: 10.1016/B978-0-12-384947-2.00186-0.
[88] Y. Zhao *et al.*, "Comprehensive review of polysaccharide-based materials in edible packaging: A sustainable approach," *Foods*, vol. 10, no. 8, p. 1845, 2021, doi: 10.3390/foods10081845.
[89] T. I. Adegbolagun, O. A. Odeniyi, and M. A. Odeniyi, "Drug delivery applications and future prospects of microbial exopolysaccharides," *Polym. Med.*, vol. 53, no. 2, pp. 117–127, 2023, doi: 10.17219/pim/176590.
[90] G. Lara *et al.*, "Spray technology applications of xanthan gum-based edible coatings for fresh-cut lotus root (Nelumbo nucifera)," *Food Res. Int.*, vol. 137, p. 109723, 2020, doi: 10.1016/j.foodres.2020.109723.
[91] S. Farris, I. U. Unalan, L. Introzzi, J. M. Fuentes-Alventosa, and C. A. Cozzolino, "Pullulan-based films and coatings for food packaging: Present applications, emerging opportunities, and future challenges," *J. Appl. Polym. Sci.*, vol. 131, no. 13, 2014, doi: 10.1002/app.40539.
[92] C. H. Yang *et al.*, "Strengthening alginate/polyacrylamide hydrogels using various multivalent cations," *ACS Appl. Mater. Interfaces*, vol. 5, no. 21, pp. 10418–10422, 2013, doi: 10.1021/am403966x.
[93] V. Kadirvel and G. P. Narayana, "Edible gums—An extensive review on its diverse applications in various food sectors," *Food Bioeng.*, vol. 2, no. 4, pp. 384–405, 2023, doi: 10.1002/fbe2.12067.
[94] C. Costa *et al.*, "Emulsion formation and stabilization by biomolecules: The leading role of cellulose," *Polymers (Basel).*, vol. 11, no. 10, p. 1570, 2019, doi: 10.3390/polym11101570.
[95] A. M. Bakry *et al.*, "Microencapsulation of Oils: A Comprehensive Review of Benefits, Techniques, and Applications," *Compr. Rev. Food Sci. Food Saf.*, vol. 15, no. 1, pp. 143–182, 2015, doi: 10.1111/1541-4337.12179.
[96] G. Raguénès *et al.*, "A novel exopolymer-producing bacterium, Paracoccus zeaxanthinifaciens subsp. payriae, isolated from a 'kopara' mat located in Rangiroa, an atoll of French Polynesia," *Curr. Microbiol.*, vol. 49, no. 3, pp. 145–151, 2004, doi: 10.1007/s00284-004-4303-x.
[97] P. Concórdio-Reis *et al.*, "Novel exopolysaccharide produced by the marine dinoflagellate Heterocapsa AC210: Production, characterization, and biological properties," *Algal Res.*, vol. 70, p. 103014, 2023, doi: 10.1016/j.algal.2023.103014.

[98] F. F. Concórdio-Reis, Patrícia, Sónia S. Ferreira, Vítor D. Alves, Xavier Moppert, Jean Guézennec, Manuel A. Coimbra, Maria A.M. Reis, "Rheological characterization of the exopolysaccharide produced by Alteromonas macleodii Mo 169," *Int. J. Biol. Macromol.*, vol. 227, pp. 619–629, 2023, doi: 10.1016/j.ijbiomac.2022.12.117.
[99] L. A. N. Patrícia Concórdio-Reis, João R. Pereira, Vítor D. Alves, Ana R. Nabais, "Characterisation of Films Based on Exopolysaccharides from Alteromonas Strains Isolated from French Polynesia Marine Environments," *Polymers (Basel).*, vol. 14, no. 20, p. 4442, 2022, doi: 10.3390/polym14204442.
[100] P. Concórdio-Reis, V. D. Alves, X. Moppert, J. Guézennec, F. Freitas, and M. A. M. Reis, "Characterization and biotechnological potential of extracellular polysaccharides synthesized by alteromonas strains isolated from french polynesia marine environments," *Mar. Drugs*, vol. 19, no. 9, p. 522, 2021, doi: 10.3390/md19090522.
[101] P. Priyanka, A. B. Arun, and P. D. Rekha, "Sulfated exopolysaccharide produced by Labrenzia sp. PRIM-30, characterization and prospective applications," *Int. J. Biol. Macromol.*, vol. 69, pp. 290–295, 2014, doi: 10.1016/j.ijbiomac.2014.05.054.
[102] X. Hu, F. Li, X. Zhang, and Y. Pan, "The structure , characterization and dual-activity of exopolysaccharide produced by Bacillus enclensis AP-4 from deep-sea sediments," *Front. Mar. Sci.*, vol. 9, 2022, doi: 10.3389/fmars.2022.976543.
[103] M. I. T. René Emanuel Lobo, María Inés Gómez, Graciela Font de Valdez, "Physicochemical and antioxidant properties of a gastroprotective exopolysaccharide produced by Streptococcus thermophilus CRL1190," *Food Hydrocoll.*, vol. 96, pp. 625–633, 2019, doi: 10.1016/j.foodhyd.2019.05.036.
[104] M. Roman and W. T. Winter, "Effect of Sulfate Groups from Sulfuric Acid Hydrolysis on the Thermal Degradation Behavior of Bacterial Cellulose," *Biomacromolecules*, vol. 5, no. 5, pp. 1671–1677, 2004, doi: 10.1021/bm034519.
[105] C. A. V. Torres *et al.*, "Rheological studies of the fucose-rich exopolysaccharide FucoPol," *Int. J. Biol. Macromol.*, vol. 79, pp. 611–617, 2015, doi: 10.1016/j.ijbiomac.2015.05.029.
[106] S. Ji *et al.*, "Rheological behaviors of a novel exopolysaccharide produced by Sphingomonas WG and the potential application in enhanced oil recovery," *Int. J. Biol. Macromol.*, vol. 162, pp. 1816–1824, 2020, doi: 10.1016/j.ijbiomac.2020.08.114.
[107] M. M. Mrokowska and A. Krztoń-Maziopa, "Viscoelastic and shear-thinning effects of aqueous exopolymer solution on disk and sphere settling," *Sci. Rep.*, vol. 9, no. 1, 2019, doi: 10.1038/s41598-019-44233-z.
[108] M. Xiao *et al.*, "Preparation, structural characterization and rheological properties of a novel fucose-containing exopolysaccharide from Clavibacter michiganensis," *Food Hydrocoll.*, vol. 151, p. 109850, 2024, doi: 10.1016/j.foodhyd.2024.109850.
[109] Y. Abid *et al.*, "Rheological and emulsifying properties of an exopolysaccharide produced by potential probiotic Leuconostoc citreum-BMS strain," *Carbohydr. Polym.*, vol. 256, p. 117523, 2021, doi: 10.1016/j.carbpol.2020.117523.
[110] M. Cruz, F. Freitas, C. A. V. Torres, M. A. M. Reis, and V. D. Alves, "Influence of temperature on the rheological behavior of a new fucose-containing bacterial exopolysaccharide," *Int. J. Biol. Macromol.*, vol. 48, no. 4, pp. 695–699, 2011, doi: 10.1016/j.ijbiomac.2011.02.012.
[111] A. Haddar, A. Bouallegue, R. Methneni, and S. Ellouz-Chaabouni, "Rheological and

Thermal Properties of Levan from Bacillus mojavensis," *J. Polym. Environ.*, vol. 30, no. 2, pp. 741–751, 2022, doi: 10.1007/s10924-021-02237-9.
[112] M. Han, C. Du, Z. Y. Xu, H. Qian, and W. G. Zhang, "Rheological properties of phosphorylated exopolysaccharide produced by Sporidiobolus pararoseus JD-2," *Int. J. Biol. Macromol.*, vol. 88, pp. 603–613, 2016, doi: 10.1016/j.ijbiomac.2016.04.035.
[113] J. Li *et al.*, "Characterization of an exopolysaccharide with distinct rheological properties from Paenibacillus edaphicus NUST16," *Int. J. Biol. Macromol.*, vol. 105, pp. 1–8, 2017, doi: 10.1016/j.ijbiomac.2017.06.030.
[114] R. Kohn and P. Kovác, "Dissociation constants of D-galacturonic and D-glucuronic acid and their O-methyl derivatives," *Chem. Zvesti*, vol. 32, no. 4, pp. 478–485, 1978.
[115] W. Gongi, J. L. G. Pinchetti, N. Cordeiro, S. Sadok, and H. B. Ouada, "Characterization of biodegradable films based on extracellular polymeric substances extracted from the thermophilic microalga Graesiella sp.," *Algal Res.*, vol. 61, p. 102565, 2022, doi: 10.1016/j.algal.2021.102565.
[116] Y. A. Shah *et al.*, "Mechanical Properties of Protein-Based Food Packaging Materials," *Polymers (Basel).*, vol. 15, no. 7, p. 1724, 2023, doi: 10.3390/polym15071724.
[117] N. Vivek *et al.*, "Synthesis and Characterization of Transparent Biodegradable Chitosan: Exopolysaccharide Composite Films Plasticized by Bio-Derived 1,3-Propanediol," *Sustain. Chem.*, vol. 2, no. 1, pp. 49–62, 2021, doi: 10.3390/suschem2010004.
[118] J. A. Piermaria, A. Pinotti, M. A. Garcia, and A. G. Abraham, "Films based on kefiran, an exopolysaccharide obtained from kefir grain: Development and characterization," *Food Hydrocoll.*, vol. 23, no. 3, pp. 684–690, 2009, doi: 10.1016/j.foodhyd.2008.05.003.
[119] P. Paolicelli *et al.*, "Effect of glycerol on the physical and mechanical properties of thin gellan gum films for oral drug delivery," *Int. J. Pharm.*, vol. 547, no. 1–2, pp. 226–234, 2018, doi: 10.1016/j.ijpharm.2018.05.046.
[120] and K. de la C. Iratxe Zarandona, Mónica Estupiñán, Carla Pérez, Laura Alonso-Sáez, Pedro Guerrero, "Chitosan Films Incorporated with Exopolysaccharides," *Mar. Drugs*, vol. 18, no. 9, p. 447, 2020, doi: 10.3390/md18090447.
[121] F. Freitas *et al.*, "Controlled production of exopolysaccharides from enterobacter A47 as a function of carbon source with demonstration of their film and emulsifying abilities," *Appl. Biochem. Biotechnol.*, vol. 172, no. 2, pp. 641–657, 2013, doi: 10.1007/s12010-013-0560-0.
[122] S. Galus and A. Lenart, "Development and characterization of composite edible films based on sodium alginate and pectin," *J. Food Eng.*, vol. 115, no. 4, pp. 459–465, 2013, doi: 10.1016/j.jfoodeng.2012.03.006.
[123] V. K. Joseph Robert Nastasi, Melissa A. Fitzgerald, "International Journal of Biological Macromolecules Tuning the mechanical properties of pectin films with polyphenol-rich plant extracts," *Int. J. Biol. Macromol.*, vol. 253, p. 127536, 2023, doi: 10.1016/j.ijbiomac.2023.127536.
[124] S. Paudel, S. Regmi, and S. Janaswamy, "Effect of glycerol and sorbitol on cellulose-based biodegradable films," *Food Packag. Shelf Life*, vol. 37, p. 101090, 2023, doi: 10.1016/j.fpsl.2023.101090.
[125] G. I. Olivas and G. V. Barbosa-Cánovas, "Alginate-calcium films: Water vapor permeability and mechanical properties as affected by plasticizer and relative humidity," *Lwt*, vol. 41, no. 2, pp. 359–366, 2008, doi: 10.1016/j.lwt.2007.02.015.

[126] N. Umesh *et al.*, "A hydrogel based on Fe(ii)-GMP demonstrates tunable emission, self-healing mechanical strength and Fenton chemistry-mediated notable antibacterial properties," *Nanoscale*, vol. 16, no. 27, pp. 13050–13060, 2024, doi: 10.1039/d4nr01011f.
[127] L. Wang *et al.*, "Ferrous/Ferric Ions Crosslinked Type II Collagen Multifunctional Hydrogel for Advanced Osteoarthritis Treatment," *Adv. Healthc. Mater.*, vol. 13, no. 10, 2024, doi: 10.1002/adhm.202302833.
[128] I. MacHida-Sano, S. Ogawa, H. Ueda, Y. Kimura, N. Satoh, and H. Namiki, "Effects of composition of iron-cross-linked alginate hydrogels for cultivation of human dermal fibroblasts," *Int. J. Biomater.*, vol. 2012, pp. 1–8, 2012, doi: 10.1155/2012/820513.
[129] D. M. Roquero and E. K. Ali Othman, Artem Melman, "Iron(iii)-cross-linked alginate hydrogels: A critical review," *Mater. Adv.*, vol. 3, no. 4, pp. 1849–1873, 2022, doi: 10.1039/d1ma00959a.
[130] W. Klinkajon and P. Supaphol, "Novel copper (II) alginate hydrogels and their potential for use as anti-bacterial wound dressings," *Biomed. Mater.*, vol. 9, no. 4, p. 045008, 2014, doi: 10.1088/1748-6041/9/4/045008.
[131] A. V. Shibaev, D. A. Muravlev, A. K. Muravleva, V. V. Matveev, A. E. Chalykh, and O. E. Philippova, "pH-Dependent gelation of a stiffanionic polysaccharide in the presence of metal ions," *Polymers (Basel).*, vol. 12, no. 4, p. 868, 2020, doi: 10.3390/POLYM12040868.
[132] X. Moppert *et al.*, "Investigations into the uptake of copper, iron and selenium by a highly sulphated bacterial exopolysaccharide isolated from microbial mats," *J. Ind. Microbiol. Biotechnol.*, vol. 36, no. 4, pp. 599–604, 2009, doi: 10.1007/s10295-009-0529-8.
[133] V. M. F. Lai, P. A. L. Wong, and C. Y. Lii, "Effects of cation properties on sol-gel transition and gel properties of κ-carrageenan," *J. Food Sci.*, vol. 65, no. 8, pp. 1332–1337, 2000, doi: 10.1111/j.1365-2621.2000.tb10607.x.
[134] P. Concórdio-Reis *et al.*, "Iron(III) cross-linked hydrogels based on Alteromonas macleodii Mo 169 exopolysaccharide," *Int. J. Biol. Macromol.*, vol. 274, p. 133312, 2024, doi: 10.1016/j.ijbiomac.2024.133312.
[135] A. Torres, L. Rego, M. S. Martins, M. S. Ferreira, M. T. Cruz, and I. F. Almeida, "How to Promote Skin Repair ? In-Depth Look at Pharmaceutical and Cosmetic Strategies," *Pharmaceuticals*, vol. 16, no. 4, p. 573, 2023, doi: 10.3390/ph16040573.
[136] I. T. Lorenzo Flori, Sandra Donnini, Vincenzo Calderone, Angela Zinnai and L. T. Francesca Venturi, "The Nutraceutical Value of Olive Oil and Its Bioactive Constituents on the Cardiovascular System. Focusing on Main Strategies to Slow Down Its Quality Decay during Production and Storage," *Nutrients*, vol. 11, no. 9, p. 1962, 2019, doi: 10.3390/nu11091962.
[137] Z. Ahmad, "The uses and properties of almond oil," *Complement. Ther. Clin. Pract.*, vol. 16, no. 1, pp. 10–12, 2010, doi: 10.1016/j.ctcp.2009.06.015.
[138] E. G. de M. L. Tereza Cristina Luque Castellanea, João Carlos Campanharo, Luiz Alberto Colnago, Isabel Duarte Coutinho, Érica Mendes Lopes, Manoel Victor Franco Lemos, "Characterization of new exopolysaccharide production by Rhizobium tropici during growth on hydrocarbon substrate," *Int. J. Biol. Macromol.*, vol. 96, pp. 361–369, 2017, doi: 10.1016/j.ijbiomac.2016.11.123.

[139] P. Shao, J. Feng, P. Sun, N. Xiang, B. Lu, and D. Qiu, "Recent advances in improving stability of food emulsion by plant polysaccharides," *Food Res. Int.*, vol. 137, p. 109376, 2020, doi: 10.1016/j.foodres.2020.109376.
[140] D. J. McClements, *Food Emulsions: Principles, Practices, and Techniques*, 3rd Editio. CRC Press, 2015. doi: 10.1201/b18868.
[141] D. Kavitake, S. Balyan, and P. Bruntha, "Evaluation of oil-in-water (O / W) emulsifying properties of galactan exopolysaccharide from Weissella confusa KR780676," *J. Food Sci. Technol.*, vol. 57, no. 4, pp. 1579–1585, 2020, doi: 10.1007/s13197-020-04262-3.
[142] T. F. Tadros, *Emulsion Formation and Stability*. Wiley, 2013. doi: 10.1002/9783527647941.
[143] S. Mirarab Razi, A. Motamedzadegan, S. A. Shahidi, and A. Rashidinejad, "The physical and rheological properties of egg albumin emulsions are influenced by basil seed gum as the stabilizer," *J. Food Bioprocess Eng.*, vol. 3, no. 1, pp. 61–68, 2020, doi: 10.22059/jfabe.2020.76607.
[144] D. H. El-Ghonemy, "Antioxidant and antimicrobial activities of exopolysaccharides produced by a novel Aspergillus sp. DHE6 under optimized submerged fermentation conditions," *Biocatal. Agric. Biotechnol.*, vol. 36, p. 102150, 2021, doi: 10.1016/j.bcab.2021.102150.
[145] E. H. Zaghloul and M. I. A. Ibrahim, "Production and Characterization of Exopolysaccharide From Newly Isolated Marine Probiotic Lactiplantibacillus plantarum EI6 With in vitro Wound Healing Activity," *Front. Microbiol.*, vol. 13, 2022, doi: 10.3389/fmicb.2022.903363.
[146] E. E. and S. Kusmartsev and Abstract, "Identification of ROS Using Oxidized DCFDA and Flow-Cytometry," in *Advanced Protocols in Oxidative Stress II. Methods in Molecular Biology*, vol. 594, Totowa, NJ: Humana Press, 2010, ch. 4, pp. 57–72. doi: 10.1007/978-1-60761-411-1_4.
[147] P. Patlevič, J. Vašková, P. Švorc, L. Vaško, and P. Švorc, "Reactive oxygen species and antioxidant defense in human gastrointestinal diseases," *Integr. Med. Res.*, vol. 5, no. 4, pp. 250–258, 2016, doi: 10.1016/j.imr.2016.07.004.
[148] K. Jomova, S. Y. Alomar, S. H. Alwasel, E. Nepovimova, K. Kuca, and M. Valko, "Several lines of antioxidant defense against oxidative stress: antioxidant enzymes, nanomaterials with multiple enzyme-mimicking activities, and low-molecular-weight antioxidants," *Arch. Toxicol.*, vol. 98, no. 5, pp. 1323–1367, 2024, doi: 10.1007/s00204-024-03696-4.
[149] T. Feng and J. Wang, "Oxidative stress tolerance and antioxidant capacity of lactic acid bacteria as probiotic: a systematic review," *Gut Microbes*, vol. 12, no. 1, p. 1801944, 2020, doi: 10.1080/19490976.2020.1801944.
[150] B. M. Guerreiro, J. C. Silva, J. C. Lima, M. A. M. Reis, and F. Freitas, "Antioxidant potential of the bio-based fucose-rich polysaccharide fucopol supports its use in oxidative stress-inducing systems," *Polymers (Basel).*, vol. 13, no. 18, p. 3020, 2021, doi: 10.3390/polym13183020.
[151] M. M. J. P. E. Lara L. Reys, Vijayaganapathy Vaithilingam, "Fucoidan Hydrogels Significantly Alleviate Oxidative Stress and Enhance the Endocrine Function of Encapsulated Beta Cells," *Adv. Funct. Mater.*, vol. 31, no. 35, p. 2011205, 2021, doi: 10.1002/adfm.202011205.

[152] A. R. Young, J. Claveau, and A. B. Rossi, "Ultraviolet radiation and the skin: Photobiology and sunscreen photoprotection," *J. Am. Acad. Dermatol.*, vol. 76, no. 3, pp. S100–S109, 2017, doi: 10.1016/j.jaad.2016.09.038.
[153] Rona M. MacKie, "Long-term health risk to the skin of ultraviolet radiation," *Prog. Biophys. Mol. Biol.*, vol. 92, no. 1, pp. 92–96, 2006, doi: 10.1016/j.pbiomolbio.2006.02.008.
[154] J. Zhao *et al.*, "Protective effects of Lactobacillus reuteri SJ - 47 strain exopolysaccharides on human skin fibroblasts damaged by UVA radiation," *Bioresour. Bioprocess.*, vol. 9, no. 1, 2022, doi: 10.1186/s40643-022-00617-0.
[155] R. Li *et al.*, "Bioactive Materials Promote Wound Healing through Modulation of Cell Behaviors," *Adv. Sci.*, vol. 9, no. 10, p. 2105152, 2022, doi: 10.1002/advs.202105152.
[156] L. Zhu *et al.*, "Polysaccharides composite materials for rapid hemostasis," *J. Drug Deliv. Sci. Technol.*, vol. 66, p. 102890, 2021, doi: 10.1016/j.jddst.2021.102890.
[157] A. Thomas, K. Farah, and R. M. Millis, "Epigenetic Influences on Wound Healing and Hypertrophic-Keloid Scarring: A Review for Basic Scientists and Clinicians," *Cureus*, vol. 14, no. 3, 2022, doi: 10.7759/cureus.23503.
[158] C. Oliveira, D. Sousa, J. A. Teixeira, P. Ferreira-Santos, and C. M. Botelho, "Polymeric biomaterials for wound healing," *Front. Bioeng. Biotechnol.*, vol. 11, 2023, doi: 10.3389/fbioe.2023.1136077.
[159] P. V. K. Marwan Salem Bahaj, Marwan Abdelmahmoud Abdelkarim Maki, KRS Sambasiva Rao, "Progressive exploration on the influence of natural polymers and emerging biomateria in advanced wound care strategies," *Indian J. o f Biochem. Biophys.*, vol. 61, pp. 127–144, 2024, doi: 10.56042/ijbb.v61i3.6881.
[160] W. Wen *et al.*, "Fucoidan promotes angiogenesis and accelerates wound healing through AKT/Nrf2/HIF-1α signalling pathway," *Int. Wound J.*, vol. 20, no. 9, pp. 3606–3618, 2023, doi: 10.1111/iwj.14239.
[161] T. Vieira, J. Carvalho, A. M. Botelho, and J. P. Borges, "Electrospun biodegradable chitosan based-poly(urethane urea) scaffolds for soft tissue engineering," *Mater. Sci. Eng. C*, vol. 103, p. 109819, 2019, doi: 10.1016/j.msec.2019.109819.
[162] A. Nunes *et al.*, "Investigations of Olive Oil Industry By-Products Extracts with Potential Skin Benefits in Topical Formulations," *Pharmaceutics*, vol. 13, no. 4, p. 465, 2021, doi: 10.3390/ pharmaceutics13040465.
[163] R. Komeri, N. Kasoju, and P. R. Anil Kumar, "In vitro cytotoxicity and cytocompatibility assays for biomaterial testing under regulatory platform," in *Biomedical Product and Materials Evaluation: Standards and Ethics*, Elsevier, 2022, pp. 329–353. doi: 10.1016/B978-0-12-823966-7.00009-8.
[164] A. M. Wojtowicz, S. Oliveira, M. W. Carlson, A. Zawadzka, C. F. Rousseau, and D. Baksh, "The importance of both fibroblasts and keratinocytes in a bilayered living cellular construct used in wound healing," *Wound Repair Regen.*, vol. 22, no. 2, pp. 246–255, 2014, doi: 10.1111/wrr.12154.
[165] "ISO/EN 10993-5, Biological Evaluation ofMedical Devices - Part 5 Testes for Cytotoxicity," International Organization for Standardization. [Online]. Available: https://www.iso.org/standard/36406.html
[166] R. Rai, S. Shanmuga, and C. R. Srinivas, "Update on photoprotection," *Indian J. Dermatol.*, vol. 57, no. 5, pp. 335–342, 2012, doi: 10.4103/0019-5154.100472.

[167] X. Xu *et al.*, "The structural characterization and UV-protective properties of an exopolysaccharide from a Paenibacillus isolate," *Front. Pharmacol.*, vol. 15, 2024, doi: 10.3389/fphar.2024.1434136.
[168] Y.-J. J. Lei Wang, Jae-Young Oh, Young-Sang Kim, Hyo-Geun Lee, Jung-Suck Lee, "Anti-Photoaging and Anti-Melanogenesis Effects of Fucoidan Isolated from Hizikia fusiforme and Its Underlying Mechanisms," *Mar. Drugs*, vol. 18, no. 8, p. 427, 2020, doi: 10.3390/md18080427.
[169] W. Su, L. Wang, X. Fu, L. Ni, D. Duan, and J. Xu, "Protective Effect of a Fucose-Rich Fucoidan Isolated from Saccharina japonica against Ultraviolet B-Induced Photodamage In Vitro in Human Keratinocytes and In Vivo in Zebrafish," *Mar. Drugs*, vol. 18, no. 6, p. 316, 2020, doi: 10.3390/md18060316.
[170] C. Zhou *et al.*, "Preliminary characterization, antioxidant and hepatoprotective activities of polysaccharides from Taishan Pinus massoniana pollen," *Molecules*, vol. 23, no. 2, p. 281, 2018, doi: 10.3390/molecules23020281.
[171] X. Li, J. Wei, L. Lin, J. Li, and G. Zheng, "Structural characterization, antioxidant and antimicrobial activities of polysaccharide from Akebia trifoliata (Thunb.) Koidz stem," *Colloids Surfaces B Biointerfaces*, vol. 231, p. 113573, 2023, doi: 10.1016/j.colsurfb.2023.113573.
[172] Y. Q. Wang, J. X. Huang, and W. W. Zhou, "Isolation, characterization and cytoprotective effects against UV radiation of exopolysaccharide produced from Paenibacillus polymyxa PYQ1," *J. Biosci. Bioeng.*, vol. 130, no. 3, pp. 283–289, 2020, doi: 10.1016/j.jbiosc.2020.05.001.
[173] A. E. Shaheen, H. M. Gebreel, L. A. Moussa, A. E. Zakaria, and W. A. Nemr, "Photoprotection Against UV-Induced Skin Damage Using Hyaluronic Acid Produced by Lactiplantibacillus plantarum and Enterococcus durans," *Curr. Microbiol.*, vol. 80, no. 8, 2023, doi: 10.1007/s00284-023-03377-y.
[174] A. Jesus, S. Mota, A. Torres, M. T. Cruz, I. F. Almeida, and H. Cidade, "Antioxidants in Sunscreens: Which and What For?," *Antioxidants*, vol. 12, no. 1, p. 138, 2023, doi: 10.3390/antiox12010138.
[175] M. Nowak, W. Tryniszewski, A. Sarniak, A. Wlodarczyk, P. J. Nowak, and D. Nowak, "Effect of physiological concentrations of vitamin C on the inhibitation of hydroxyl radical induced light emission from Fe2+-EGTA-H2 O2 and Fe3+-EGTA-H2 O2 systems in vitro," *Molecules*, vol. 26, no. 7, p. 1993, 2021, doi: 10.3390/molecules26071993.
[176] A. Nagaraj, Y. Subramaniyan, S. Surya, and P. D. Rekha, "Burn Wound Healing Abilities of a Uronic Acid Containing Exopolysaccharide Produced by the Marine Bacterium Halomonas malpeensis YU-PRIM-29 T," *Appl. Biochem. Biotechnol.*, 2024, doi: 10.1007/s12010-024-04966-8.
[177] F. Bouaziz *et al.*, "Healing efficiency of oligosaccharides generated from almond gum (Prunus amygdalus) on dermal wounds of adult rats," *J. Tissue Viability*, vol. 23, no. 3, pp. 98–108, 2014, doi: 10.1016/j.jtv.2014.07.001.
[178] M. Xu *et al.*, "Arabinose confers protection against intestinal injury by improving integrity of intestinal mucosal barrier," *Int. Immunopharmacol.*, vol. 126, p. 111188, 2024, doi: 10.1016/j.intimp.2023.111188.

A

APPENDIX

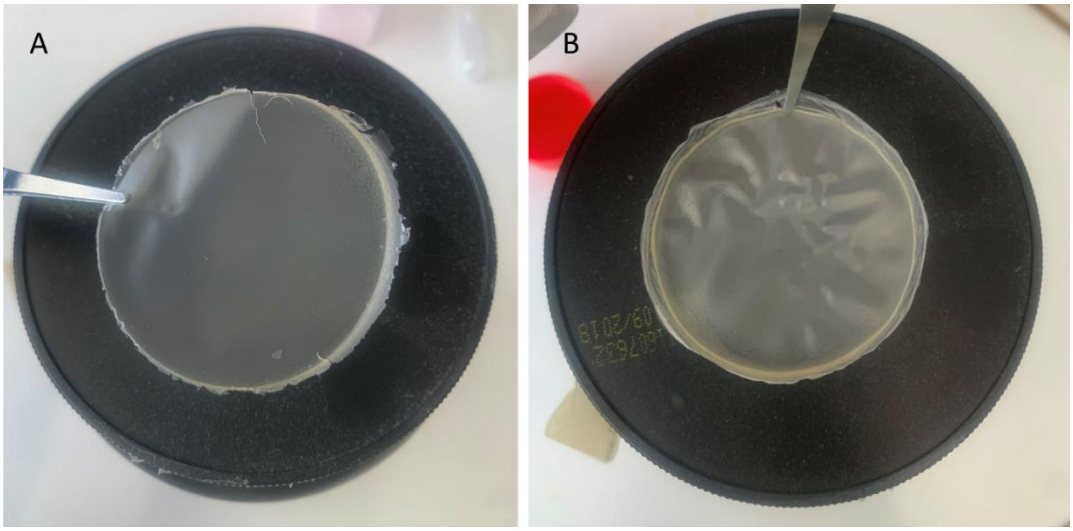

Figure A1. Photographs of the films with (A) 1.5wt.%; and (B) 3 wt.% EPS RA19.

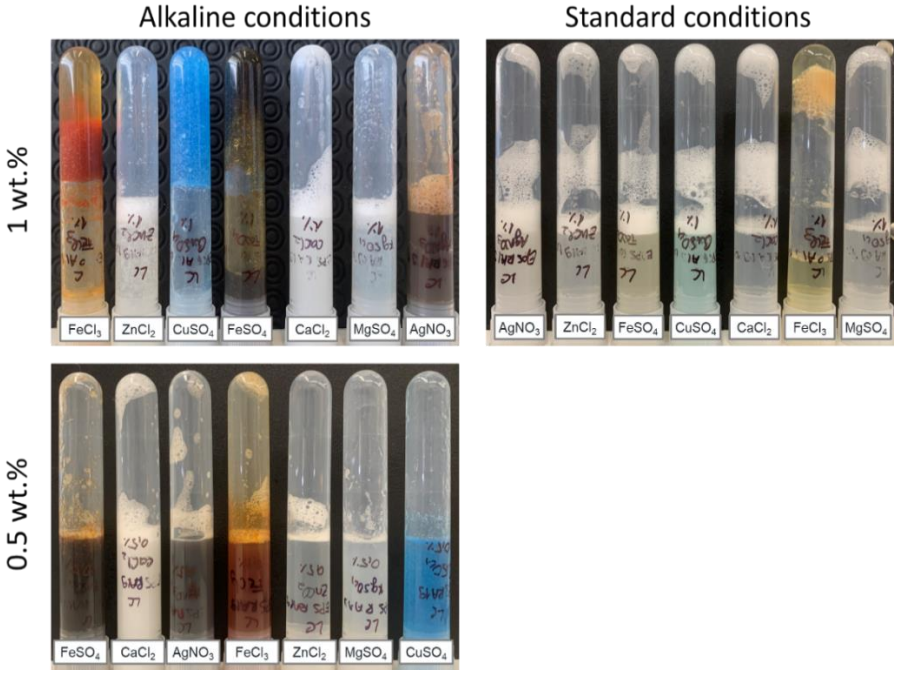

Figure A2. Results of screening cations in order to assess gel formation, under alkaline and standard conditions for 0.5 and 1 wt.% EPS.

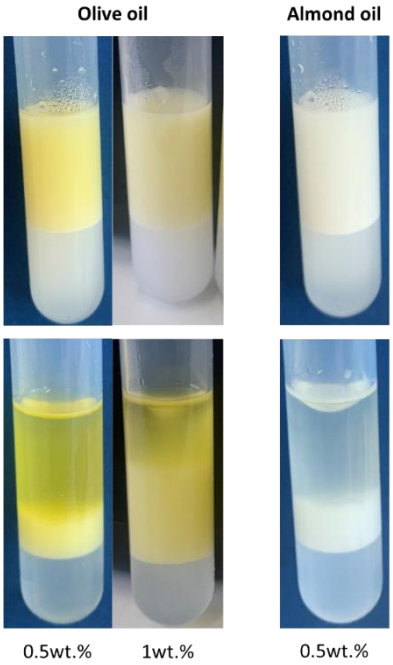

Figure A3. Emulsions formulated with EPS RA19 at 0.5 and 1.0 wt.%, with O:W weight ratios of 2:3 and 3:2, using almond and olive oil.

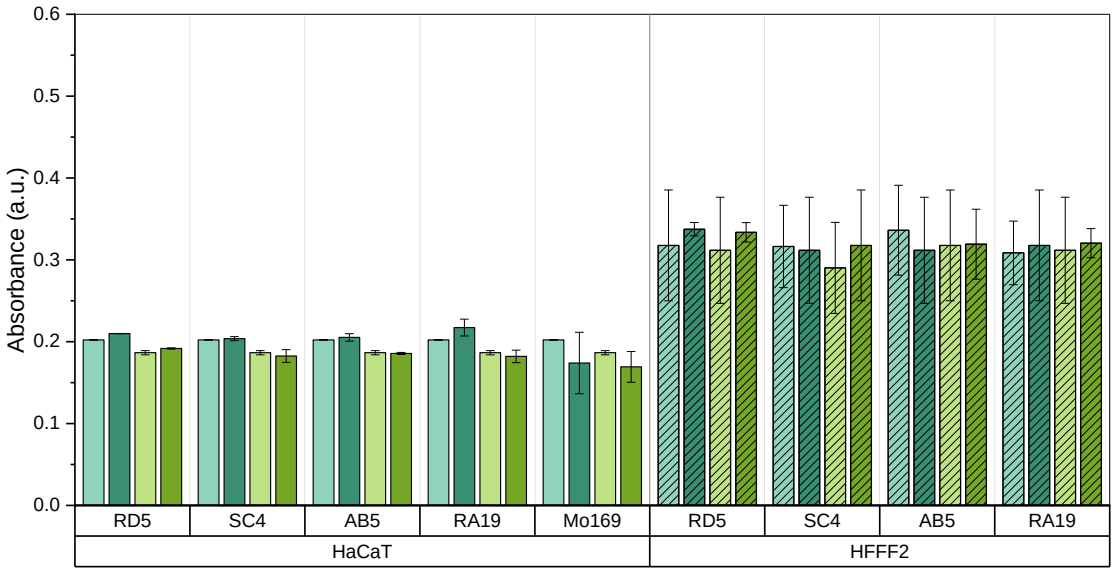

Figure A4. Metabolic viability of irradiated and non-irradiated HaCaT (clear bars) and HFFF2 (striped bars) 2h post exposure to UV radiation, for four EPS, RD5, SC4, AB5 and RA19. Non irradiated cells supplemented with only medium, C-, (▫); Non irradiated cells supplemented with EPS, C+, (▪); Irradiated cells supplemented with only medium, I-, (▫); Irradiated cells supplemented with EPS, I+, (▪). Statistically significant differences comparing samples were determined according to Two way ANOVA (*, p≤0.05, **, p≤0.01, ***, p≤0.001, **** p≤0.0001).

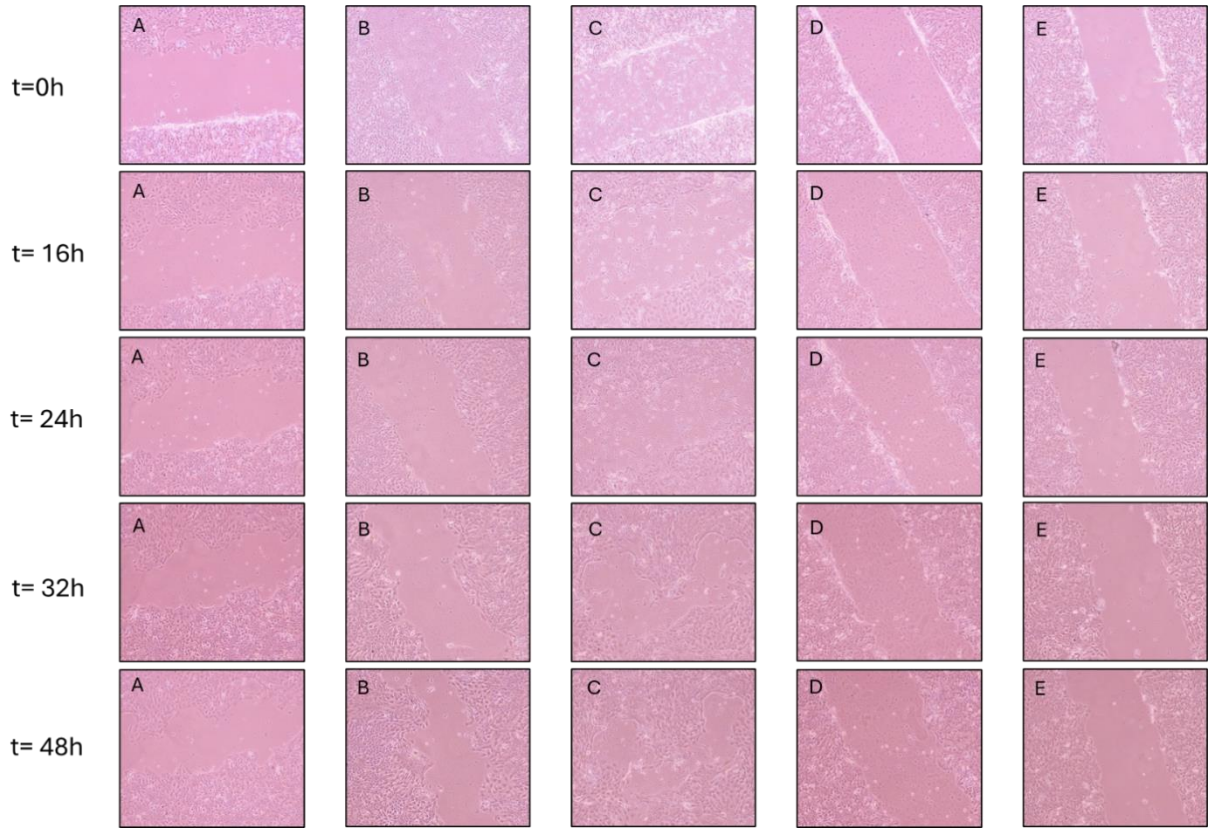

Figure A5. Evolution of wound healing in HaCaT cells line after treatment medium (A), EPS RD5 (B), SC4 (C), RA19 (D), Mo169 (E) at time 0, 16, 32, 48h.